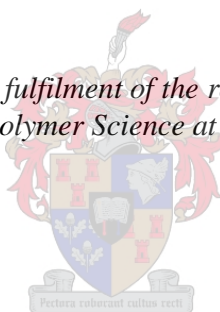


Silk-cellulose nanofiber membranes for application in water treatment

by

Priscilla Nyakombi

*Dissertation presented in fulfilment of the requirements for the degree
Master of Science in Polymer Science at Stellenbosch University*



Supervisor: Dr Nonjabulo Prudence Gule
Co-supervisors: Prof Bert Klumperman and Prof Fritz Vollrath

Faculty of Science

Department of Chemistry and Polymer Science

December 2019

Declaration

By submitting this dissertation electronically, I declare that the entirety of the work contained therein is my own, original work, that I am the sole author thereof (save to the extent explicitly otherwise stated), that reproduction and publication thereof by Stellenbosch University will not infringe any third party rights and that I have not previously in its entirety or in part submitted it for obtaining any qualification.

Priscilla Nyakombi

December 2019

Copyright © 2019 University of Stellenbosch

All rights reserved

Abstract

Electrospinning (ES) of biopolymers down to nanoscale size has received considerable interest in efforts to address specific millennia problems, which include materials for application in medical and water treatment spheres. The main aim of this study was to fabricate silk fibroin (SF) and cellulose (CE) nanofiber membranes via the ES method, then characterized for morphology using scanning electron microscopy and transmission electron microscopy, structurally using X-ray diffraction, Fourier Transform Infra-red spectrometry, Raman spectroscopy and Solid-State NMR. To establish thermal stability of the fabricated nanofibers when compared to the pure polymers, differential scanning calorimetry and thermal gravimetric studies were conducted. Several properties such as biodegradability, biocompatibility and non-toxic were considered with applications in filter media and tissue engineering in mind. Both cellulose and silk are natural fibers that degrade naturally, and they have remarkable mechanical properties, which, from an environmental friendliness point of view, a blended material from these biopolymers can be a good candidate, and secondly utilize the blended nanofibers as candidates in filtration media. Furthermore, both materials are mechanically strong and therefore can withstand the pressures associated with water treatment. A further advantage is that both silk and cellulose fibers have been reported to exhibit antimicrobial properties. Hence, it was envisaged that fiber combinations from these two biopolymers may have some degree of antimicrobial activity, which would open a wide range of applications.

Randomly oriented SF/CMC nanofibrous mats were fabricated with average diameters of about 153 ± 20 nm. The electrospun mats were also crosslinked with *N*-(3-dimethylaminopropyl)-*N'*-ethylcarbodiimide hydrochloride (a nontoxic crosslinking agent) and *N*-hydroxysuccinimide to enhance water stability for water treatment applications. The antimicrobial activity of the fibers was examined against different bacteria including *Staphylococcus aureus* (Gram-positive) and *Escherichia coli* (Gram-negative). Various methods were used to assess the antibacterial activity, including zone inhibition and fluorescence imaging. Enzymatic biodegradation of the materials was studied using cellulase (*Aspergillus niger*) and protease type XIV (*Streptomyces griseus*). The degradation of the electrospun mats was confirmed using SEM and FTIR.

From the results, SF/CMC fibers displayed diameter increases when compared to fibers obtained from pure silk solutions. Structural characterization using ATR-FTIR, XRD, Raman,

and SolSt-¹³C NMR showed the transfiguration of SF from a random coil to a β -sheet in the electrospun blends with CMC. The TGA results of the SF/CMC blended nanofibers exhibited thermal behavior very similar or better than that of SF nanofibers. The SF and SF/CMC blends nanofibers were all successfully crosslinked by EDC/NHS crosslinking agent. After crosslinking, it was observed that the nanofiber mats became more pliable and their average diameter increased compared to the non-crosslinked nanofiber mats and achieved more water stability as the crosslinking agent was increased. The results from zone inhibition tests showed that SF is slightly active against *E. coli* and CMC indicated positive result towards *E. coli* and moderate results towards *S. aureus*. The degradation of all electrospun nanofibers was investigated through the action of enzymes. Results show that SF/CMC nanocomposites can be classified as enzymatically degradable. The increase in weight loss as the degradation period increased was observed. From the findings, it was concluded that protease XIV degrades SF by breaking down the peptide bonds of the SF into amino acids and cellulase degrades CMC.

Opsomming

Die Elektrospinn (ES) van biopolimere tot nanoskaalgrootte het groot belangstelling getrek in pogings om millennia-kwessies soos mediese materiale en velde wat verband hou met waterbehandeling aan te spreek. Die hoofdoel van hierdie studie was om syfibrien-sellulose nanovesel membraan via die ES tegniek te fabriseer en karakteriseer. Verskeie eienskappe was oorweeg met toepassings in filtermedia en weefselingenieurswese as agtergrond. Beide sellulose en sy, is natuurlike vesels wat natuurlik afbreek en interessante meganiese eienskappe besit wat hulle, vanuit 'n omgewingsvriendelike oogpunt voordelig maak. Verder is albei materiale meganies sterk en kan dus die druk wat met waterbehandeling gepaard gaan hanteer. Nóg 'n voordeel is dat syvesels as antimikrobies aangetoon word. Daar was dus beoog dat veselkombinasies tussen die twee biopolimere antimikrobies kon wees, wat 'n wye verskeidenheid toepassings sou oplewer.

Willekeurig georiënteerde SF/CMC nanovesel matte met gemiddelde diameters van ongeveer 153 ± 20 nm was vervaardig. Die morfologie van die matte was gekenmerk deur gebruik te maak van skanderingselektronmikroskopie (SEM) en transmissie-elektronmikroskopie, terwyl hul struktuur met behulp van X-straaldiffraksie, Fourier-transform infrarooi spektrometrie (FTIR), vastestandse kernmagnetiese resonansie en Raman-spektroskopie bepaal was. Om die termiese stabiliteit van die vervaardigde membraan, in vergelyking met dié van die suiwer polimere was met behulp van differensiële skanderingskalorimetrie en termiese gravimetrie studies uitgevoer. Die elektrospinn matte was ook gekruis met N-(3-dimethylaminopropyl)-N'-ethylcarbodiimide hydrochloride ('n nie-toksiese kruisingsagent) en N-hydroxysuccinimide. Die antimikrobiese aktiwiteit van die vesels was in vergelyking met verskillende bakterieë, insluitend *Staphylococcus aureus* (Gram-positief) en *Escherichia coli* (Gram-negatief) ondersoek. Verskeie metodes soos sone inhibisie en fluoressensie beelding was gebruik om vir antimikrobiese aktiwiteit te toets. Die ensiematiese biodegradering van die materiale was met behulp van sellulase (*Aspergillus niger*) en protease tipe XIV (*Streptomyces griseus*) bestuddeer. Die agteruitgang van die elektrospun matte was ondersoek deur SEM en FTIR te gebruik.

Resultate het getoon dat die deursnee van die elektrospinn matte geleidelik toegeneem het na mate CMC toegevoeg is. Strukturele karakterisering met behulp van ATR-FTIR, XRD, Raman, en SolSt-¹³C NMR het die transformasie van SF vanaf 'n ewekansige spoel na 'n β -vel in die elektrospinn mengsels met CE getoon. Die SF/CMC gemengde nanovesels het hittegedrag

getoon wat baie soortgelyk of beter is as dié van SF nanovesels was. Die SF en SF/CMC mengsel nanovesels was almal suksesvol gekruis deur 'n EDC/NHS kruismiddel te gebruik. Na kruising was dit waargeneem dat die nanovesel matte meer buigbaar geword het en hul gemiddelde deursnee toegeneem het in vergelyking met die nie-gekruisde nanoveselmatte sowel as dat dit meer waterstabiliteit verkry het namate die kruisingsmiddel verhoog was. Die resultate van sone inhibisie toetse het getoon dat SF effens aktief is teen *E. coli* en CMC het positiewe aktiwiteit teenoor *E. coli* en matige aktiwiteit teenoor *S. aureus* getoon. Die afbreek van alle elektrospun nanofibers was deur die werking van ensieme ondersoek. Resultate het toon dat SF/CMC membraan as ensimaties afbreekbaar geklassifiseer kon word. Die toename in gewigsverlies namate die afbreekperiode verhoog was, is waargeneem. Uit die bevindinge was gevind dat protease XIV, SF degradeer, deur die peptiedbindings van die SF na aminosure af te breek en dat CMC afbreek van sellulose.

List of Publications

Aspects of this thesis have been presented at international conferences.

Oral presentations

[1] April 2018: Invited speaker, NanoAfrica conference. Durban, South Africa.

Lecture title: Natural polymer nanofibers - A cellulose and silk fibroin perspective
Priscilla Nyakombi and Nonjabulo Prudence Gule

[2] August 2018: Oral presentation. 5th Early Career Symposium, Liverpool, UK.

Title of talk: Opportunities and challenges for the advancement of natural polymer-based nanomaterials: A silk and Cellulose perspective

Poster presentations

[1] January 2018: Electrospinning conference, Stellenbosch, South Africa.

Title of Poster: Novel silk-cellulose nanofiber membranes for application in water treatment.

Acknowledgements

I would like to thank the following people and institutions/groups who contributed towards the success of this project:

- I am forever grateful to God for the gift of life, and for being my Saviour. I am grateful for the love, the strength and courage, He gave me throughout my studies.
- Dr. Nonjabulo Gule, my supervisor, to provide me with the wonderful opportunity of conducting this study under her supervision – for her support, patience and encouragement, and for always seeing the best in me. Thank you!
- Prof. B. Klumperman and Prof. F. Vollrath, my co-supervisors, for their valued contributions to this study, and to offer me a chance to perform this work under their leadership/guidance.
- To the Oxford Silk group (Oxford University) for their contributions to the study.
- My family, for their prayers, love and the support. My loving parents, for always believing in me even at times when I did not believe in myself. My wonderful sisters and brothers, for always being supportive.
- Prof Khan and her group (Microbiology Department, Stellenbosch University) to welcome me and for guidance during the time I spent in their laboratory. Special thanks to Dr. Thando Ndlovu for the assistance with biodegradation and antimicrobial activity experiments.
- The Free Radical group (Polymer Science, Stellenbosch University) for all the assistance and support. Special thanks to Dr Waled Hadasha and Dr Siyasanga Mbizana.
- The Staff at the Central Analytical Facilities (CAF, Stellenbosch University) for assistance with sample analysis.
- The National Research Foundation for funding.

Table of Contents

Declaration	ii
Abstract	iii
Opsomming	v
List of Publications.....	vii
Acknowledgements	viii
List of Figures	xii
List of Schemes	xv
List of Tables.....	xvi
List of Abbreviations.....	xvii
Chapter 1: Introduction and Objectives	1
1.1. Background.....	1
1.2. Motivation	2
1.3. Problem statement	2
1.4. Overall aim of the study	3
1.5. Objectives	3
1.6. Layout of the thesis.....	3
1.7. References	5
Chapter 2: Literature review	7
2.0. Chapter summary.....	7
2.1. Introduction	7
2.1.1. Classes of natural polymers	8
2.1.2. Natural polymers and synthetic polymers.....	9
2.1.3. Sources and uses of natural polymers	10
2.1.4. Polymers used in this study.....	11
2.2. Silk.....	11
2.2.1. Sources, extraction and production of silk.....	11
2.2.2. Composition of the silk thread	13
2.2.3. Structure of silk.....	14
2.2.4. Physical properties of silk.....	17
2.3. Cellulose	17
2.3.1. Sources, extraction and application of cellulose.....	17
2.3.2. Molecular structure of cellulose.....	18

2.3.3. Properties of cellulose.....	20
2.3.4. Chemical modification of cellulose	21
2.3.5. Derivative of cellulose used in this study: Carboxymethyl cellulose	22
2.4. Nanofiber membranes of SF and CE	24
2.4.1. Fabrication of the nanofiber blends	24
2.4.3. Applications of the nanofiber membranes	30
2.5. References	31
Chapter 3: Experimental approach: Preparation and characterization of electrospun nanofibers of SF/CMC blends.....	42
3.0. Background.....	42
3.1. Materials	42
3.2. Processing of silk fibroin (SF).....	43
3.2.1. Degumming of silkworm cocoons	43
3.2.2. Preparation of regenerated silk fibroin (RSF).....	43
3.2.3. Preparation of aqueous solutions of silk protein fibroin.....	43
3.2.4. Development of carboxymethylcellulose (CMC) solutions	43
3.2.5. Preparation of nanofiber membranes	44
3.3. Electrospinning.....	44
3.3.1 Equipment and setup used	44
3.3.2. ES parameters	44
3.3.3. Preparation of electrospun nanofibers	44
3.4. Characterization of fibers	45
3.4.1. Morphological characterization	45
3.4.2. Chemical characterization.....	46
3.4.3. Thermal characterization	47
3.5. Results and discussion	47
3.5.1. Preparation of pure SF nanofibers	47
3.5.2. Preparation of SF/CMC blend nanofibers.....	53
3.5.3. Characterization of the SF/CMC blend nanofibers.....	53
3.5.4. Morphological study	53
3.5.7. Thermal characterization	60
3.6. Conclusion.....	63
3.7. References	64

Chapter 4: Biodegradation and antimicrobial evaluation of the electrospun mats	67
4.0. Summary.....	67
4.1. Introduction	67
4.1.1. The biodegradation behavior of SF and CMC nanofiber membranes	67
4.2. Crosslinking of silk and cellulose nanofibers.....	68
4.3. Materials and techniques	70
4.3.1. Crosslinking of the electrospun nanofibers.....	70
4.3.2. Antimicrobial characterization.....	71
4.3.3. Biodegradation evaluation	72
4.4. Results and discussion	73
4.4.1. Effect of the crosslinking agent on the crosslinked nanofibers	73
4.4.2. Characterization of crosslinked nanofiber membranes.....	77
4.4.3. Antimicrobial evaluation of the crosslinked nanofibers	81
4.4.4. Biodegradation evaluation	84
4.5. Conclusion.....	88
4.6. References	90
Chapter 5: Conclusions and recommendations for future research.....	92
5.0. Summary.....	92
5.1. Conclusions	92
5.2. Recommendations	93

 List of Figures

Figure 2. 1: Classification of Natural Polymers.	8
Figure 2. 2: The life cycle of the mulberry silkworm from silk moth.....	13
Figure 2. 3: Interaction between polypeptide chains forming a β -sheet structure of fibroin. ..	15
Figure 2. 4: Physical structure of silk.....	16
Figure 2. 5: Properties of Silk Fibroin. Adapted from reference	17
Figure 2. 7: Representation of a cellulose chain showing the anhydroglucose unit in the chair conformation along with atom numbering, the glycosidic link, and both reducing and non-reducing ends of the polymer.	19
Figure 2. 8: Intramolecular hydrogen bonding in cellulose molecules.	20
Figure 2. 9: Functions and Properties of CMC. Adapted from	23
Figure 2. 10: Schematic illustration of solution casting	24
Figure 2. 11: Schematic diagram of ES setup.	26
Figure 2. 12: Potential applications of nanofibers.....	30
Figure 3.1: SEM images of electrospun SF nanofibers generated from SF solutions of different concentrations (8-12%) (distance between the collector and spinning electrode 16 cm, voltage 15 kV).....	48
Figure 3.2: SEM images of electrospun SF nanofibers formed from 10 wt% SF solution, using different distances between the electrodes (12, 14, 16 cm).	50
Figure 3.3: FTIR spectrum of electrospun SF nanofibers.....	51
Figure 3.4: XRD spectrum of SF electrospun nanofibers.	52
Figure 3.5: TGA thermogram of the electrospun SF nanofibers.....	53
Figure 3.6: FE-SEM images of electrospun nanofibers: SF/CMC(1), SF/CMC(2) and SF/CMC(3).....	54
Figure 3.7: FE-SEM images of SF/CMC/SS electrospun nanofibers	55
Figure 3.8: TEM images of electrospun SF/CMC (1) blend nanofibers.....	56
Figure 3.9: FTIR spectra of the electrospun SF and SF/CMC blends.....	57
Figure 3. 10: SolSt- ¹³ C NMR of SF and CE, and SF/CMC (1) nanofibers.	58
Figure 3.11: XRD spectra of the electrospun SF and SF/CMC blends nanofibers.....	59
Figure 3. 12: Raman spectra of (A) CMC, (B) SF, and (C) SF/CMC(1) blends.	60
Figure 3. 13: TGA curves of the SF, CMC, and SF/CMC blends.	61

Figure 3. 14: DSC thermograms of the second heating runs of (A) CMC, (B) SF, and (C) SF/CMC (1) blend.....	62
Figure 4.1: Final Mass loss of SF and SF/CMC(1) nanofiber mats as the EDC/NHS concentration increases.	73
Figure 4.2: FESEM images of SF crosslinked nanofibers (A) uncrosslinked nanofiber mats, (B) 3 wt% EDC/NHS, (C) 5 wt% EDC/NHS, and (D) 7.5 wt% EDC/NHS.....	74
Figure 4.3: FESEM images of SF/CMC(1) crosslinked nanofibers (A) uncrosslinked nanofiber mats, (B) 3 wt% EDC/NHS, (C) 5 wt% EDC/NHS, and (D) 7.5wt% EDC/NHS.....	75
Figure 4.4: FE-SEM images of SF, (A) untreated SF nanofiber mats, (B) untreated SF nanofiber mats after soaking in water, (C) SF nanofiber mats exposed for 24 h to the 7.5wt% EDC/NHS, (D) after soaking in water, (E) SF nanofibers mats exposed for 48 h to the 7.5wt% EDC/NHS and (F) after soaking in water.	76
Figure 4.5: FE-SEM images of SF/CMC (1) fibers, (A) untreated nanofiber mats, (B) untreated nanofiber mats after soaking in water, (C) nanofiber mats exposed for 24 h to the 7.5wt% EDC/NHS , (D) after soaking in water, (E) nanofibers mats exposed for 48 h to the 7.5wt% EDC/NHS and (F) after soaking in water.	77
Figure 4.6: FTIR spectra of SF crosslinked nanofibers with different concentrations of the crosslinking agent: 0%, 3 wt%, 5 wt%, 7.5 wt% EDC/NHS.	78
Figure 4.7: FTIR spectra of SF/CMC(1) crosslinked nanofibers with different concentrations of the crosslinking agent: 0%, 3 wt%, 5 wt%, 7.5 wt% EDC/NHS.	79
Figure 4.8: TGA spectra of SF crosslinked nanofibers with different concentrations of the crosslinking agent: (a) 7.5 wt% EDC/NHS, (b) 5 wt% EDC/NHS, (c) 3 wt% EDC/NHS; and (d) uncrosslinked SF nanofibers.....	80
Figure 4.9: TGA spectrum of SF/CMC(1) crosslinked nanofibers with different concentration of the crosslinking agent: (a) 7.5 wt% EDC/NHS, (b) 5 wt% EDC/NHS, and (c) 3 wt% EDC/NHS; and (d) uncrosslinked SF nanofibers.....	81
Figure 4.10: Results of the zone-inhibition method used to determine the susceptibility of <i>E. coli</i> (Gram-negative) and <i>S. aureus</i> (Gram-positive) to (A) SF, CMC, SF/CMC, (C) SS and (E) SF/CMC/SS blend nanofiber composites.....	82
Figure 4.11: Fluorescent microscope images of incubated fibers, SF, and SF/CMC blend <i>with S. aureus</i> and <i>E. coli</i> in saline solution.	84

Figure 4.12: Degradation behavior of SF, SF/CMC(1), and SF/CMC(2) after incubation in the following solutions: (A) PBS solution (controls), (B) protease XIV solution, (C) cellulase solution, and (D) a solution of both enzymes.....	85
Figure 4.13: SEM images of the SF nanofibers after incubation in PBS (controls) and protease XIV solution at 37 °C for 3, 7, and 14 days.	86
Figure 4.14: SEM images of the SF/CMC blends nanofibers after incubation in PBS and enzymatic solution at 37°C for 3–14 days.	87
Figure 4.15: FTIR spectra of the CMC, SF, and SF/CMC blend nanofibers: (A) before degradation, (B) after 3 days degradation, (C) after 7 days degradation, and (D) after 14 days degradation.	88

List of Schemes

Scheme 2. 1: Etherification of CE to form carboxymethyl cellulose.....	23
Scheme 4. 1: Crosslinking reaction of SF.	69
Scheme 4. 2: Crosslinking reaction process of SF/CMC blend nanofibers.	70

List of Tables

Table 2.1: Classification of some silk moths found around the world.....	12
Table 2.2: composition of the silk.....	14
Table 2.3: Amino acid composition	14
Table 2. 4 : Cellulose derivatives and applications	21
Table 2.5: Advantages and disadvantages of various scaffold fabrication techniques.	25
Table 2.6: Parameters affecting electrospinning/fiber morphology.....	27
Table 2.7: Various SF–biopolymer blend based scaffolds and their applications	29
Table 3. 1: Experimental parameters used for electrospinning of SF, SF/CMC and SF/CMC/SS blend nanofibers	45
Table 4. 1: Summary of antimicrobial activity of the electrospun nanofiber composites	83

List of Abbreviations

AGU	Anhydroglucose unit
ATR-FTIR	Attenuated total reflectance-Fourier transform infrared spectroscopy
CA	Cellulose acetate
CE	Cellulose
CMC	Carboxymethylcellulose
CS	Chitosan
DI	Deionized
DP	Degree of polymerization
DSC	Differential scanning calorimetry
DS	Degree of substitution
<i>E. coli</i>	<i>Escherichia coli</i>
EDC	Ethylcarbodiimide hydrochloride
ES	Electrospinning
EU	European Union
FA	Formic acid
LB	Luria Bertani
NHS	<i>N</i> -hydroxysuccinimide
PBS	Phosphate buffered saline
PI	Propidium iodide
RSF	Regenerated silk fibroin
RT	Room temperature
<i>S. aureus</i>	<i>Staphylococcus aureus</i>
SF	Silk fibroin
SF/CE	Silk fibroin-cellulose
SEM	Scanning electron microscopy
SolSt-NMR	Solid State-Nuclear magnetic resonance spectroscopy
SS	Silk sericin
TGA	Thermogravimetric analysis
T _g	Glass transition temperature
TEM	Transmission electron microscopy
UTS	Ultimate tensile strength
WAXD	Wide-angle X-ray diffraction

XCT	X-ray computerized tomography
XRD	X-ray diffraction

Chapter 1: Introduction and Objectives

1.1. Background

Insufficient gateway to potable water is the unique vital concern affecting humanity. Statistics indicate that by the year 2040 water insufficiency will have reached alarming levels. This could be, in part, attributed to climate change, which has brought about extreme weather events like droughts.¹ About a third of the world's population lacks or has very little access to potable water supplies. According to the United Nations: "In 2016, an estimated 52 million children under the age of five years from developing countries died annually from intestinal parasitic infections".² Problems related to sanitation and poor water quality are also on the rise globally due to the rapidly growing population.^{3,4} According to Ostioch *et al.*,⁵ waterborne diseases are caused by microorganisms (protozoa, bacteria and viruses) which can emanate from human and animal excretory substances. In developing countries, where there is either poor infrastructure or none at all, water impurity may be credited to infiltration, drain and surface run-off between pastures, and leakage of sewage discarding systems into drinking water bodies.⁶ These statistics further reiterate the seriousness of the problem and the urgency with which solutions to either control or solve this problem is needed.

The production of nanofibers has obtained plenty of attention in the development of materials with properties that are suitable to direct problems associated to water treatment.⁷ Nanofibers are a quite new group of nanomaterials that can be produced through electrospinning (ES). ES is the process that generates submicron to nanoscale fibers between an electrically charged jet of polymer solution. Both man-made polymer and natural have been effectively used for manufacturing nanofibers that have the diameter fluctuating from ten to hundreds of nanometer, with manageable morphology and functionality.⁸

In the application of water filtration, majority porous polymeric membranes, produced by the ordinary phase-inversion technique, have their existing drawbacks, like low flux and high fouling because of the asymmetric void structure developing of pores across the membrane's width and the equivalent pore size diffusion. Electrospun nanofiber-based membranes are good replacements which can exceed standard membranes due to their high porosity (normally around 80%), completely connected open pore structures and controlled pore size distribution from microns to sub-microns, hence giving high penetrable for water filtration.¹⁴

Synthetic polymer fibers were initially manufactured for their longevity and impenetrable to all forms of degradation, including biodegradation, and for special performance characteristics achieved through control of molecular weight and functionality.⁹ However, these properties have contributed to disposal problems. Synthetic polymers have received the brunt of media attention, largely because of their visibility in the environment as litter and their obvious contribution to landfills depletion.¹⁰ These side effects of synthetic polymers may be controlled by switching to natural polymers.

Natural fiber composites have attracted much attention over the past few years because of the advantages that these fibers offer over synthetic nanofibers.¹¹ They are biodegradable, biocompatible and nonabrasive, unlike synthetic fibers. They are also readily available.¹² The suitable uses of electrospun fibers involves: high-performance air filters, protective textiles, sensors, advanced composites, photovoltaics cells, wound dressings, in tissue engineering as scaffolds and, once again, as membrane filters for water treatment.¹³

1.2. Motivation

Natural polymers are mainly polysaccharides or proteins that are derived from natural sources. Natural polymers are highly renewable and biological accepted. Natural polymers are viable alternatives to replace potentially environmentally hazardous synthetic materials and may be accessible at a low overall cost compared to their chemically produced counterparts. Both cellulose (CE) and silk are natural fibers which degrade naturally. Therefore, from an environmental friendliness point of view, their use would offer advantages. They also have exceptional mechanical properties; hence they would be able to withstand the pressures associated with water treatment, offering further advantage. Furthermore, some silk fibers are thought to be antimicrobial,^{15,16} which led us to hope that fibers from these two biopolymers could also be antimicrobial. This would then open unlimited uses.

1.3. Problem statement

With the increasing world population, management of water is progressively strained. Most regions all over the universe are diverting to recycling of water to increase their drinkable water supply. Conventional water purification technique have ability of eliminating small solid particles, organic components and nutrients.¹⁷ Although, these standard technologies may not take off most components of importance like, pathogenic organisms and viruses, traces of pharmaceutical and self-care hygiene, also endocrine-disrupting chemicals.

Membrane processes providing the straightforward treatment that have ability to eliminate not only viruses, as well as the remains of concern mentioned above.

Despite its unlimited and good pertinence, technology of membrane filtration residues available because of membrane contamination and poor mechanical properties. Both silk and CE are recognized for their excellent mechanical robustness and their antimicrobial properties have been reported.¹⁶ Nanofibers from SF and CE should be promising candidates to address these problems.¹⁸ Synthetic polymers are manmade polymers that can be manufactured in the laboratory via a chain of chemical reactions.¹⁹ They have various industrial uses and applications; however, they may be harmful to the environment due to associated pollution problems

1.4. Overall aim of the study

The main aim of this study was to fabricate silk fibroin-cellulose nanofiber blends using an ES method and then to evaluate them for use in water filtration applications.

1.5. Objectives

Certain goals were the following:

- i. To fabricate SF/CMC blend nanofibers using ES methods (optimization process)
- ii. To characterize for morphology using SEM and TEM, structurally using XRD, FTIR, Raman spectroscopy and SS NMR.
- iii. To establish thermal stability of the fabricated nanofiber membranes when compared to the pure polymers, DSC and TGA studies were conducted.
- iv. To determine antimicrobial properties of the fabricated nanofibers, using fluorescent imaging techniques and zone inhibition tests.
- v. To evaluate the biodegradation behavior of the fabricated nanofibers.

1.6. Layout of the thesis

Chapter 1: The background of the study is sketched. Motivation for the study is stated. The problem statement puts forth the overall aim of fabricating natural polymers for the preparation of nanofiber filters to address the challenges associated with water treatment.

Chapter 2: A brief description from other studies and fundamental concepts related to this study are described. First, the classification of natural polymers and their applications are presented. Second, the ES process, which is the technique used in this study to fabricate the nanofibers, is described.

Chapter 3: This is the experimental chapter; it describes the materials and research methods used, and the analytical techniques used to characterize all the materials fabricated in this study.

Chapter 4: The antimicrobial evaluation of the nanofiber mats fabricated while this study towards *S. aureus* and *E. coli* organisms are defined. Biodegradation studies of the electrospun mats by enzyme action are also described.

Chapter 5: In this chapter the conclusions drawn from experimental results, and briefly offers recommendations for future research.

1.7. References

- (1) Judd, S. The Status of Membrane Bioreactor Technology. *Trends Biotechnol.* **2008**, *26* (2), 109–116.
- (2) Wu, H. The Sustainable Development Goals Report. United National Department of Economic and Social Affairs **2017**, (<https://doi.org/10.18356/4d038e1e-en>).
- (3) Hassan Rashid, M. A. U.; Manzoor, M. M.; Mukhtar, S. Urbanization and Its Effects on Water Resources: An Exploratory Analysis. *Asian J. Water, Environ. Pollut.* **2018**, *15* (1), 67–74.
- (4) Scroccaro, I.; Ostoich, M.; Umgiesser, G.; De Pascalis, F.; Colugnati, L.; Mattassi, G.; Vazzoler, M.; Cuomo, M. Submarine Wastewater Discharges: Dispersion Modelling in the Northern Adriatic Sea. *Environ. Sci. Pollut. Res.* **2010**, *17* (4), 844–855.
- (5) Ostoich, M.; Serena, F.; Tomiato, L. Environmental Controls for Wastewater Treatment Plants: Hierarchical Planning, Integrated Approach, and Functionality Assessment. *J. Integr. Environ. Sci.* **2010**, *7* (4), 251–270.
- (6) Yavuz Corapcioglu, M.; Haridas, A. Transport and Fate of Microorganisms in Porous Media: A Theoretical Investigation. *J. Hydrol.* **1984**, *72* (1–2), 149–169.
- (7) Mokhena, T. C.; Jacobs, V.; Luyt, A. S. A Review on Electrospun Bio-Based Polymers for Water Treatment. *Express Polym. Lett.* **2015**, *9* (10), 839–880.
- (8) Wang, X.; Hsiao, B. S. Electrospun Nanofiber Membranes. *Curr. Opin. Chem. Eng.* **2016**, *12*, 62–81.
- (9) Swift, G. Directions for Environmentally Biodegradable Polymer Research. *Acc. Chem. Res.* **1993**, *26* (3), 105–110.
- (10) Andrady, A. L. Microplastics in the Marine Environment. *Mar. Pollut. Bull.* **2011**, *62* (8), 1596–1605.
- (11) Saheb, D. N.; Jog, J. P.; Nabi Saheb, D.; Jog, J. P. Natural Fiber Polymer Composites : A Review. *Adv. Polym. Technol.* **1999**, *18* (4), 351–363.
- (12) Olatunji, O.; Richards, O. Processing and Characterization of Natural Polymers. *Natural Polymers*. Springer International, **2017**.
- (13) Jamshaid, A.; Hamid, A.; Muhammad, N.; Naseer, A.; Ghauri, M.; Iqbal, J.; Rafiq, S.;

- Shah, N. S. Cellulose-Based Materials for the Removal of Heavy Metals from Wastewater - An Overview. *ChemBioEng Rev.* **2017**, *4* (4), 240–256.
- (14) Ahmed, A. E. S. I.; Moustafa, H. Y.; El-Masry, A. M.; Hassan, S. A. Natural and Synthetic Polymers for Water Treatment against Dissolved Pharmaceuticals. *J. Appl. Polym. Sci.* **2014**, *131* (13), 1–10.
- (15) Rajendran, R.; Balakumar, C.; Sivakumar, R.; Amruta, T.; Devaki, N. Extraction and Application of Natural Silk Protein Sericin from Bombyx Mori as Antimicrobial Finish for Cotton Fabrics. *J. Text. Inst.* **2012**, *103* (4), 458–462.
- (16) Jassim, K. N.; Alsaree, O. J. Study of the Antimicrobial Activity of Silk Sericin from Silkworm Bombyx Mori. *J. Comm. Med.* **2010**, *23*, 130–133.
- (17) Markandya, A. Water Quality Issues in Developing Countries. *Essay Environ. Dev* **2006**, University of Bath, MSc.
- (18) Mai, Z. Membrane Processes for Water and Wastewater Treatment : Study and Modeling of Interactions between Membrane and Organic Matter. Ecole Central Paris. *English* **2014**.
- (19) Ramakrishna, S.; Fujihara, K.; Teo, W. E.; Yong, T.; Ma, Z.; Ramaseshan, R. Electrospun Nanofibers: Solving Global Issues. *Mater. Today* **2006**, *9* (3), 40–50.

Chapter 2: Literature review

2.0. Chapter summary

In this chapter a brief description of natural polymers, with the focus on SF, CE and CMC polymers is given. This is followed by the classification of natural polymers, and the advantages and disadvantages of natural over synthetic polymers. The sources and isolation of SF and CE are described. The extraction, purification and application of SF and CE is discussed followed by the derivatization of CMC from CE. The chapter concludes with the fabrication techniques and the applications of SF/CMC blends nanofibers.

2.1. Introduction

Polymers are long-chain molecules (macromolecules) which then joined together by a building blocks of monomers.¹ A chemical reaction by which these monomer molecules are joined is known as a polymerization reaction.² Polymer molecule can be made up of hundreds, thousands or more monomers. Natural polymers are a group of polymers extracted from plant or animal sources. Natural polymers involves mostly carbohydrates and proteins that survive in plant and animals, these polymers perform dissimilar duties and consists of different monomers.³ Carbohydrates made up of sugar monomers called monosaccharide and are necessary for energy storage, glucose is an important monosaccharide that is broken down during cellular respiration to be used as energy source. Proteins are biomolecules that have the ability of making compound structures which consists of building blocks of amino acids, and has a wide variation of purposes including movement of molecules, the representatives of proteins are enzymes.⁴ Most natural polymers are naturally built by condensation polymerization.⁵ Natural polymers are examined as the most acceptable scaffolding substances for most uses, including filtration. Collagen, chitosan (CS), silk fibroin (SF), cellulose (CE), CE derivatives and gelatin are examined as possible substances for the manufacturing of scaffolds. Such materials provides superior cell adhesion, developing and proliferation properties.⁶ Natural polymers are usually not harmful to the environment compared with synthetic polymers; they are also biocompatible, cost effective and, in most cases, readily available and renewable. Natural polymers have been used as clarifying agents in water treatment because they can destabilize the particles contained

in the water in a liquid medium through the process of neutralization and adsorption, and flocculate colloids, followed by their sedimentation.⁷

2.1.1. Classes of natural polymers

Natural polymers can be grouped according to their sources and structures. They can be grouped into three fundamental categories according to their origins: polysaccharides, proteins and polynucleotides.⁸ See Figure 2.1.

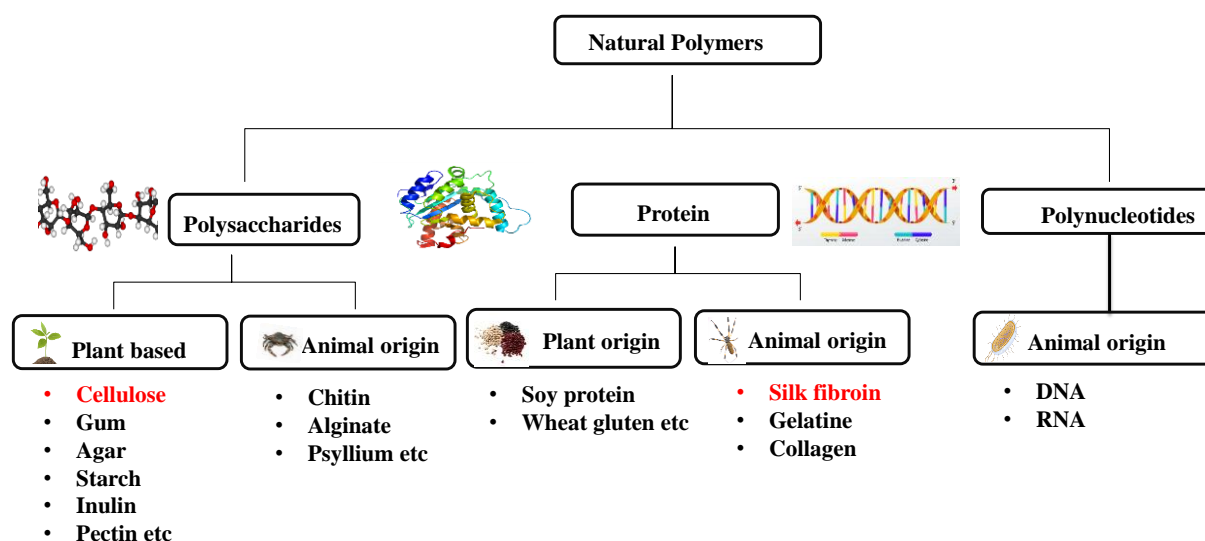


Figure 2. 1: Classification of Natural Polymers.⁸

2.1.1.1. Polysaccharides

Polysaccharides are defined as carbohydrate polymers, with building blocks of monosaccharide $C_nH_{2n}O_n$ units that are covalently linked in linear or branched configuration by *O*-glycosidic bonds ($R'-O-R$).⁹ These building blocks of monosaccharides are by far the most abundant renewable resources. They act as energy supplier, in a form of starch (amylopectin and amylose) and glycogen (branched polysaccharide of glucose), and as a structural component of bacterial cell walls. CE is the principal structural element of plants, close by hemicellulose, pectin, and lignin, whereas chitin is the most important structural constituent in some animals such as crustaceans.¹⁰

The classification and characterization of many polysaccharides can be challenging due to their irregular properties.¹¹ Thus, most researchers are studying towards synthetic polymers in the place of natural polymers, especially polysaccharides, which exhibit most irregularities on their

structures and properties. Nevertheless, due to their biodegradability and biocompatibility tendencies, polysaccharides have become increasingly attractive.

2.1.1.2. Proteins

Proteins are large biomolecules, or macromolecules, made up of building blocks of amino acid fragments.⁹ They are essential area for the cell wall of the plant and both acting as useful and configurational fragments: and establish application also identifying nature of the structure.¹² Classification of proteins may be made considering their shape, size, solubility, composition, including functionality.¹³ The two types of polymers that are based on shape and size are globular and fibrous proteins. Globular proteins are soluble in water type, which are rather frangible in nature. The classic examples of globular proteinase antibodies, enzymes and hormones. Fibrous proteins are water insoluble, tougher proteins found in structural tissues such as hair, nail and skin.

2.1.1.3. Polynucleotides

A polynucleotide molecule is a biopolymer comprising a long, linear series of nucleotides joined together by phosphoester linkages. Individual nucleotide monomer is made up of a pentose (five carbon) sugar that is connected to the phosphate group and a nitrogenous base.¹⁴ These nucleotides are covalently bonded in a chain. Polynucleotides occur naturally in all organisms.¹⁵ Ribonucleic acid (RNA) and deoxyribonucleic acid (DNA) are polynucleotides that act as the building blocks of life that comprise the order necessary for a cell to carry out its functions.

2.1.2. Natural polymers and synthetic polymers

2.1.2.1. Advantages of natural polymers

Natural polymers are extracted from natural sources and thus are biodegradable. Composites of natural polymers are coming out very rapidly as possible substitutes to metal or ceramic based uses that incorporate the automotive, marine, sporting goods and electronic industries.¹⁶ Natural fiber composites substances has been a demand topic recently due to the increasing environmental awareness.¹⁷ Because of their advantageous properties, like affordability, high strength to weight ratio, low density and non-corrosiveness, natural fibers are of interest to scientist. Natural polymers are environmentally friendly in contract with glass fibers-based compounds. Natural fibers have been performed in the growth of highly thermally stable and

acoustic insulator substances and are also emerging as a feasible alternative to glass fiber. Natural polymers can be adjusted into different structures, according to their functional groups.⁸

2.1.2.2. Disadvantages of natural polymers

A production of natural polymers cannot be maintained with predetermined amount of components, as in the case of synthetic polymers; their production is hanging on environmental and diverse physical circumstances.^{18,19} A percentages of chemical fragments existing in a stated natural polymer substances might differ because of dissimilarity in the assembly of the natural matters at various times, as well as difference in the source areas, species and climate conditions.⁸ They have gradual rate of manufacturing, because their production hangs on the environment and most circumstances are unchanged.⁹

2.1.3. Sources and uses of natural polymers

Agars are polysaccharides that are made up of agarose and agarpectin. Agarose is the firmly gelling complex sugar and the major component of agar-agar. It is a linear polymer consists of the continuous monomer fragment of agarobiose that consists of D-galactose and 3,6-anhydro-L-galactopyranose.⁸ The main applications of agars are related to the formation of thermoreversible gels at low concentration in water. This biopolymer has been extensively performed in both the food and pharmaceutical industries as a stabilizing and gelling agent.²⁰ It has many biological activities: anticoagulant, antiviral, anticancer, and immunomodulation.²¹ Chitin or poly(β -(1,4)-*N*-acetyl-D-glucosamine) is another tremendously available structural polysaccharide found in nature. Various living organisms can synthesize this biopolymer. The main sources of the chitin are cuticles of numerous crustaceans (shellfish), main shrimps and crabs.²² Chitin chemical structure is alike to that of CE, except that the CE has hydroxyl groups while chitin contains with the amino and acetyl group (acetamido group).²³ Uses of chitin are restricted because it does not dissolve in most solvent and awkwardness in handling. So, to produce CS, it is prepared by partial alkaline *N*-deacetylation. Thus, chitin is very often joined with CS to give related applications.²⁴

Collagen is the protein polymer, which can be defined as the fibrous structural protein exist in the extracellular matrix and connective tissue of animals. The pig skin; bovine, pork and battle bones are the most extraordinary origins of collagen and established as extended fibrils constituting about 1–2% of muscle tissue, where it is the foremost component of the endomysium.²⁵ It is present invertebrates body walls including cuticles, whereas is not found

in plants and unicellular organisms. Made of protein content of 20-30% for the whole body especially in mammals. It consists of extensive uses in many uses like pharmaceutical, medical, biomedical, the food industry, cosmetics, etc.

2.1.4. Polymers used in this study

SF and CE are both natural polymers that degrade naturally. CE is the predominant constituent of plant cell walls, making up about half of the biomass of photosynthesis organisms. Hence, regarded as the most abundant molecule on earth. SF is a fibrous protein found in silkworm (*Bombyx mori*); it is very versatile and can be prepared into different designs such as gels, films, fibers and powder.²⁶

These natural polymers are attractive for environmental uses because of properties like biodegradability, biocompatibility and nontoxicity. As the bonus, these biopolymers have advantageous mechanical and chemical properties, making them excellent composites for use in different applications.²⁷

2.2. Silk

2.2.1. Sources, extraction and production of silk

Silk is a protein polymer of animal origin produced by a variety of spiders and insect larvae (as well as a rare shrimp,²⁸), all in the phylum Arthropoda.²⁹ A number of animals secrete silk, which they use for anchorage, e.g., in shrimp and spider (and even a so called 'silk' in a mussel),³⁰ intertwining their prey (spiders),³¹ or forming a protective sheath with or without other material (Lepidopteran cocoons).³² The favorable silks are from the protein secretions of the *Bombycidae* moth/butterflies, such as the domesticated moth *Bombyx mori* (*B. mori*), sub-family *Bombycid*; the wild Chinese Tasar moth *Antheraea pernyi* and Indian Tasar moth *Antheraea mylitta*, from sub-family Saturniidae. Important African silks come from the communal caterpillar *Anaphe moloneyi*, sub-family *Thaumetopoeidae*.^{19,29,33} Or the interesting *Gonometa spp.* The ranking of a silk manufacturing moth is generally based to their varying families, such as *Bombycidae*, *Saturniidae*, *Lasiocampidae*, *Thaumetopoeidae*, etc., as summarized in Table 2.1. Close to 400–500 species are known to manufacture silk but only limited are commercially utilized.

Table 2.1: Grouping of some silk moths found around the world.

Silkworm species	Host plant	Distribution	Ref
Bombycidae <i>B. mori</i> <i>B. mandarina</i>	Mulberry	India, China, Japan, Korea, Russia	29,34,35
Saturniidae <i>Antheraea</i> <i>polyphemus</i> <i>Antheraea mylitta</i>	<i>Acer saccharum, Acer negundo, Alnus incana</i> <i>Terminalia alata, Terminalia arjuna, Shrea robust</i>	Northern America, Canada, United states India, Korea, Japan	36,37
Lasiocampidae <i>Gonometa potica</i> <i>G. rufobrunnae</i>	<i>Vachellia erioloba, A. tortillis, A. Senegalia mellifera, Burker Africana, Prosopis glandulosa</i> <i>Colophospermum mopane</i>	Southern Africa, Africa, Kenya Botswana, Zimbabwe,	38
Thaumetopoeidae <i>Anaphe infracta</i> <i>Anaphe venata</i> <i>A. panda</i>	<i>Bridelia minrantha,</i> <i>Pseudolachaostylis maprouneifolia,</i> <i>Cynometra ulexandri, Triumfetta manrophylla</i>	Nigeria, Uganda, Kenya, Congo, Cameroon, Togo	38,39

The manufacturing of silk is normally related with Asia, in which silk development was initially prepared over 4500 years ago in China;⁴⁰ traders and travelers introduced silk to other countries.^{41,42} The route they travelled is still called the “Silk Route”, even today. Trading silks are mainly grouped as mulberry (cultivated) silk and nonmulberry (wild) silk.⁴³ The silkworm, which is the larva or caterpillar of the domesticated silk moth *Bombyx mori*, is the best producer

of cultivated silk. Its favored food is the white mulberry leaves or the leaves of any other mulberry tree (such as *Morus rubra* or *Morus nigra*), as well as the Osage orange.⁴⁴

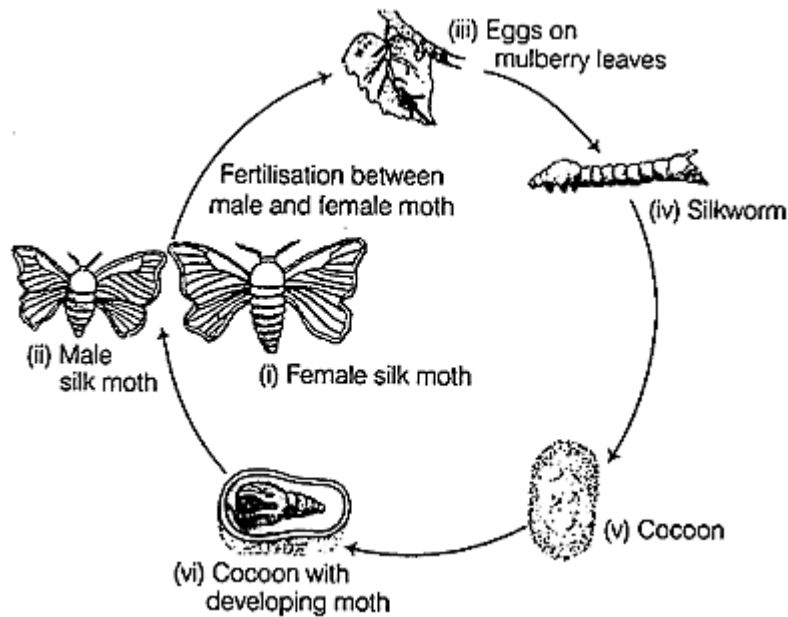


Figure 2. 2: The life cycle of the mulberry silkworm from silk moth.⁴⁴

The life process of the mulberry silkworm usually takes about 55–60 days but may be longer depending on the type of eggs laid and rearing conditions. The female silkworm deposits 300–400 eggs at a time and then dies, while the male lives only a short time. The small eggs of the silkworm moth are incubated for about 10 days until they hatch into larvae (caterpillars). Once hatched, the larvae are placed under a fine layer of gauze and fed huge amounts of chopped mulberry leaves, Osage orange or lettuce. At this time, they shed their skin four times. Then the pupation period starts, where a silkworm attaches itself to a compartmented frame, twig, tree, or shrub in a rearing house to spin a silk cocoon. This takes place over a 3–8 day period.^{16,45,46}

2.2.2. Composition of the silk thread

The silkworm *Bombyx mori* possesses a pair of long tubular organs called silk glands.^{29,47} The silk gland has three distinct regions as per the anatomical and functional aspect: the anterior, middle and posterior regions.⁴⁸ The silk proteins are manufactured in a detailed gland of the silkworm and fibers are produced by stretching the liquid silk through the head movement of the silkworm. Fibroin (about 70–80%) and sericin (about 20–30%) are the two proteins in the silk thread that are secreted by the silk gland. Fibroin, which is the most important silk protein, with a simple amino acid composition, is synthesized very rapidly in the posterior gland and then transferred into the middle silk gland where it is stored before spinning.⁴⁹ The fibroin in

the anterior gland is present in a very small amount, such that it is neglected in the calculations. The sericin is synthesized in the middle gland of *B. mori* and is secreted into the lumen.^{50,51} During spinning, the sericin coats the fibroin and acts as the gum binder to maintain the structural integrity of the cocoon.⁵² Other substances such as fat, wax, inorganic salt and coloring matter are also present in the cocoon. The composition of silk is given in Table 2.2.

Table 2.2: Composition of the silk.⁵²

Component	Percentage (wt%)
Fibroin	70–80
Sericin	20–30
Carbohydrates	1.2–1.6
Inorganic matter	0.7
Wax matter	0.4–0.8
Pigment	0.2

2.2.3. Structure of silk

Silk is a protein polymer comprising various amino acids. The amino acid compositions of *B. mori*, sericin and fibroin are close; however, hydrophilic amino acids, especially serine, are more abundant in sericin.^{52–54} Sericin is primarily amorphous and unstructured. The amino acid composition of fibroin and sericin in silk is tabulated in Table 2.1

Table 2.3: Amino acid composition.⁵²

Amino acid	Fibroin	Sericin
Glycine (Gly)	45	14
Alanine (Ala)	29	5
Serine (Ser)	12	33
Tyrosine (Tyr)	5	3
Valine (Val)	2	3
Aspartic acid (Asp)	1	15
Arginine (Arg)	1	3
Glutamic acid (Glu)	1	8
Isoleucine (Ile)	1	1
Leucine (Leu)	1	1
Phenylalanine (Phe)	1	1

Threonine (Thr)	1	8
Histidine (His)	0	1
Lysine (Lys)	0	4
Methionine (Met)	0	0
Proline (Pro)	0	1
Tryptophan (Trp)	0	0
Cysteine (Cys)	0	0

The amino acid sequence of the main structural protein, fibroin, contains repetitive glycine–alanine–glycine–alanine–glycine–serine (GAGAS) repeat units.⁵⁵ These amino acids self-assemble into antiparallel β -sheet structures that are highly crystalline essentially crosslinks the protein through strong intra and intermolecular hydrogen bonds, as well as strong van der Waals interactions between stacked β -sheets.^{50,54,56,57} Initialization of the hydrogen bonding network between these β -sheet crystallites act an important character in defining the strength and rigidity of this material, while the nanocrystalline area adopt a enough flexible conformation and contribute to elasticity.^{58,59}

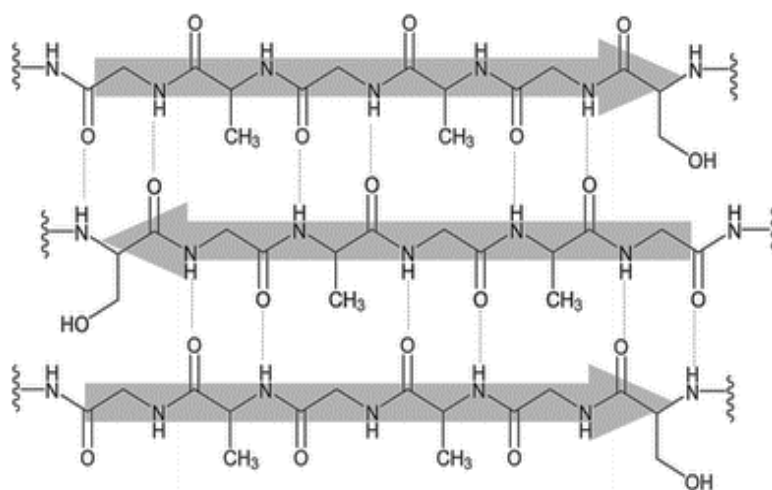


Figure 2. 3: Interaction between polypeptide chains forming a β -sheet structure of fibroin.^{29,60}

The main crystal structures of silkworm SF are silk I and silk II. The lesser structure or unstable silk III structure also exists in regenerated silk fibroin (RSF) solution at the air/water interface. Silk I is a metastable structure with a S zig-zag structure spatial conformation, belonging to the orthorhombic system. Silk II has an antiparallel β -sheet structure, belonging to the monoclinic system.^{61,62,63} The key element of this structure is the extensive hydrogen bonding between

adjacent polypeptide chains, forming large interconnected sheets. The silk I structure can be easily converted to silk II through methanol or potassium treatment.

Concerning the physical structure of silk, fibers are main of two protein microfilaments (known as brins) rooted in the glue-like glycoprotein coating,⁶⁴ see Figure 2.4. The brins are fibroin filaments composed of bundles of nanofibrils that are preferentially aligned with the long axis of the fiber. The microfilaments comprise a 6:6:1 complex of three different proteins: a heavy chain (H-chain) fibroin, which is hydrophobic (molar mass approx. 350 kDa), that is linked to a light chain (L-chain) fibroin, which is relatively hydrophilic (molar mass 25 kDa), that are joined together by disulfide bonds, and the third small glycoprotein, P25 protein (molar mass 30 kDa) that is linked via hydrophobic interactions.⁶⁵ The H-chain has the highly repetitive sequence of approximately 5263 amino acid residues, typically rich in glycine, alanine, and serine, which are known to form anisotropic β -sheet rich nanocrystals.⁶⁶ The L-chain polypeptide has about 262 amino acids residues, dominated by leucine, isoleucine, valine, and acidic amino acids. The P25 is believed for taking a part in keeping decency of the structure. The fibroin organic composition, solubility and structural organization enable crosslinking, copolymerization, and combinations with other polymers, which together convey different properties to sericin, e.g., antioxidizing, moisturizing, healing, antibacterial, antimicrobial, protection against ultraviolet radiation, and antitumor.⁴⁹

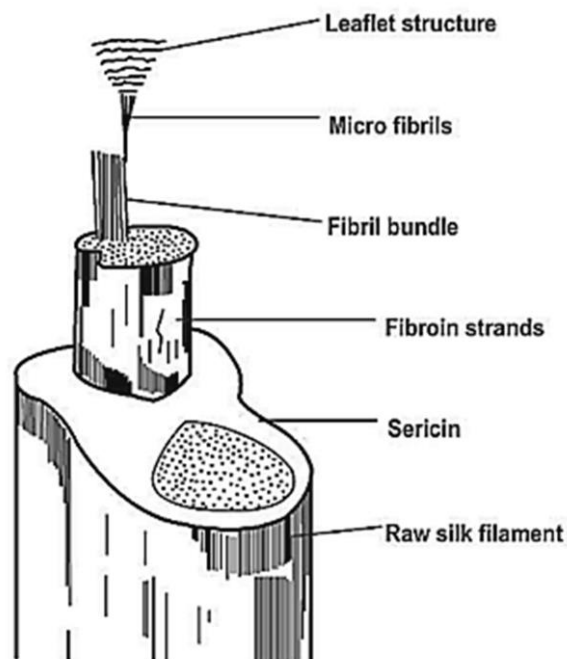


Figure 2. 4: Physical structure of silk.⁶⁷

2.2.4. Physical properties of silk

The physical properties of silk are due to the hydrophobic nature of the protein, extensive hydrogen bonding, and significant crystallinity.⁶⁸ Silk is insoluble in most solvents, including water and diluted alkaline solutions, but it is soluble in formic acid (FA) and trifluoroacetic acid (TFA). Silk is an attractive renewable fibrous biopolymer with outstanding biocompatibility properties. These properties strongly endorse its application to various fields, such as alternatives for the anterior cruciate ligaments, bioactive dressing and scaffolds for connective tissue engineering.⁶⁹ Recently, many researches have been investigating SF as one of the promising sources of biotechnology and biomedical materials due to its unique properties, including biodegradability, good biocompatibility, good oxygen and water vapor permeability, and minimal inflammatory reaction.⁷⁰ Because of these properties, SF is an applicable material not only in the field of textile but also in biomedical applications.

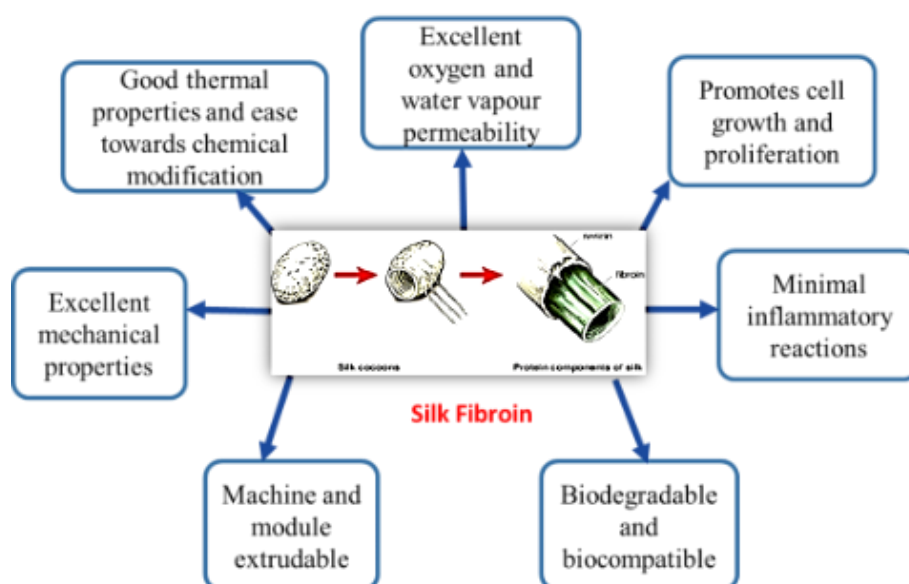


Figure 2. 5: Properties of Silk Fibroin. Adapted from reference ²⁹

2.3. Cellulose

2.3.1. Sources, extraction and application of cellulose

CE was discovered in 1838 by the French chemist Anselme Payen.¹ CE known as most extensive biopolymer on its creation;⁷¹ mainly derived on large number of CE-obtaining sources such as plants, animals including bacteria.⁷² Also known as the main structural component that confers strength and stability to plant cell walls. It is arranged into microfibrils in the cell wall,

interrupted by hemicellulose and surrounded by a lignin matrix.⁷³ There are many existing in plentiful quantities of cellulose: cotton, wood, bamboo, flax, hemp, sisal, and jute.

To extract cellulose involves three steps to isolate alpha-cellulose (Which is defined as the purified, not soluble form of cellulose manufactured from cotton or wood pulp). Followed by rinsing step-by-step. The rinsing process involves treatment in a Soxhlet system with toluene and ethanol to remove waxes, fats, oils and other compounds soluble in organic solvents. Holocellulose is a water-insoluble carbohydrates fraction of wood materials. The separation of holocellulose involves bleaching with a mixture of sodium chlorite and acetic acid to remove lignins. The final step is the isolation of α -cellulose.¹⁰

CE has wide application, for example, in paper, cotton, lubricants, fillers, adhesives and also in the form of fibers, because of its very large quantity, affordability and properties.⁷⁴ Up to early 1900s, CE (and other renewable biomaterials) was the main source of fuel, chemicals and material production. It does not dissolve in water organic solvents. Its poor solubility is attributed primarily the strong intramolecular and intermolecular hydrogen bonding between the individual chains.⁷⁵ Regardless of its poor solubility, CE can operate in many uses, including composites, netting, upholstery, coatings, packaging, paper, etc. the chemical modification of CE is performed to improve its processability and to produce CE derivatives that can be tailored for specific industrial applications.

2.3.2. Molecular structure of cellulose

The macromolecular nature of CE was finally recognized and accepted in the 1920s by Haworth.^{76,77} CE is a nonbranched polysaccharide, meaning that the compound is linear. It is a chemically bound chain of hydroglucose units in a glucan chain attached together by $\beta(1-4)$ linkages, forming a crystalline structure that can be readily broken down into monomeric sugars. The repeat units of cellulose are called cellobiose. Each glucose unit is oriented 180

degrees to its neighbors. Obtaining carbon (44.44%), hydrogen (6.17%) and oxygen (49.39%).⁷⁸

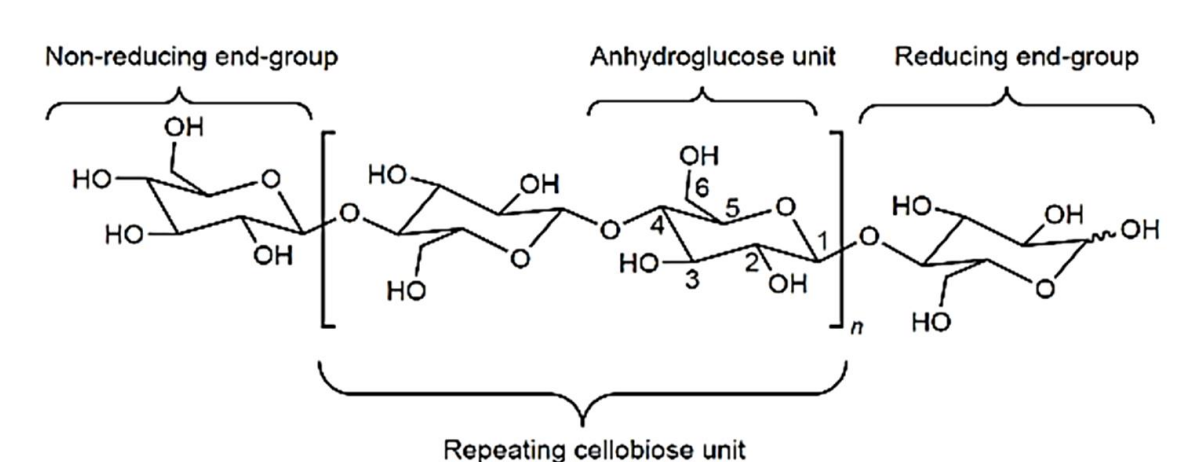


Figure 2. 6: Representation of a cellulose chain showing the anhydroglucose unit in the chair conformation along with atom numbering, the glycosidic link, and both reducing and non-reducing ends of the polymer.⁷⁹

The chemical formula for CE is $(C_6H_{10}O_5)_n$, where n is the degree of polymerization (DP), which denotes the number of glucose groups (monomers), ranging from hundreds to thousands or even tens of thousands.⁸⁰ The terminal groups at the either end of the CE molecule are quite different in nature from each other. The C-1 OH at the end of the molecule is an aldehyde group with reducing activity. The aldehyde groups form a pyranose ring through an intramolecular hemiacetal form.⁸¹⁻⁸³ Then on the other end chain, C-4 OH is an alcohol-borne OH constituent; this is called the nonreducing end. The ionic hydroxyl groups do not only play a role in the typical reactions of primary and secondary alcohols that are carried out on CE, but also facilitate intermolecular hydrogen bonding with other polymers, leading to good miscibility, new functions and properties. CE is insoluble in common organic solvents as well as in water. This

is because the hydroxyl groups are responsible for the extensive hydrogen bonding network forms: intra and intermolecular hydrogen bonding,^{82,83} see Figure 2.8.

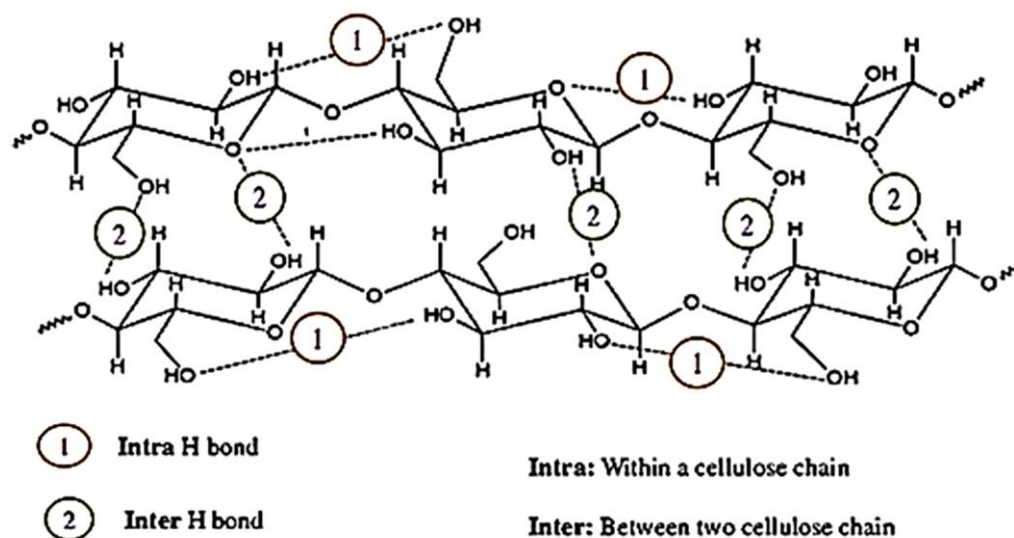


Figure 2. 7: Intramolecular hydrogen bonding in cellulose molecules.⁸⁴

The CE molecular chains are biosynthesized by enzymes, deposited in continuous fashion and aggregated to form microfibrils through intra and intermolecular hydrogen bonding. These microfibrils have crystalline and amorphous regions, the crystalline regions are impermeable to water, while the alkaline degradation takes place in the amorphous regions of CE. The microfibrils further aggregate on the macroscale to form fibers; the natural fibers themselves act as composite materials, assembling in a mainly lignin matrix.⁸⁴

2.3.3. Properties of cellulose

CE is a distinctive polymeric product; it holds favorable characteristics, like fine cross section, the capacity to absorb moisture, affordability, good biocompatibility and low density, yet good mechanical properties.⁸⁵ It is a strong, fibrous, water-insoluble material that act important character in keeping the structure of the plant cell. It is a nontoxic, biodegradable solid homopolymers. In its pure state; cellulose is white in color, with a molecular weight of 1621,406 kg/mol, and density of 1.52–1.54 g/cm³ (at 20 °C). Cellulose has high tensile and compressive strength. It is also thermally stable; it shows thermal softening at 231–253 °C. The application of cellulose in the textile field is increasing because of its superior moisture absorbing property and biodegradability. Cellulose has also recently been an icon because of its suitable

applications in the generation of biofuels. However, cellulose has shown versatility in numerous applications. Furthermore, it can be chemically adjusted to produce cellulose derivatives.⁸⁶

2.3.4. Chemical modification of cellulose

As mentioned earlier, cellulose got randomly intrinsic challenges, such as not easily dissolve in most solvents, poor crease resistance, poor dimensional stability, lack of thermoplasticity, high hydrophilicity and lack of antimicrobial properties.⁸⁶ CE can however be chemically modified to yield derivatives that have wider applications. CE contains three free hydroxyl groups per anhydroglucose part (AGU); these hydroxyl groups can be completely or partially converted to ether or ester linkages. The conversion of these hydroxyl groups helps to reduce the regularity of the chain and improves solubility in organic solvents. When cellulose is chemically modified, the extent of modification is defined as the degree of substitution (DS), which is the number of positions modified per monosaccharide. Table 2.4 summarizes cellulose derivatives and their application sectors.⁸⁷

Table 2.4 : Cellulose derivatives and applications.^{88–90}

Cellulose derivative	Degree of substitution (DS)	Solubility	Functional group	Applications
Cellulose acetate	0.6–0.9 1.2–1.8 2.2–2.7 2.8–3.0	DCM/ethanol 2-methoxy-ethanol Acetone/water	–OAc	Textiles, plastic films
Cellulose nitrate	1.8–2.0 2.0–2.3 2.2–2.8	Ethanol Methanol/acetone	–NO ₂	Membranes and explosives
Cellulose xanthane	0.5–0.6	NaOH/water	–C(S)SNa	Textiles
Carboxymethyl cellulose	0.5–2.9	Water Formic acid	–CH ₂ COONa	Coatings, paints, adhesives and pharmaceuticals
Methyl cellulose	0.4–0.6 1.3–2.6 2.5–3.0	4% aq NaOH Cold water Organic solvents	–CH ₃	Films, textiles and in food and tobacco industries

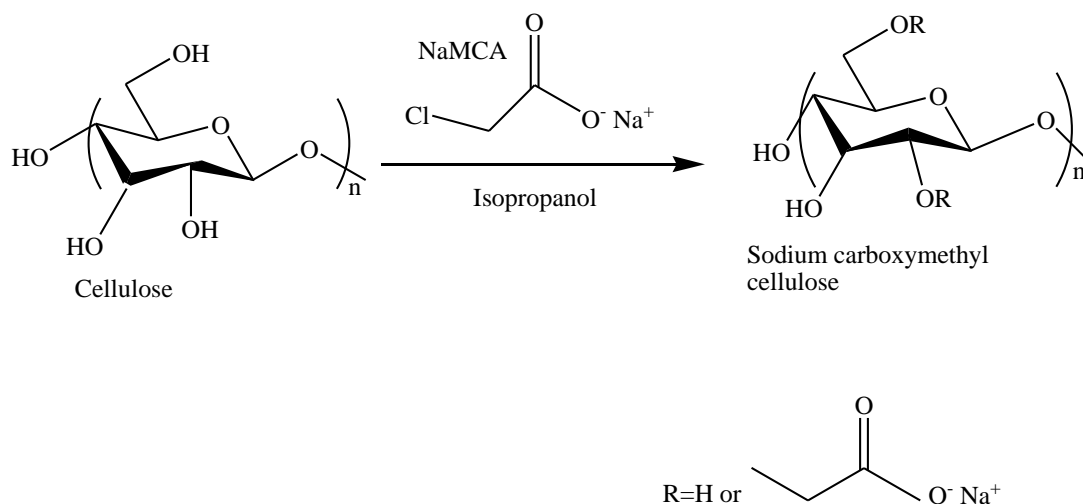
Ethyl cellulose	0.5–0.7	4% aq NaOH	$-\text{CH}_2\text{CH}_3$	Pharmaceutical industry
	0.8–1.7	Cold water		
	2.3–2.6	Organic solvents		
Hydroxyethyl cellulose	0.1–0.5	4% aq NaOH	$-\text{CH}_2\text{CH}_2\text{OH}$	Paints, coatings, films and cosmetics
	0.6–1.5	Water		

2.3.5. Derivative of cellulose used in this study: Carboxymethyl cellulose

Carboxymethyl cellulose (CMC) is a polymer derived from natural CE. It is one of the most important CE derivatives, it is of great industrial importance and also in our daily life.⁹¹ CMC is a linear, long chain, normally anionic polysaccharide that is water soluble;⁷⁶ it is often applied as its sodium salt, sodium CMC. Manufacture with an alkali-catalyzed reaction of CE with chloroacetic acid, see Scheme 2.1. Hydroxyl groups on the 2-glucopyranose residue of cellulose are substituted with carboxymethyl groups ($-\text{CH}_2-\text{COOH}$); the DS is determined as the average number of sodium carboxymethyl groups substituted per AGU, which have extremely influence on the properties and applications of CMC.⁸⁶ The chain length of the cellulose backbone and DS determines the solubility, viscosity and gel strength of CMC. The theoretical maximum DS of CMC is 3 (i.e., all OH groups per AGU have been replaced). In this study, the DS was 0.6–0.95 derivatives per monomer unit. For food uses, the DS levels of CMC are ranging between 0.2–1.5.^{82,83}

Several techniques have been described for the synthesis of CMC, involving homogeneous carboxymethylation, a fluidized bed technique, sheet carboxymethylation, a rotating drum technique, and a solventless method using a double screw press and a paddle reactor.⁸⁴ The development of CMC requires two steps: mercerization (an alkali treatment of cellulose fibers which is dependent on the type and concentration of the solution) and etherification by a slurry process. In the slurry method, CE is suspended in a mixture of NaOH/water/alcohol at 20–30 °C with an excess of alcohol (ethanol or propanol), ensuring a good mixing efficiency. The liquid phase (water/alcohol mixture), which acts as the solvating agent in the mercerization processes, dissolves the NaOH and distributes it evenly to the hydroxyl groups, forming alkali cellulose. The aqueous NaOH penetrates the crystalline structure of cellulose, and then solvates

its hydroxyl groups by making them available for the etherification reaction by cleaving the hydrogen bonds.^{92,93}



Scheme 2. 1: Etherification of CE to form carboxymethyl cellulose.

2.3.5.1. Properties and uses of CMC

The various properties of CMC depend upon three factors: molecular weight of the polymer, average number of carboxyl content per AGU and the distribution of carboxyl substituents along the polymer chains. CMC is used in drug formulations, as binder for drugs, as film coating agent for drugs, as an ointment base, and as lubricant in nonvolatile eye drops (artificial tears),⁸⁸ see Figure 2.9.

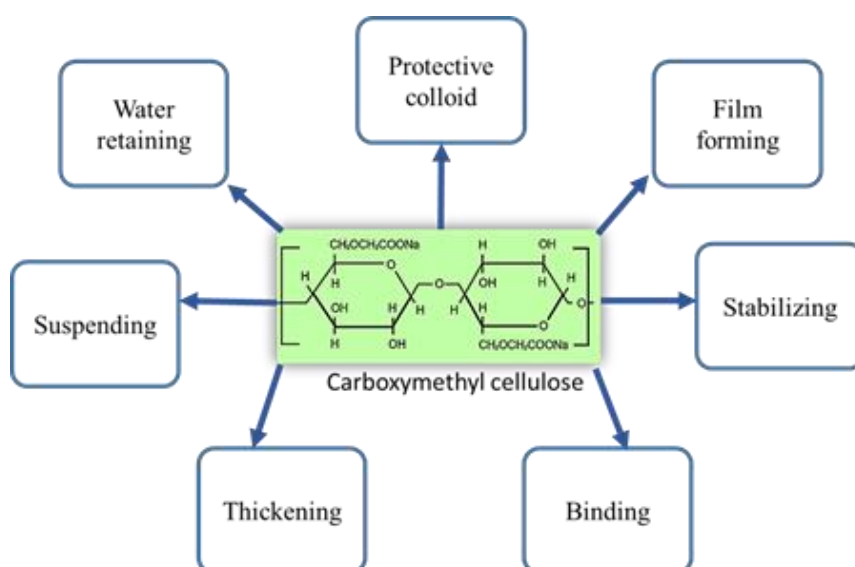


Figure 2. 8: Functions and Properties of CMC. Adapted from⁹⁴

2.4. Nanofiber membranes of SF and CE

2.4.1. Fabrication of the nanofiber blends

There are diverse methods that can be used to fabricate blends, like ES, self-assembly, phase separation, solution casting and drawing, etc. Here, various techniques for the fabrication of composites are briefly discussed; ES is addressed in more detail.

2.4.1.1. Solution casting

The senior technology in plastic films production is the ongoing solvent cast process, established more than hundred years ago, driven by the needs of an emerging photographic industry. Solvent casting is commonly employed for forming polymer films as illustrated on Figure 2.10. A capacity of polymers in order to create films is vital for diverse uses like packaging, transdermal drug delivery and wound healing.⁹⁵ Films can be applied as coatings. The key characteristic of films for any applications is uniformity. For obtaining stability in film development, either from pure polymers or blended polymers, fixed processes are taken. Methods for film formation include self-absorption of monolayers, spin coating, thermal spraying, solvent casting, the floating technique and the Langmuir–Blodgett film technique. Among these methods, prevalent methods are solvent casting and spin coating.⁹⁶



Figure 2. 9: Schematic illustration of solution casting.⁹⁷

2.4.1.2. Self-assembly

Self-assembly, the spontaneous organization of components into larger, well defined, and stable aggregates.⁹⁸ The self-assembly process is driven by an unfavorable mixing enthalpy coupled with a small mixing entropy.⁹⁹ It is based on interaction between the hydrophilic and hydrophobic domain of amphiphilic peptides, which further assemble into nanofibrous structure through weak noncovalent bonding such as hydrogen, van der Waals interaction, and ionic interaction, etc. Besides forming peptides, this method can be used to fabricate nanofibers.¹⁰⁰

Some advantages and disadvantages of various scaffold fabrication techniques are summarized in Table 2.5.

Table 2.5: Advantages and disadvantages of various scaffold fabrication techniques.

Process	Production scale	Advantages	Disadvantages	Ref
Solvent casting/ particulate leaching	Laboratory	Control over porosity, pore size and crystallinity	Limited mechanical properties, residual solvents and porogen material	95,96
Phase separation	Laboratory	No decrease in the activity of the molecule	Difficult to control scaffold morphology precisely	26
Self-assembly	Laboratory	Control over organization of biomolecule, fiber diameter, porosity	Complicated and elaborated process, high cost of synthesis biomaterial	101
Fiber bonding	Laboratory	High surface to volume ratio, high porosity	Poor mechanical properties, limited application to other polymers	26
Electrospinning	Laboratory and industrial	Control over porosity, pore size and fiber diameter	Limited mechanical properties, jet instability	26,29,102
Melting molding	Laboratory	Independent control over porosity and pore size	Requires high temperatures for non-amorphous polymers	103

2.4.1.3. Electrospinning

ES is a rather old technique. It was initially created by Formhals in 1934 and has been upgraded by different groups of researchers over the years.¹⁰⁴ In the 1960s, jet forming processes were studied fundamentally by Taylor. He studied the cone shape of the polymer droplet at the needle

tip when an electric field was applied, leading to the name ‘the Taylor cone’ in subsequent literature. The electrohydrodynamical phenomenon called ES launched polymer nanofibers into broader realms of nanotechnology and materials science during the decades starting in 1990 and 2000.¹⁰⁵ A brief background of ES will be presented, followed by a description of some factors influencing ES process and nature of resulting nanofibers in subsequent sections.

ES is an efficient technique to make fibers with diameters fluctuating from a few nanometers to a few micrometers. The ES process is relatively simple, suitable, constructive and extensively applied for the production of nanofibrous membranes.¹⁰⁴ Development of fibers through ES depends on uniaxial stretching of a viscoelastic jet manufactured from a polymer solution. Figure 2.11 is a schematic diagram of the basic system used for single needle ES. Three major substances are examined in the ES setup: a high voltage power supply; a spinneret, which is a needle; and then the collector, which is a petri dish covered with aluminium foil.

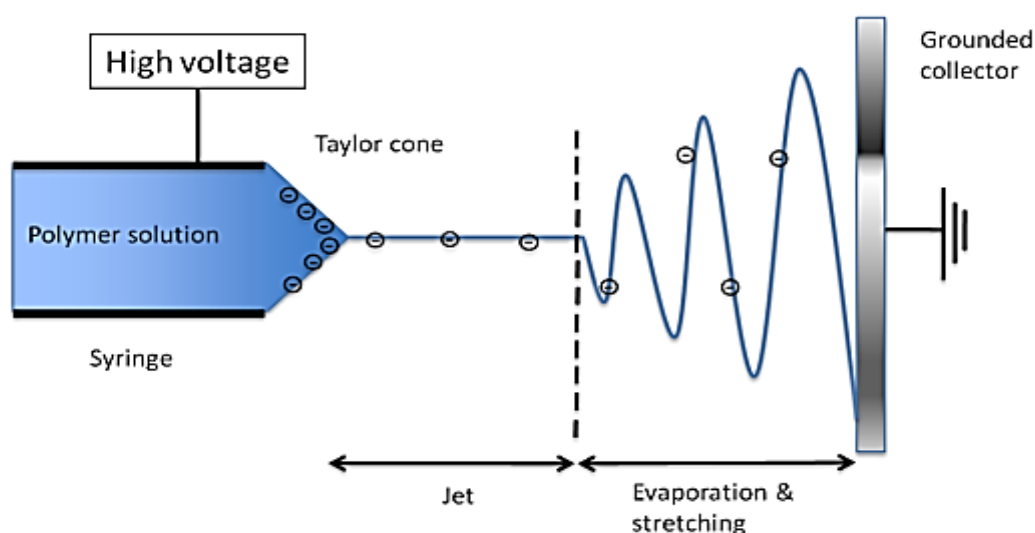


Figure 2. 10: Schematic diagram of ES setup.¹⁰⁶

During the process of ES, the polymer solution is driven from the syringe into the needle by the syringe pump at a constant and manageable rate. When the electrical field is applied, a drop of the polymer solution is presented from the needle tip.¹⁰⁷ As the strength of the electrical field is increased, a pendent droplet at the tip of the needle will become highly electrified, dramatically altering the droplet shape to form a Taylor cone. Then charge repulsion surpasses the surface tension and a jet of solution is ejected from the Taylor cone towards the ground collector acting as the counter electrode. During this process the solvent evaporates, leaving behind polymer fibers in the form of nonwoven mats.¹⁰⁸ The inside and outside charge forces

causes the flogging motion, which permit the polymer chains within the solution to stretch and slide past each other, resulting in the fabrication of fibers with diameters small enough to be called nanofibers. Electrospinning process has been attracting many scientists over the past decades, because ES has ability to continually fabricate fibers in the submicron range, which is not an easy thing to obtain when using standard mechanical fiber spinning techniques. And because of its versatility in spinning a wide variety of polymeric fibers.

Electrospinning parameters are summarized in Table 2.6. There are many factors that affect the ES process. These factors are grouped as process, solution and environmental ES parameters. All these parameters directly affect the generation of smooth and bead-free electrospun fibers. Therefore, to better understand ES techniques and ES development of polymeric nanofibers, it is important to thoroughly understand the effect of these governing parameters.¹⁰⁴

Table 2.6: Parameters affecting electrospinning/fiber morphology

Ambient parameters	Effect on fiber morphology	Ref
Relative humidity	Humidity causes changes in the nanofiber diameter by controlling the solidification process of the charged jet.	109,110
Temperature	Temperature influences the average diameter of the nanofibers. High temperatures increase the rate of evaporation of the solvent and decreases the viscosity of the solution, which leads to a decrease in the mean fiber diameter.	111
Solution parameters	Effect on fiber morphology	Ref
Polymer molecular weight and concentration	This determines the number of entanglements in the solvent. At very low concentrations, electrospinning occurs and beaded nanofibers are formed.	112,113
Solution viscosity	Viscosity is proportional to the polymer concentration. An increase in viscosity increases the fiber diameter.	29,114

	High viscosity hinders pumping of the polymer solution through the syringe needle.	
Solvent volatility	Solvents with a high boiling point may not evaporate completely before reaching the collector, thereby resulting in ribbon-like flat nanofiber morphology.	115,116
Solution conductivity	An increase in conductivity of the solution allows for more charges to be carried by the electrospinning jet. A solution with higher conductivity leads to electrospun nanofibers with smaller diameters.	116,117
Process parameters	Effect on fiber morphology	Ref
Applied voltage	The surface charge on the jet is controlled by the applied voltage. Increase in voltage leads to a decrease in nanofiber diameter. High voltage, beyond the critical value, decreases the Taylor cone and resulting in the formation of beads.	111
Flow rate	The flow rate through the capillary influences the nanofiber diameter, porosity, and geometry of the electrospun nanofibers. Low flow rate results in smooth continuous nanofibers	111,118
Tip to collector distance	Short distances result in the formation of beads. Increasing the distance results in a decrease of average fiber diameter.	29,119

2.4.2. Properties of nanofiber membranes

The ES process is the prevalently used tool for the development of nonwoven nanofibrous.²⁶ Park *et al.* reported the successful production of ES nanofibers of SF/CS blends that were prepared in formic acid, which demonstrated significant conformational changes of the as-spun SF/CS blends nanofibers with improved β -sheet content.¹²⁰ Morsano et al studied the blend nanofibers of SF and CE, which were composed of 70% CE and 30% SF developed through wet spinning of the two polymers in DMAc/LiCl, using ethanol as the coagulant. From the

study, the materials demonstrated good mechanical properties, modulus and breaking strength in comparison to the pure CE fibers obtained using the same operation conditions.⁷⁴

Shang et al. reported the work that has been done by Freddi *et al.*¹²¹ about the development of the SF/CE blend film using cuoxam solution. However, the disadvantage of this procedure included the environmental apprehensions, like unwanted metal complex waste solution and the difficulty to remove Cu from the regenerated materials.¹²² Biomaterials of CE and its derivatives are operated for many uses like carrier for immobilization of enzymes, hemodialysis and drug releasing scaffold.²⁶ Zhou *et al.* studied the ES of SF/cellulose acetate (CA) blend nanofiber and demonstrated the applications of the composites to remove heavy metal ions from wastewater.¹²³ Table 2.7, summarizing the uses of various SF and other polymer blend based scaffold.

Table 2.7: Various SF–biopolymer blend based scaffolds and their applications

SI. No.	Polymer–polymer blend	Morphological form	Application	Ref
1	Silk fibroin/ Gelatin	Nanofiber, cable	Vascular and ligament tissue engineering	^{124,109}
2	Silk fibroin/ Chitosan	Nanofiber, porous	Bone and cartilage tissue engineering	²⁶
3	Silk fibroin/ Cellulose acetate	Nanofiber	Heavy metal ion adsorption	¹²²
4	Silk fibroin/ Carboxymethyl cellulose	Film	Biotechnological application	¹²⁵
5	Silk fibroin/ Pectin	Hydrogel	Various biomedical applications	¹²³
6	Silk fibroin/ PEO	Nanofiber	Cell culture	¹²⁶
7	Silk fibroin/ PLA	Nanofiber	Drug delivery	²⁹

2.4.3. Applications of the nanofiber membranes

Blended films of SF and CMC have been prepared by Kundu *et al.* using the solution casting method to obtain biomaterials that can provide good performance for biotechnological applications, concerning both mechanical and biological features.¹²⁵ The chemical interactions, morphologies, thermal, mechanical properties, and biocompatibility of the blended films were explored. Based on the results, the blended films were found to be a potential substrate for supporting cell adhesion and proliferation.

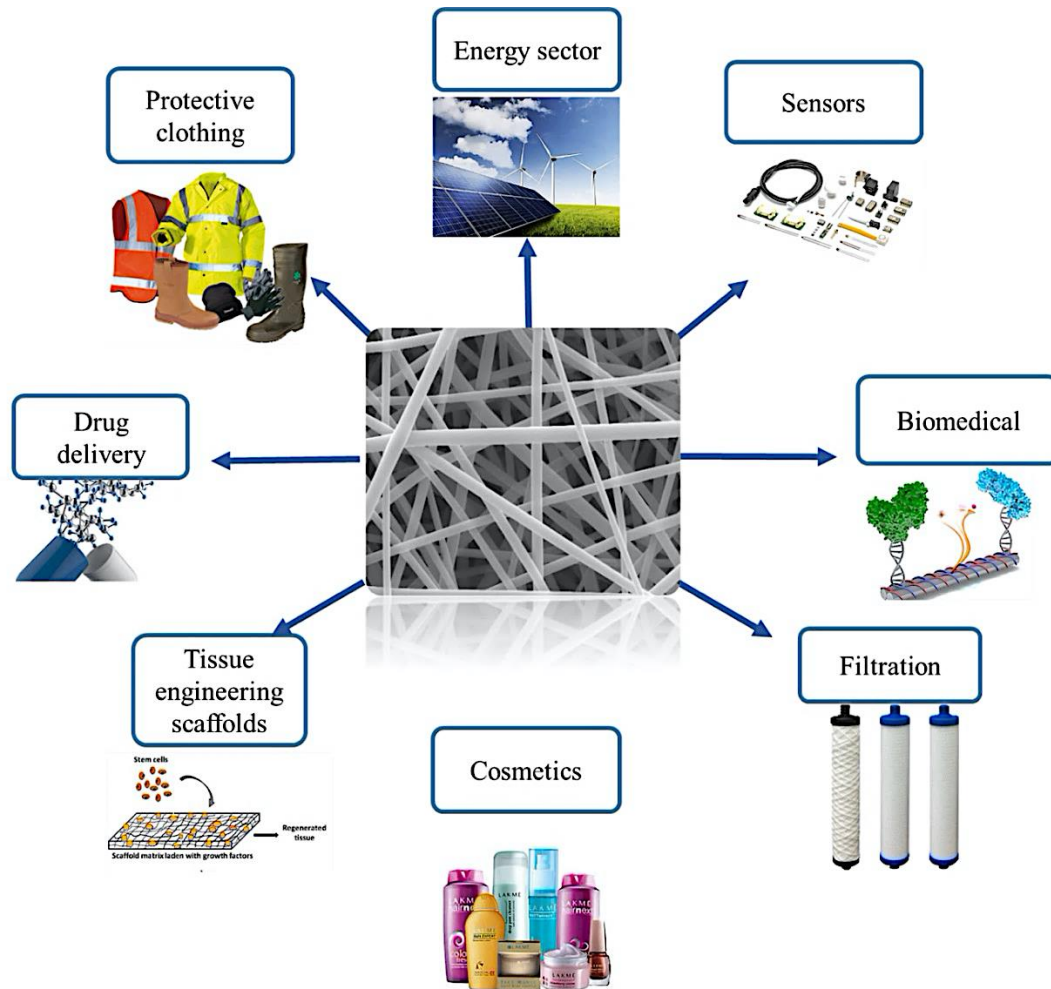


Figure 2. 11: Potential applications of nanofibers.¹²⁷

Bhisham has reported the electrospun scaffolds of SF and CMC for bone tissue engineering application. The scaffolds showed enough strength to support many types of bone tissue regeneration. They also exhibited higher water uptake capacity, hydrophilicity, and bioactivity.²⁶ The characteristics and performances of the electrospun membranes prepared with SF and CA were investigated for heavy ions metal adsorption by Zhou *et al.* who observed that the adsorption of heavy metals increased in the blends compared to pure polymers.¹²³

2.5. References

- (1) Kulkarni Vishakha, S.; Butte Kishor, D.; Rathod Sudha, S. Natural Polymers – A Comprehensive Review. *Int. J. Res. Pharm. Biomed. Sci.* **2017**, *3* (4).
- (2) Gacitua, W.; Ballerini, A.; Zhang, J. Polymer Nanocomposites: Synthetic and Natural Fillers a Review. *Environ. Sci. Technol.* **2005**, *7* (3), 159–178.
- (3) Aravamudhan, A. *Natural Polymers: Polysaccharides and Their Derivatives for Biomedical Applications*; 2014.
- (4) Bangar, B.; Shinde, N.; Deshmukh, S.; Kale, B. Natural Polymers in Drug Delivery Development. *Research J. Pharm. Dos. Forms Technol.* **2014**, *6* (1), 54–57.
- (5) Sperling, L. H. *Introduction to Physical Polymer Science*; **2006**; Vol. 78.
- (6) Weinberger, C. B. Instructional Module on Synthetic Fiber Manufacturing. *Dept. Chem. Eng. Drexel University* **1996**, 43.
- (7) Carpenter, A. W.; De Lannoy, C. F.; Wiesner, M. R. Cellulose Nanomaterials in Water Treatment Technologies. *Environ. Sci. Technol.* **2015**, *49* (9), 5277–5287.
- (8) Kaushik, K.; Sharma, R. B.; Agarwal, S.; Pradesh, H. Review Article Natural Polymers and Their Applications. *Int. J. Pharm. Sci. Rev. Res.* **2016**, *37* (05), 30–36.
- (9) Finkenstadt, V. L. Natural Polysaccharides as Electroactive Polymers. *Appl. Microbiol. Biotechnol.* **2005**, *67* (6), 735–745.
- (10) Olatunji, O.; Richard, O. *Processing and Characterization of Natural Polymers*; **2016**.
- (11) Prabakaran, M.; Mano, J. F. Stimuli-Responsive Hydrogels Based on Polysaccharides Incorporated with Thermo-Responsive Polymers as Novel Biomaterials. *Macromol. Biosci.* **2006**, *6* (12), 991–1008.
- (12) Chen, F. M. C. Compared to Synthetic Polymers , Proteins Are Awesome. *J. Chinese Chem. Soc.* **2004**, *51*, 1051–1057.
- (13) Murata, H.; Carmali, S.; Baker, S. L.; Matyjaszewski, K.; Russell, A. J. Reversible Immobilization Supports. *Nat. Commun.* **2018**, No. 9, 845.
- (14) I, R. I. M. Physiological Levels and Properties of Polynucleotide Phosphorylase of *Rhizobium Meliloti*. *J. Genet. Microbiol.* **1977**, No. 102, 403–411.

- (15) Heppel, L. A.; Singer, M. F.; Hilmoie, R. J. The mechanism of action of polynucleotide phosphorylase. *Ann. N. Y. Acad. Sci.* **1959**, 4 (81), 44-635.
- (16) Vollrath, F.; Porter, D. Silks as Ancient Models for Modern Polymers. *Polymer (Guildf)*. **2009**, 50 (24), 5623–5632.
- (17) Sanjay, M. R.; Arpitha, G. R.; Naik, L. L.; Gopalakrishna, K.; Yogesha, B. Applications of Natural Fibers and Its Composites: An Overview. *Nat. Resour.* **2016**, 07 (03), 108–114.
- (18) Vivekanandhan, S.; Christensen, L.; Misra, M.; Kumar Mohanty, A. Green Process for Impregnation of Silver Nanoparticles into Microcrystalline Cellulose and Their Antimicrobial Bionanocomposite Films. *J. Biomater. Nanobiotechnol.* **2012**, 03 (03), 371–376.
- (19) Wang, J.; Vermerris, W. Antimicrobial Nanomaterials Derived from Natural Products-a Review. *Materials (Basel)*. **2016**, 9 (4), 1–19.
- (20) Lim, Y.; Lee, W. K.; Leow, A. T. C.; Namasivayam, P.; Abdullah, J. O.; Ho, C. L. Sulfated Galactans from Red Seaweeds and Their Potential Applications Sulfated Galactans From Red Seaweeds and Their Potential Applications. *PJSRR*. **2018**, 3(2), 1-17.
- (21) Ancheeva, E.; El-neketi, M.; Song, W.; Lin, W.; Daletos, G.; Ebrahim, W.; Proksch, P. Structurally Unprecedented Metabolites from Marine Sponges. *Curr. Org. Chem.* **2017**, 21 (January 2017), 426–449.
- (22) Younes, I.; Rinaudo, M. Chitin and Chitosan Preparation from Marine Sources. Structure, Properties and Applications. *Mar. Drugs* **2015**, 13 (3), 1133–1174.
- (23) Isa, M. T.; Ameh, A. O.; Gabriel, J. O.; Adama, K. K. Extraction and Characterization of Chitin from Nigerian Sources. *Leonardo Electron. J. Pract. Technol.* **2012**, 11 (21), 73–81.
- (24) Pichyangkura, R. Application of Chitin-Chitosan from Marine by-Products in Thailand. 70–75.
- (25) Khajavi, R.; Abbasipour, M. Sharif University of Technology Electrospinning as a Versatile Method for Fabricating Coreshell , Hollow and Porous Nanofibers. *Sci. Iran.* **2012**, 19 (6), 2029–2034.

- (26) Singh, B. N. Development of Novel Silk Fibroin / Carboxymethyl Cellulose Based Electrospun Nanofibrous Scaffolds for Bone Tissue Engineering Application. **2017**, *National Institute of Technology Rouker*, (PhD).
- (27) Sirichaisit, J.; Brookes, V. L.; Young, R. J.; Vollrath, F. Analysis of Structure/Property Relationships in Silkworm (*Bombyx Mori*) and Spider Dragline (*Nephila Edulis*) Silks Using Raman Spectroscopy. *Biomacromolecules* **2003**, *4* (2), 387–394.
- (28) Kronenberger, K.; Vollrath, F.; Moore, P. G.; Halcrow, K. Spinning A Marine Silk for the Purpose of Tube-Building. *J. Crustac. Biol.* **2012**, *32* (2), 191–202.
- (29) Mhuka, V. Characterization of Silk Protein from African Wild Silkworm Cocoons and Application of Fibroin Matrices as Biomaterials. **2014**, *PhD* (University of South Africa), 19.
- (30) Wang, H.; Mao, N.; Hu, X.; Shao, H.; Jin, X. The Properties of Native Silk Fibroin (SF) Solution/Gel from *Bombyx Mori* Silkworms during the Full Fifth Instar Larval Stage. *J. Wuhan Univ. Technol. Mater. Sci. Ed.* **2011**, *26* (2), 262–268.
- (31) Raghu, A.; Somashekar, R.; Ananthamurthy, S. Microrheological Studies of Regenerated Silk Fibroin Solution by Video Microscopy. *J. Polym. Sci. Part B Polym. Phys.* **2007**, *45* (18), 2555–2562.
- (32) Hardy, J. G.; Römer, L. M.; Scheibel, T. R. Polymeric Materials Based on Silk Proteins. *Polymer (Guildf)*. **2008**, *49* (20), 4309–4327.
- (33) Jinnai, H.; Spontak, R. J.; Nishi, T. Transmission Electron Microtomography and Polymer Nanostructures. *Macromolecules*. **2010**, *43* (4), 1675–1688.
- (34) Kômoto, N.; Kuwabara, N.; Yukuhiro, K. Absence of Hybrids between the Domesticated Silkworm, *Bombyx Mori*, and the Wild Mulberry Silkworm, *B. Mandarina*, in Natural Populations around Sericulture Farms. *J. Insect Biotechnol. Sericology*. **2016**, *85* (3), 67–71.
- (35) Kômoto, N. Behavior of the Larvae of Wild Mulberry Silkworm *Bombyx Mandarina*, Domesticated Silkworm *B. Mori* and Their Hybrid. *J. Insect Biotechnol. Sericology*. **2017**, *86* (January), 17–20. https://doi.org/10.11416/jibs.86.1_017.
- (36) Yukuhiro, K.; Kuwabara, N.; Kômoto, N. Pheromone Dose and Set Height of Pheromone Traps for Efficient Collection of Wild Mulberry Silkworms, *Bombyx*

- Mandarina. *J. Insect Biotechnol. Sericology* **2017**, *86*, 55–57.
- (37) Lalronunga, S.; Lalrinchhana, C. Morphological and Molecular Characterization of *Theioderma Moloch* (Anura : Rhacophoridae) from Indo-Burma Biodiversity Hotspot of Northeast India Morphological and Molecular Characterization of *Theioderma Moloch* (Anura : Rhacophoridae) from Indo-Burma. *Sci. Vis.* **2017**, *17* (3), 148–159.
- (38) Akite, P.; Telford, R. J.; Waring, P.; Akol, A. M.; Vandvik, V. Temporal Patterns in Saturnidae (Silk Moth) and Sphingidae (Hawk Moth) Assemblages in Protected Forests of Central Uganda. *Ecol. Evol.* **2015**, *5* (8), 1746–1757.
- (39) Lalhmingliani, E.; Gurusubramanian, G.; Laliemsanga, H. T.; Lalrinchhana, C.; Lalronunga, S. Wild silk moths (Lepidoptera; Saturniidae) of Hmuifang community forest. *Conf. Pap.* **2014**. No. January.
- (40) Yilmaz, O. Biology of Silkworm (*Bombyx Mori*) in Turkey. *Conf. Pap.* **2015**, No. October.
- (41) Sundari, K. T. An Analysis of Silk Production in India. *Int. J. Bus. Manag.* **2015**, *3* (3), 151–161.
- (42) Rahmathulla, V. K. Management of Climatic Factors for Successful Silkworm (*Bombyx Mori* L .) Crop and Higher Silk Production : A Review. *Rev. Artic.* **2012**, *2012*.
- (43) Rahman, M. A Review on Mulberry Silk and Spider Silk Fiber, and Their Mechanical Behavior. **2015**, *MSc*.
- (44) Anjana, K. G. .; Balamurugan, T. S. .; Manivasagan, V.; Ramesh, B. N. . Phytochemical , Antioxidant and Antitumor Activity of Edible Mushroom *Pleurotus Ostreatus*. *Int. J. Adv. Res. Biol. Sci.* **2016**, *3* (9), 170–177..
- (45) Wani, A. .; Jaiswal, Y. . Health Hazards of Rearing Silkworm and Environmental Impact Assessment of Rearing Households of Kashmir, India. *Indian J. Public Heal. Res. Dev.* **2011**, *2* (2).
- (46) Zafar, I. .; Nazir, A. .; Muzafar, A. . Molecular Marker Systems with Special Reference to the Silkworm *Bombyx Mori* L. *Int. J. Bioassays* **2016**, *5* (11), 5025–5040.
- (47) Tashiro, Y.; Morimoto, T.; Matsuura, S. Studies on the Podterior Silk Gland of the Silkworm, *Bombyx Mori*. *J. Cell Biol.* **1968**, *38*, 574–588.

- (48) Copeland, C. G. Production of Synthetic Spider Silk Fibers. **2016**, No. All Graduate Theses and Dissertations, 4879.
- (49) Mondal, M.; Trivedy, K.; Kumar, S. N. The Silk Proteins, Sericin and Fibroin in Silkworm, *Bombyx Mori* Linn. A Review. *Casp. J. Environ. Sci.* **2007**, 5 (2), 63–76.
- (50) Kunz, R. I.; Brancalhão, R. M. C.; Ribeiro, L. D. F. C.; Natali, M. R. M. Silkworm Sericin: Properties and Biomedical Applications. *Biomed Res. Int.* **2016**, 2016.
- (51) Zhang, Q.; Yan, S.; Li, M. Silk Fibroin Based Porous Materials. *Materials (Basel)*. **2009**, No. 2, 2276–2295.
- (52) Padamwar, M. N.; Pawar, A. P. Silk Sericin and Its Applications : A Review. *J. Sci. Ind. Res.* **2004**, 63 (April), 323–329.
- (53) Vepari, C.; Kaplan, D. L. Silk as a Biomaterial. *Program. Polym. Sci.* **2009**, 32, 991–1007.
- (54) Cao, Y.; Wang, B. Biodegradation of Silk Biomaterials. *Int. J. Mol. Sci.* **2009**, No. 10, 1514–1524.
- (55) Liu, R.; Zhang, F.; Zuo, B.; Zhang, H. EDC-Crosslinked Electrospun Silk-Fibroin Fiber Mats. *Adv. Mater. Res.* **2011**, 175–176, 170–175.
- (56) Rangi, A.; Jajpura, L. The Biopolymer Sericin : Extraction and Applications. *J. Text. Sci. Eng.* **2015**, 5 (1), 1–5.
- (57) Jaramillo-quiceno, N.; Álvarez-lópez, C.; Restrepo-osorio, A. Structural and Thermal Properties of Silk Fibroin Films Obtained From Cocoon and Waste Silk Fibers as Raw Materials. *Procedia Eng.* **2017**, 200, 384–388.
- (58) Rousseau, M.; Pe, M. Protein Secondary Structure and Orientation in Silk as Revealed by Raman Spectromicroscopy. *Biophys. J.* **2007**, 92 (April), 2885–2895.
- (59) Koh, L. D.; Cheng, Y.; Teng, C. P.; Khin, Y. W.; Loh, X. J.; Tee, S. Y.; Low, M.; Ye, E.; Yu, H. D.; Zhang, Y. W.; et al. Structures, Mechanical Properties and Applications of Silk Fibroin Materials. *Prog. Polym. Sci.* **2015**, 46, 86–110.
- (60) Murphy, A. R.; Kaplan, D. L. Biomedical Applications of Chemically-Modified Silk Fibroin. *J. Mater. Chem.* **2009**, 19, 6443–6450.
- (61) Vollrath, F.; Porter, D. Spider Silk as Archetypal Protein Elastomer. *Soft Matter* **2006**, 2

- (5), 377.
- (62) Liu, L.; Yang, X.; Yu, H.; Ma, C.; Yao, J. Biomimicking the Structure of Silk Fibers via Cellulose Nanocrystal as β -Sheet Crystallite. *RSC Adv.* **2014**, *4* (27), 14304–14313.
- (63) Cranford, S. W.; Tarakanova, A.; Pugno, N. M.; Buehler, M. J. Nonlinear Material Behaviour of Spider Silk Yields Robust Webs. *Nature* **2012**, *482* (7383), 72–76.
- (64) Hashimoto, T.; Taniguchi, Y.; Kameda, T.; Tamada, Y.; Kurosu, H. Changes in the Properties and Protein Structure of Silk Fibroin Molecules in Autoclaved Fabrics. *Polym. Degrad. Stab.* **2015**, *112*, 20–26.
- (65) Kundu, B.; Rajkhowa, R.; Kundu, S. C.; Wang, X. Silk Fibroin Biomaterials for Tissue Regenerations. *Adv. Drug Deliv. Rev.* **2013**, *65* (4), 457–470.
- (66) Mottaghitalab, F.; Farokhi, M.; Shokrgozar, M. A.; Atyabi, F.; Hosseinkhani, H. Silk Fibroin Nanoparticle as a Novel Drug Delivery System. *J. Control. Release* **2015**, *206*, 161–176.
- (67) Sonthisombat, A.; Ph, D.; Speakman, P. T.; Ph, D. Silk : Queen of Fibres - The Concise Story. **2003**, *1* (4), 1–28.
- (68) Chen, F.; Porter, D.; Vollrath, F. Structure and Physical Properties of Silkworm Cocoons. *J. R. Soc.* **2012**, *9* (74), 2299–2308.
- (69) Kweon, H.; Yeo, J.; Lee, K.; Lee, H. C.; Na, H. S.; Won, Y. H.; Cho, C. S. Semi-Interpenetrating Polymer Networks Composed of Silk Fibroin and Poly(Ethylene Glycol) for Wound Dressing. *Biomed. Mater.* **2008**, *3* (3), 034115. <https://doi.org/10.1088/1748-6041/3/3/034115>.
- (70) Yang, G.; Zhang, L.; Feng, H. Role of Polyethylene Glycol in Formation and Structure of Regenerated Cellulose Microporous Membrane. *J. Memb. Sci.* **1999**, *161* (1–2), 31–40. [https://doi.org/10.1016/S0376-7388\(99\)00095-2](https://doi.org/10.1016/S0376-7388(99)00095-2).
- (71) Maheswari, C. U.; Reddy, K. O.; Dhlamini, M. S.; Mothudi, B. M.; Kommula, V. P.; Rajulu, A. V. Extraction and Structural Characterization of Cellulose from Milkweed Floss. *Sep. Sci. Technol.* **2017**, *52* (17), 2677–2683. <https://doi.org/10.1080/01496395.2017.1374406>.
- (72) Mokhena, T. C.; Jacobs, V.; Luyt, A. S. A Review on Electrospun Bio-Based Polymers for Water Treatment. *Express Polym. Lett.* **2015**, *9* (10), 839–880.

<https://doi.org/10.3144/expresspolymlett.2015.79>.

- (73) Penjumras, P.; Abdul, R. B.; Talib, R. A.; Abdan, K. Extraction and Characterization of Cellulose from Durian Rind. *Agric. Agric. Sci. Procedia* **2014**, *2*, 237–243. <https://doi.org/10.1016/j.aaspro.2014.11.034>.
- (74) Marsano, E.; Corsini, P.; Canetti, M.; Freddi, G. Regenerated Cellulose-Silk Fibroin Blends Fibers. *Int. J. Biol. Macromol.* **2008**, *43* (2), 106–114. <https://doi.org/10.1016/j.ijbiomac.2008.03.009>.
- (75) Ma, Z.; Kotaki, M.; Ramakrishna, S. Electrospun Cellulose Nanofiber as Affinity Membrane. *J. Memb. Sci.* **2005**, *265*, 115–123.
- (76) Casaburi, A.; Montoya, Ú.; Cerrutti, P.; Analía, V.; Laura, M. Carboxymethyl Cellulose with Tailored Degree of Substitution Obtained from Cellulose. *Food Hydrocoll.* **2018**, *75* (2018), 147–156.
- (77) Rusman, R.; Majid, R. A.; Aizan, W.; Abd, W.; Low, J. H. Carboxymethyl Cassava Starch / Polyurethane Dispersion Blend as Surface Carboxymethyl Cassava Starch / Polyurethane Dispersion Blend as Surface Sizing Agent. *Chem. Eng. Trans.* **2017**, *56*, 1171–1176.
- (78) Ahmad, M. I.; Ismail, M.; Riffat, S. Renewable Energy and Sustainable Technologies for Building and Environmental Applications: Options for a Greener Future. *Rev. Artic.* **2016**, 1–252.
- (79) Eyley, S.; Thielemans, W. Surface Modification of Cellulose Nanocrystals. *Nanoscale* **2014**, *6*, 7764–7779.
- (80) Kumar, S.; Kruth, J. P. Composites by Rapid Prototyping Technology. *Mater. Des.* **2010**, *31* (2), 850–856.
- (81) Kim, C. W.; Kim, D. S.; Kang, S. Y.; Marquez, M.; Joo, Y. L. Structural Studies of Electrospun Cellulose Nanofibers. *Polymer (Guildf)*. **2006**, *47*, 5097–5107.
- (82) Marks, J. A.; Edgar, K. J.; Taylor, L. S.; Riffle, J. S.; Turner, S. R. Synthesis and Applications of Cellulose Derivatives for Drug Delivery Synthesis and Applications of Cellulose Derivatives for Drug Delivery. **2015**, *PhD*, Virginia Polytechnic Institute and State Universit.
- (83) Asl, S. A.; Mousavi, M.; Labbafi, M. Synthesis and Characterization of Carboxymethyl

- Cellulose from Sugarcane. *J. Food Process. Technol.* **2017**, 8 (8), 2157–7110.
- (84) Roy, D.; Semsarilar, M.; Guthrie, J. T.; Perrier, S.; Tada, H.; Roy, D.; Semsarilar, M.; Guthrie, T. Cellulose Modification by Polymer Grafting : A Review. *Chem. Soc. Rev.* **2009**, 38 (7), 2046–2064.
- (85) Wang, Y. Cellulose Fiber Dissolution in Sodium Hydroxide Solution at Low Temperature: Dissolution Kinetics and Solubility Improvement. **2008**, *PhD*, Georgia Institute of Technology.
- (86) Granström, M. Cellulose Derivatives: Synthesis, Properties and Applications; 2009; Vol. PhD.
- (87) Siqueira, E. J.; Botaro, V. R.; Novack, K. M. Thermal and Mechanical Properties of Films Prepared with Purified and Unpurified Carboxymethylcellulose (CMC). *Conf. Pap.* **2014**.
- (88) Ardizzone, S. *et al.* Microcrystalline Cellulose Powders: Structure, Surface Features and Water Sorption Capability. *Cellulose* **1999**, 6(1), 57–69.
- (89) Battista, O. A.; Smith, P. A. Microcrystalline Cellulose. *Ind. Eng. Chem.* **1962**, 54 (9), 20–29.
- (90) Law, M. F. L.; Deasy, P. B. Use of Hydrophilic Polymers with Microcrystalline Cellulose to Improve Extrusion-Spheronization. *Eur. J. Pharm. Biopharm.* **1998**, 45 (1), 57–65.
- (91) Nechifor, C. D.; Dorohoi, D. O.; Ciobanu, C. The Influence of Gamma Radiations on Physico-Chemical Properties of Some Polymer Membranes. *Rom. Reports Phys.* **2009**, 54 (3–4), 349–359.
- (92) Blomstedt, M. Modification of Cellulosic Fibers by Carboxymethyl Cellulose- Effects on Fiber and Sheet Properties, Helsinki University of Technology, **2007**. PhD.
- (93) Ali, H. E.; Atta, A.; Senna, M. M. Physico-Chemical Properties of Carboxymethyl Cellulose (CMC)/ Nanosized Titanium Oxide (TiO 2) Gamma Irradiated Composite. *Arab J. Nucl. Sci. Appl.* **2015**, 48 (4), 44–52.
- (94) Kelco, C. The World Leader in Carboxymethylcellulose (CMC) Production, 1st Edition.; **2009**.

- (95) Mukherjee, T. *et al.* Chemically Imaging the Interaction of Acetylated Nanocrystalline Cellulose (NCC) with a Polylactic Acid (PLA) Polymer Matrix. *Cellulose* **2017**, *24* (4), 1717–1729.
- (96) Azizi Samir, M. A. S.; Alloin, F.; Dufresne, A. Review of Recent Research into Cellulosic Whiskers, Their Properties and Their Application in Nanocomposite Field. *Biomacromolecules* **2005**, *6* (2), 612–626.
- (97) Sayyar, S.; Gambhir, S.; Chung, J.; Officer, D. L.; Wallace, G. G. 3D Printable Conducting Hydrogels Containing Chemically Converted Graphene. *Nanoscale* **2017**, *9* (5), 2038–2050.
- (98) Lu, W.; Sastry, A. M. Self-Assembly for Semiconductor Industry. *IEEE Trans. Semicond. Manuf.* **2007**, *20*.
- (99) Feng, H.; Lu, X.; Wang, W.; Kang, N.; Mays, J. W.; Wang, W. Block Copolymers: Synthesis, Self-Assembly,. *Polymer (Guildf)*. **2017**, *9*, 494.
- (100) Cooper, T. M.; Campbell, A. L.; Crane, R. L. Formation of Polypeptide-Dye Multilayers by an Electrostatic Self-Assembly Technique. *Langmuir* **2009**, *29* (3), 663–668..
- (101) Zhang, L.; Menkhaus, T. J.; Fong, H. Fabrication and Bioseparation Studies of Adsorptive Membranes/Felts Made from Electrospun Cellulose Acetate Nanofibers. *J. Memb. Sci.* **2008**, *319* (1–2), 176–184.
- (102) Meli, L.; Miao, J.; Dordick, J. S.; Linhardt, R. J. Electrospinning from Room Temperature Ionic Liquids for Biopolymer Fiber Formation. *Green Chem.* **2010**, *12* (11), 1883–1892. <https://doi.org/10.1039/c0gc00283f>.
- (103) Rockwood, D. N.; Preda, R. C.; Wang, X.; Yucel, T.; Lovett, M. L. Materials Fabrication from Bombyx Mori Silk Fibroin. *Natl. Protoc.* **2013**, *6* (10).
- (104) Bhardwaj, N.; Kundu, S. C. Electrospinning: A Fascinating Fiber Fabrication Technique. *Biotechnol. Adv.* **2010**, *28* (3), 325–347.
- (105) Haider, A.; Haider, S.; Kang, I. K. A Comprehensive Review Summarizing the Effect of Electrospinning Parameters and Potential Applications of Nanofibers in Biomedical and Biotechnology. *Arab. J. Chem.* **2015**.
- (106) Grafe, T.; Graham, K. Nanofiber Webs from Electrospinning. *Nonwovens Filtr. Int. Conf.* **2003**, No. March, 1–5.

- (107) Diedericks, H. Controlled Release of an Antimicrobial Substance from Polymeric Matrices. **2016**, MSc (March), Stellenbosch University.
- (108) Shenoy, S. L.; Bates, W. D.; Frisch, H. L.; Wnek, G. E. Role of Chain Entanglements on Fiber Formation during Electrospinning of Polymer Solutions: Good Solvent, Non-Specific Polymer-Polymer Interaction Limit. *Polymer (Guildf)*. **2005**, *46* (10), 3372–3384.
- (109) Baji, A.; Mai, Y. W.; Wong, S. C.; Abtahi, M.; Chen, P. Electrospinning of Polymer Nanofibers: Effects on Oriented Morphology, Structures and Tensile Properties. *Compos. Sci. Technol.* **2010**, *70* (5), 703–718.
- (110) Kriel, H. Polylactic Acid Core-Shell Fibres by Coaxial Electrospinning. **2010**, MSc, Stellenbosch University.
- (111) Pillay, V.; Dott, C.; Choonara, Y. E.; Tyagi, C.; Tomar, L.; Kumar, P.; Du Toit, L. C.; Ndesendo, V. M. K. A Review of the Effect of Processing Variables on the Fabrication of Electrospun Nanofibers for Drug Delivery Applications. *J. Nanomater.* **2012**, *2013*.
- (112) Luo, C. J.; Edirisinghe, M. Core-Liquid-Induced Transition from Coaxial Electro spray to Electrospinning of Low-Viscosity Poly (Lactide- Co -Glycolide) Sheath Solution. *Macromolecules* **2014**.
- (113) Yu, D. G.; White, K.; Chatterton, N. P.; Zhu, L. M.; Huang, L. Y.; Wang, B. A Modified Coaxial Electrospinning for Preparing Fibers from a High Concentration Polymer Solution. *Express Polym. Lett.* **2011**, *5* (8), 732–741.
- (114) Kurban, Z.; Lovell, A.; Bennington, S. M.; Jenkins, D. W. K.; Ryan, K. R.; Jones, M. O.; Skipper, N. T.; David, W. I. F. A Solution Selection Model for Coaxial Electrospinning and Its Application to Nanostructured Hydrogen Storage Materials. *J. Phys. Chem. C* **2010**, *114* (49), 21201–21213.
- (115) Elahi, F.; Lu, W.; Guoping, G.; Khan, F. Core-Shell Fibers for Biomedical Applications- A Review Bioengineering & Biomedical Science. *J. Bioeng. Biomed. Sci.* **2013**, *3* (1), 1–14.
- (116) Leach, M. K.; Feng, Z.-Q.; Tuck, S. J.; Corey, J. M. Electrospinning Fundamentals: Optimizing Solution and Apparatus Parameters. *J. Vis. Exp.* **2011**, No. 47, 2–5.
- (117) Zhou, L.; Wang, Q.; Wen, J.; Chen, X.; Shao, Z. Preparation and Characterization of

- Transparent Silk Fibroin/Cellulose Blend Films. *Polymer (Guildf)*. **2013**, *54* (18), 5035–5042.
- (118) Zhang, C.; Yuan, X.; Wu, L.; Han, Y.; Sheng, J. Study on Morphology of Electrospun Poly(Vinyl Alcohol) Mats. *Eur. Polym. J.* **2005**, *41* (3), 423–432.
- (119) Haider, A.; Haider, S.; Kang, I. A Comprehensive Review Summarizing the Effect of Electrospinning Parameters and Potential Applications of Nanofibers in Biomedical and Biotechnology. *Arab. J. Chem.* **2018**, *11* (8), 1165–1188.
- (120) Park, W. H.; Jeong, L.; Yoo, D.; Hudson, S. Effect of Chitosan on Morphology and Conformation of Electrospun Silk Fibroin Nanofibers. *Polymer (Guildf)*. **2004**, *45* (21), 7151–7157.
- (121) Freddi, G.; Romano, M.; Massafa, M. R.; Tsukada, M. Silk Fibroin/Cellulose Blend Films-Preparation, Structure, and Physical Properties. *J. Appl. Polym. Sci.* **1995**, *56*, 1537–1545.
- (122) Shang, S.; Zhu, L.; Fan, J. Physical Properties of Silk Fibroin/Cellulose Blend Films Regenerated from the Hydrophilic Ionic Liquid. *Carbohydr. Polym.* **2011**, *86* (2), 462–468.
- (123) Zhou, W.; He, J.; Cui, S.; Gao, W. Preparation of Electrospun Silk Fibroin/Cellulose Acetate Blend Nanofibers and Their Applications to Heavy Metal Ions Adsorption. *Fibers Polym.* **2011**, *12* (4), 431–437.
- (124) Sill, T. J.; von Recum, H. A. Electrospinning: Applications in Drug Delivery and Tissue Engineering. *Biomaterials* **2008**, *29* (13), 1989–2006.
- (125) Kundu, J.; Mohapatra, R.; Kundu, S. C. Silk Fibroin/Sodium Carboxymethylcellulose Blended Films for Biotechnological Applications. *J. Biomater. Sci. Polym. Ed.* **2011**, *22* (4–6), 519–539.
- (126) Numata, K.; Yamazaki, S.; Katashima, T.; Chuah, J.; Naga, N.; Sakai, T. Silk-Pectin Hydrogel with Superior Mechanical Properties, Biodegradability, and Biocompatibility. *Macromol. Biosci.* **2014**, *14* (6), 799–806.
- (127) Kemp, R. Coaxial Electrospinning for the Reinforcement of Nanofibre Mats. **2017**, *MSc* (March), Stellenbosch University.

Chapter 3: Experimental approach: Preparation and characterization of electrospun nanofibers of SF/CMC blends

3.0. Background

The ES of biopolymers down to nanoscale sizes has attracted considerable interest in efforts to address many of our millennial concerns, for example, in medical fields and fields related to water treatment.¹ CE is commonly obtained in the naturally fibrillary structures where it provide structural support and mechanical resistance that are crucial for the vital functions of plants and SF is a unique biomaterial with various superior properties such as biocompatibility, biodegradation and tunable mechanical properties.² The excellent mechanical properties of both SF and CE materials, together with their biocompatibility and biodegradability, have fostered the development of strategies able to effectively use these two biopolymers to create novel composite systems with applications in different sectors.³ However, SF lacks hydrophilicity, and flexibility, which limits its use in many applications.⁴⁻⁶ The blending of SF with other polymers has gained significant awareness by scientist to upgrade physicochemical properties of silk fibroin.

The cellulose derivative that was used in this study, CMC, is a highly hydrophilic natural polymer (polysaccharide) that has chelating abilities, biocompatibility, is biodegradable, and finds widespread applicability in wound dressing and in tissue engineering applications.⁷ Therefore, CMC was chosen as a blending polymer with SF in efforts to improve the hydrophilicity and mechanical properties of SF. Hydrophilicity is very important in filtration applications since it ensures moisture stability. In this section, ES has been described as the most common fabricating technique for the generation of polymer nanofibers.² Therefore, this chapter focuses in the preparation of SF/CMC blend electrospun nanofibers for water treatment application. The materials, procedures, and parameters used for the ES are described. Characterization of the electrospun mats using techniques such as ATR-FTIR, XRD, and determination of their morphology and thermal behavior, are discussed. The results and discussion of these experimental results are included.

3.1. Materials

All the reagents used in this study were used without any further purification unless otherwise stated. Their purity was at least 98%, unless stated otherwise. *Bombyx mori* SF and SS were obtained from Oxford University, Silk group (UK). The α -cellulose was obtained from Sigma-

Aldrich (South Africa). CMC (reagent grade, molecular weight ~700 kDa and DS ~0.65–0.85), protease XIV (from *Streptomyces griseus*), cellulase (from *Aspergillus niger*), and phosphate buffered saline (PBS) were obtained from Sigma-Aldrich. Formic acid (98%), lithium bromide, sodium carbonate, ethanol, and methanol were purchased from Merck and used as solvents. fluorescein (free acid, dye content ~95%), Rhodamine B (dye content ~95%), propidium iodide (PI) and STYO 9 dye were also obtained from Sigma-Aldrich.

3.2. Processing of silk fibroin (SF)

3.2.1. Degumming of silkworm cocoons

The *B. mori* SF was prepared according to a previously published procedure.⁸ Briefly, the silkworm cocoons (5g), were cut into pieces and added to a boiling 0.02 M aqueous solution of Na₂CO₃ (250 mL) for 20 min, then rinsed thoroughly with deionized (DI) water to remove the sericin protein. After degumming, silk fibers were dried at 37 °C overnight. Degummed silk fibers were dissolved in 9.3 M LiBr solution at 60 °C for 4 h, yielding a 20% (w/v) solution. The silk/LiBr solution was then inserted into the dialysis tubing and dialyzed against DI water using Slide-a-Lyzer dialysis cassettes (molecular weight cut off 3500 g·mol⁻¹) for 3 days to remove salt. The solution was optically clear after dialysis; it was then centrifuged to remove undissolved impurities and clumps that initiate on the process.

3.2.2. Preparation of regenerated silk fibroin (RSF)

The solution obtained after dialysis was lyophilized at –20 °C for 24 h (VirTis BenchTop freeze dryer). The RSF powder obtained was stored in a desiccator until use.

3.2.3. Preparation of aqueous solutions of silk protein fibroin

SF nanofibers were prepared by the ES of a solution of a calculated amount of RSF powder in 98% FA to obtain a homogeneous solution of various concentrations: typically, 8 wt%, 10 wt% and 12 wt%. Solutions were stirred for 3 h at room temperature (RT).

3.2.4. Development of carboxymethylcellulose (CMC) solutions

A calculated weight of CMC was dissolved in DI water at RT and slowly stirred on a magnetic stirrer for 24 h to prepare solutions of various concentrations: typically, 1 wt% and 3 wt%. The solutions were then left aside for 4 h to ensure they were free of any air bubbles, then stored at RT until required for use.

3.2.5. Preparation of nanofiber membranes

3.2.5.1. Development of silk fibroin and carboxymethyl cellulose (SF/CMC) blends solutions

To prepare SF/CMC blends, silk fibroin (10wt%) and carboxymethyl cellulose (3wt%) were prepared as stock solutions. The stock solutions were then mixed at different ratios (3:2, 3:1, and 2:1). The blends were stirred at RT for 24h. Well dispersed homogeneous solutions were obtained. The different blends were designated as follows: SF/CMC(1) for the 3:2 blend, SF/CMC(2) for the 3:1 blend and SF/CMC(3) for the 2:1 blend.

3.2.5.2. Preparation of silk fibroin, carboxymethyl cellulose and silk sericin (SF/CMC/SS) blends solutions

The SF/CMC/SS blends solution were prepared to evaluate antimicrobial activity by slowly mixing the stock solutions of silk fibroin (10wt%), carboxymethyl cellulose (3wt%) and silk sericin (3wt%) using the ratio of 3:2:1, and stirred for 24h at RT.

3.3. Electrospinning

3.3.1 Equipment and setup used

The equipment and setup used for ES was similar to the sketch in Section 2.4.1.3, Figure 2.11. This system comprised of a plastic syringe capped with a blunt needle which was used as the solution reservoir. This was connected to a programmed syringe pump (Kent Scientific Genie Plus). A high voltage positive DC power supply was used. The collector plate made up of a glass petri dish, covered with aluminium foil, connected to the power supply's negative port, while the positive was attached to the needle tip.⁹

3.3.2. ES parameters

The ES experiments was carried out in the fume hood (without the operation of the extraction fan). Humidity and temperature were both controlled with a 44 Hermos-hygrometer (TFA Dostman, Wertheim). The spinning process was manipulated by adjusting the following: gap in between the needle and the collector, the voltage, and the flow rate. Continuous and nonbeaded fibers were obtained under the parameters tabulated in Table 3.1.

3.3.3. Preparation of electrospun nanofibers

SF nanofibers were developed by ES. In the ES process, first, a plastic syringe with a blunt needle was charged with the prepared solution of SF (described earlier, Section 3.2.3), then it

was electrospun using ES machine setup shown in the previous chapter (Figure 2.11). The voltage was 15 kV and a constant flow rate of 0.027 mL/min, then distance between the collector and spinning electrode was set at 12, 14 or 16 cm. For the ES of SF/CMC blends nanofibers, a syringe with a blunt needle was charged with the polymer solution (SF/CMC) and attached to a syringe pump. A constant flow rate of 0.003 mL/min was applied. The needle was clamped to the positive electrode of a high-voltage power supply, generating 20 kV. The distance between the spinning electrode and the collector was 20 cm. See Table 3.1 (flow rate; distance: between the spinning electrode and the collector).

Table 3. 1: Experimental parameters used for electrospinning of SF, SF/CMC and SF/CMC/SS blend nanofibers

Sample codes	Flow rate (mL/min)	Distance (Tip-to-collector) (cm)	Voltage (kV)	Humidity (%)	Temperature (°C)
SF	0.027	16	15	40	25
SF/CMC(1)	0.003	20	20	50	25
SF/CMC(2)	0.003	20	20	50	25
SF/CMC(3)	0.003	20	20	50	25
SF/CMC/SS	0.006	20	15	40	25

3.4. Characterization of fibers

3.4.1. Morphological characterization

3.4.1.1. Scanning electron microscopy (SEM)

SEM gives insight into surface characteristics, such as morphology, smoothness, fiber diameter, pore size, and interfiber adhesion properties.¹⁰ Analysis was performed using a Zeiss MERLIN Field Emission Scanning Electron Microscope at the Electron Microbeam Unit of Stellenbosch University's Central Analytical Facility. Prior to imaging, the samples were mounted on aluminium stubs with double-sided carbon tape. The samples were then coated with a thin layer of gold (~10 nm thick), using a gold coater (over 3 min). SEM images of samples were captured using a Zeiss Secondary Electron (SE2) detector or the Zeiss In-lens detector using Zeiss SmartSEM software. The beam conditions during the image analysis were the following: 5 kV acceleration voltage extra-high tension target, 250 pA beam current (I-Probe), <4 mm working distance, and a high resolution column configuration (Column Mode).¹¹ The diameter of the

fibres was measured using AxioVision image analyser software; the SEM images were loaded into the software, and diameters of the fibers were measured using a two-point measuring analysis. Approximately 50 measurements were taken to determine the diameter distribution for individual fiber.

3.4.1.2. Transmission electron microscopy (TEM)

TEM analysis was operated on a JEOL 1200EX electron microscope operated at 120 kV, at the Electron Microbeam Unit of the University of Cape Town's Central Analytical Facility. Prior to sample preparation, the solution of CMC was stained with uranyl acetate before ES. Then ES fibers were developed straight by set down nanofibers onto carbon-coated copper grids (diameter 3 mm).

3.4.2. Chemical characterization

3.4.2.1. Attenuated total reflection-Fourier transform infrared (ATR-FTIR)

ATR-FTIR spectroscopy was carried out on a Nexus infrared spectrophotometer that was equipped with a smart golden gate attenuated total reflectance diamond from Thermo Nicolet with ZnSe lenses. All samples were scanned 64 times, resolution of 4.0 cm^{-1} was used and records were taken in the 400 cm^{-1} to 400 cm^{-1} . The software that was used on the system to do the data analysis was Omnic Software, version 7.2.

3.4.2.2. X-ray diffraction (XRD)

The internal molecular structure of the polymers (fibers) was studied by 2D wide-angle X-ray diffraction (WAXD) using a D2 Phaser instrument (Bruker AXS, Germany), with a Cu K_{α} radiation ($\lambda = 1.54\text{ \AA}$) source, and a PSD Lynx-Eye (Si-strip detector; 196 channels. XRD data were collected from $2\theta = 10\text{--}40\text{ kV}$, 30 mA. Units were operated at RT with the sample connected on a standard glass sample holder.

3.4.2.3. Solid-state NMR (SolSt NMR)

Solid-state (SolSt) NMR experiments were operated to examine the configuration changes in SF/CMC blend nanofibers concerning the RSF and CE. See Figure 3.11. The experiments were operated on a Varian Infinity Plus-400 wide-bore (89 mm) spectrometer running at a ^{13}C frequency of 100.5 MHz, using a standard 4 mm Vespel HX T3 MAS NMR probe. ^{13}C ramped cross-polarization (CP) NMR spectra were obtained under a magic-angle-spinning rate of 5 kHz.

3.4.2.4. Raman spectroscopy

Raman spectroscopy is a functional technique tool study the conformation of a polymer in the solid state as well as in solution. It is useful in determining chemical modification and crystallization. A WITec Raman microscope (ALPHA 300 R-confocal Raman imaging) was used. Spectra were accumulated from 512 scans at a resolution of $\sim 4 \text{ cm}^{-1}$ using a laser power $\sim 500 \text{ mW}$. The operating range was $200\text{--}3500 \text{ cm}^{-1}$, depending on the choice of detector. Raman spectra have bands that are characteristic for each molecules in a sample.⁶

3.4.3. Thermal characterization

3.4.3.1. Differential scanning calorimetry (DSC)

DSC units were recorded with a TA instruments Q100 instrument, under a nitrogen atmosphere. Samples to be analysed (5–10 mg) were sealed in aluminium pans. The sample runs where performed in a three main steps process. First the samples were heated from 0 to 300 °C at a rate of 10 °C/min, held at 300 °C for 1 min, and cooled at the same rate (10 °C/min). This cycle was repeated twice. The percentage crystallinity of the materials was defined with the use of TA Universal Analysis software.

3.4.3.2. Thermal gravimetric analysis (TGA)

Nanofibers of various blend composition of SF/CMC were chopped into little segments weighing around 3-5 mg and placed in an alumina crucible to examine the thermal behaviour of the blended nanofibers. TGA was operated with a Q500 thermogravimetric analyser under nitrogen at 5 °C/min. This tool defines the changes in weight in relation to change in temperature, with an argon gas flow of 100 ml/min. Experiment was operated at a heating rate of 20 °C/min and run from 30 °C to 900 °C.

3.5. Results and discussion

3.5.1. Preparation of pure SF nanofibers

The intensity of the polymer has an extremely impact on its spinnability, whereby affecting the development of nanofibers and their morphology.¹⁷ An impact of SF polymer intensity on development of spun nanofibers and their morphology was studied by adjusting the concentration of silk in the blends. (10–14 wt%) to establish the optimal polymer concentration that favoured fiber formation here. The ES conditions were maintained at 15 kV and 16 cm distance between the nozzle tip and the collector. Outcomes showed that the diameters of the

fibers increased with the increase in polymer concentration and the nanofiber generation was most favourable at a polymer concentration of 10 wt%. At concentrations <10 wt%, no continuous fibers were observed. And may be assigned to the very low viscosity of these polymer solutions. This resulted in sputtering of the polymer solution and fibres with much beading, as observed in Figure 3.1A. Polymer solutions with concentrations >12 wt% were very viscous and difficult to electrospun (Figure 3.1C). Overall, 10% SF solution was the optimal concentration here, proving development of continuous fiber and superior fiber diameter (Figure 3.1B).

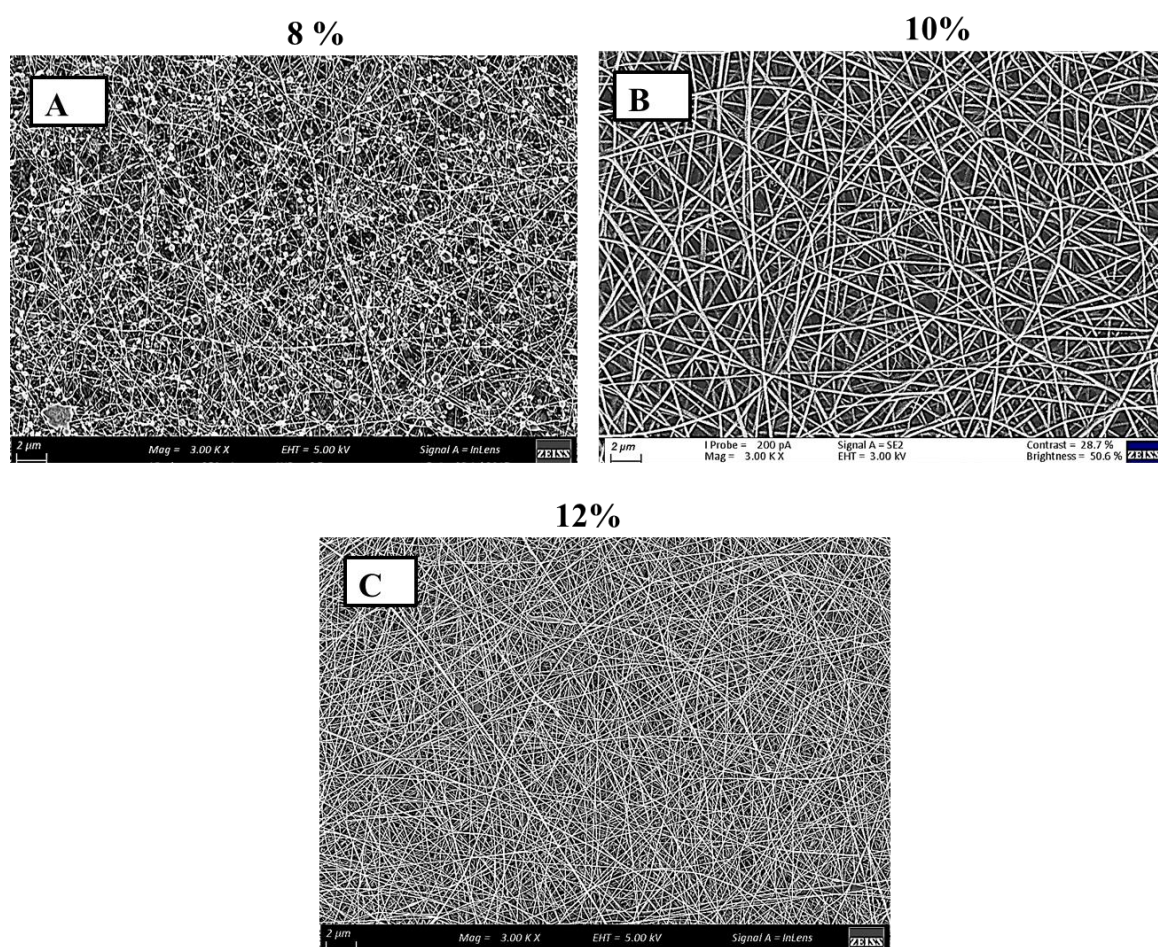


Figure 3.1: SEM images of electrospun SF nanofibers generated from SF solutions of different concentrations (8-12%) (distance between the collector and spinning electrode 16 cm, voltage 15 kV).

3.5.1.1. Fiber diameter

Fiber diameters were measured from SEM images. SF nanofibrous mats had fibers in the diameter range 20–100 nm (Figure 3.2B). Although non-specific diameter ranges for nanofibrous substance helpful in filter applications (according to the filtration theory) have been

reported, smaller fiber sizes generally give better filtration efficiency. Smaller fibers have high surface to volume ratios that are favourable for filtration applications. Hence, the very narrow nanofibers obtained in this study, with their increased surface area for filtration, can be considered advantageous.

3.5.1.2. Effect of the tip–collector distance

The development of beaded fibers is initiated by insufficient evaporation, caused by the short distance that a nanofiber travel to the collector. When the tip–to–collector distance was set to 12 cm, the nanofibers produced were found to be beaded, possibly caused by not enough period for the complete evaporation of the solvent and elongation of the nanofibers (Figure 3.2A). The fiber diameter was observed to decrease as the distance between the electrodes increased. Subsequently, using a 10 wt% SF solution and a tip–to–collector distance of 16 cm appeared to be appropriate to fabricate nanoscale fibers for water filtration.

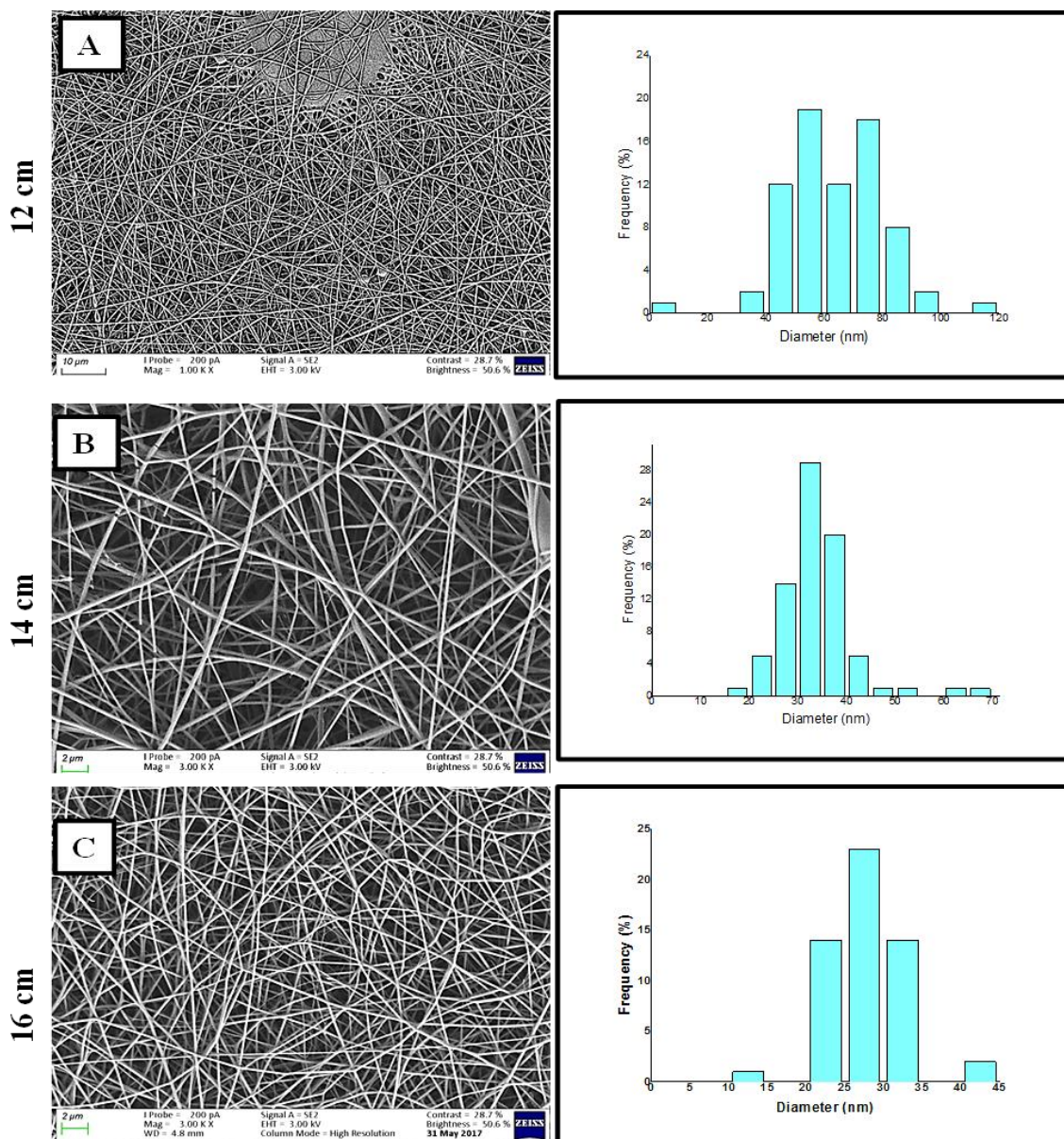


Figure 3.2: SEM images of electrospun SF nanofibers formed from 10 wt% SF solution, using different distances between the electrodes (12, 14, 16 cm).

3.5.1.3. Structural and thermal characterization

The structural and thermal properties of the SF electrospun mats determine their stability and chemical properties. These properties of SF nanofibers were described using XRD, FT-IR, and TGA. The existence of functional groups characteristic of SF nanofibers was defined by FTIR analysis. SF may exist in either of two possible conformations, a β -sheet or 'random' coil structure, showing degree of order. Both configurations reveal characteristic peaks: absorption frequencies at $1630\text{--}1660\text{ cm}^{-1}$ (amide I), 1530 cm^{-1} (amide II) and $1235\text{--}1265\text{ cm}^{-1}$ (amide III). The pure SF spectrum (Figure 3.4) shows the amide I, amide II, and amide III

conformations, corresponding to the characteristic peaks at 1630 cm^{-1} , 1530 cm^{-1} , and 1236 cm^{-1} , respectively, indicating the presence of all three conformations here.

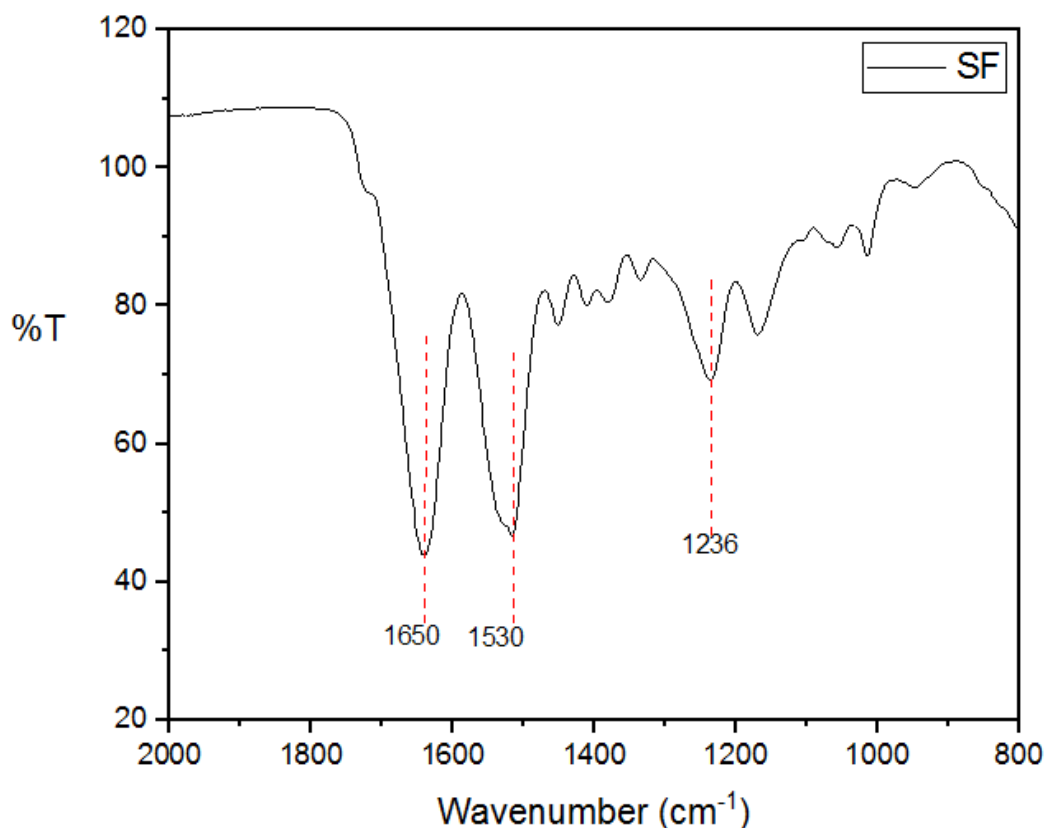


Figure 3.3: FTIR spectrum of electrospun SF nanofibers.

The conformational properties of the SF nanofibers were determined by XRD. An XRD spectrum of SF electrospun nanofibers is shown in Figure 3.5. The conformation of SF included the random coil, silk I, and silk II as major molecular structures. The silk II conformation was thought to be constituted of β -sheet and endows silk nanofibers with superior mechanical properties. The peaks at 11.7° (2θ) and 20.2° (2θ) shows the silk II conformations take part to the superior stability and mechanical properties of the SF nanofibers. A weak peak at 24.9° (2θ) has been reported to indicate the silk I structure of SF.¹⁸

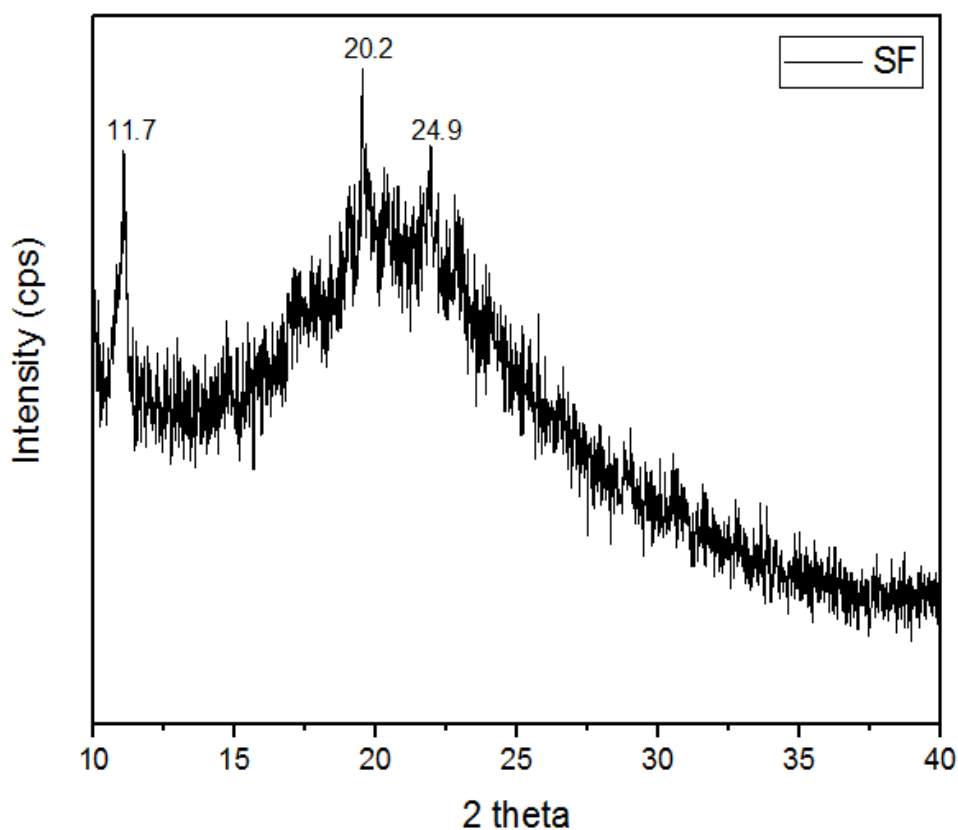


Figure 3.4: XRD spectrum of SF electrospun nanofibers.

A thermogravimetric curve of the SF nanofibers is shown in Figure 3.5. The TGA curve of SF nanofibers can be divided into three main parts, characterized by evident different mass loss rates. The first step is the initial weight loss below 150 °C, which is assigned to the evaporation of water. The second step is the slight thermal decomposition of SF molecules, which occurs from 220 to 300 °C, and which can be attributed to the loss of other low temperature volatile species.¹⁹ The third loss, from 300 to 400°C, is assigned with the breakdown of the side chain groups of amino acid residues as well as the cleavage of peptides, indicating the thermal degradation of the SF.⁴

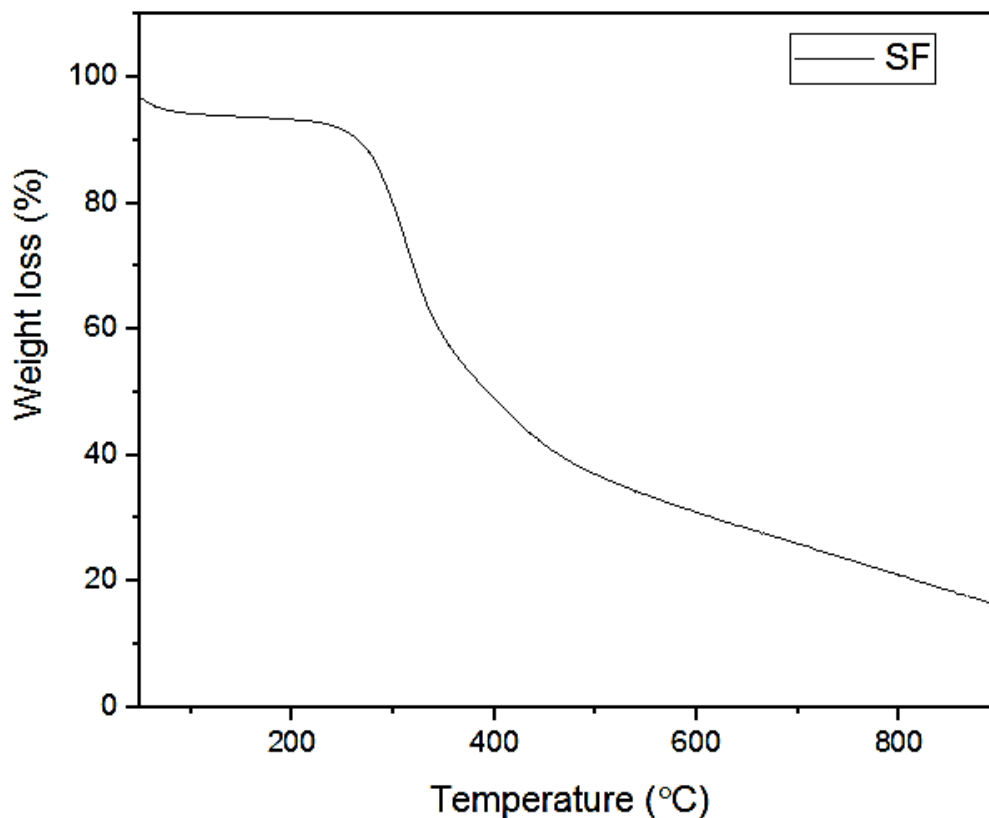


Figure 3.5: TGA thermogram of the electrospun SF nanofibers.

3.5.2. Preparation of SF/CMC blend nanofibers

Blends of SF/CMC electrospun mats were prepared by ES of various compositions of SF/CMC blend solutions (3:2, 3:1, 2:1 (w/w)). The blends are designated as described in Section 3.2.5.1 and Table 3.1. The developed blend solutions and their electrospun nanofibers were analysed by different tools.

3.5.3. Characterization of the SF/CMC blend nanofibers

3.5.4. Morphological study

3.5.4.1. Scanning electron microscopy (SEM)

The morphology of the SF, SF/CMC(1), SF/CMC(2) and SF/CMC(3) blend nanofibers was studied using FE-SEM image analysis. The SEM images shown in Figure 3.6 reveal that the ES of the SF/CMC blends from FA solutions resulted in well-defined nanofibers without the formation of beads. The increase in fiber diameter as CMC is added was observed. The average diameter of the blend nanofibers SF/CMC(1), SF/CMC(2) and SF/CMC(3) showed an increase

in the average diameter from 153 ± 28 , 135 ± 20 , and 126 ± 34 nm, respectively, whereas pure SF had an average diameter of 100 ± 20 nm.

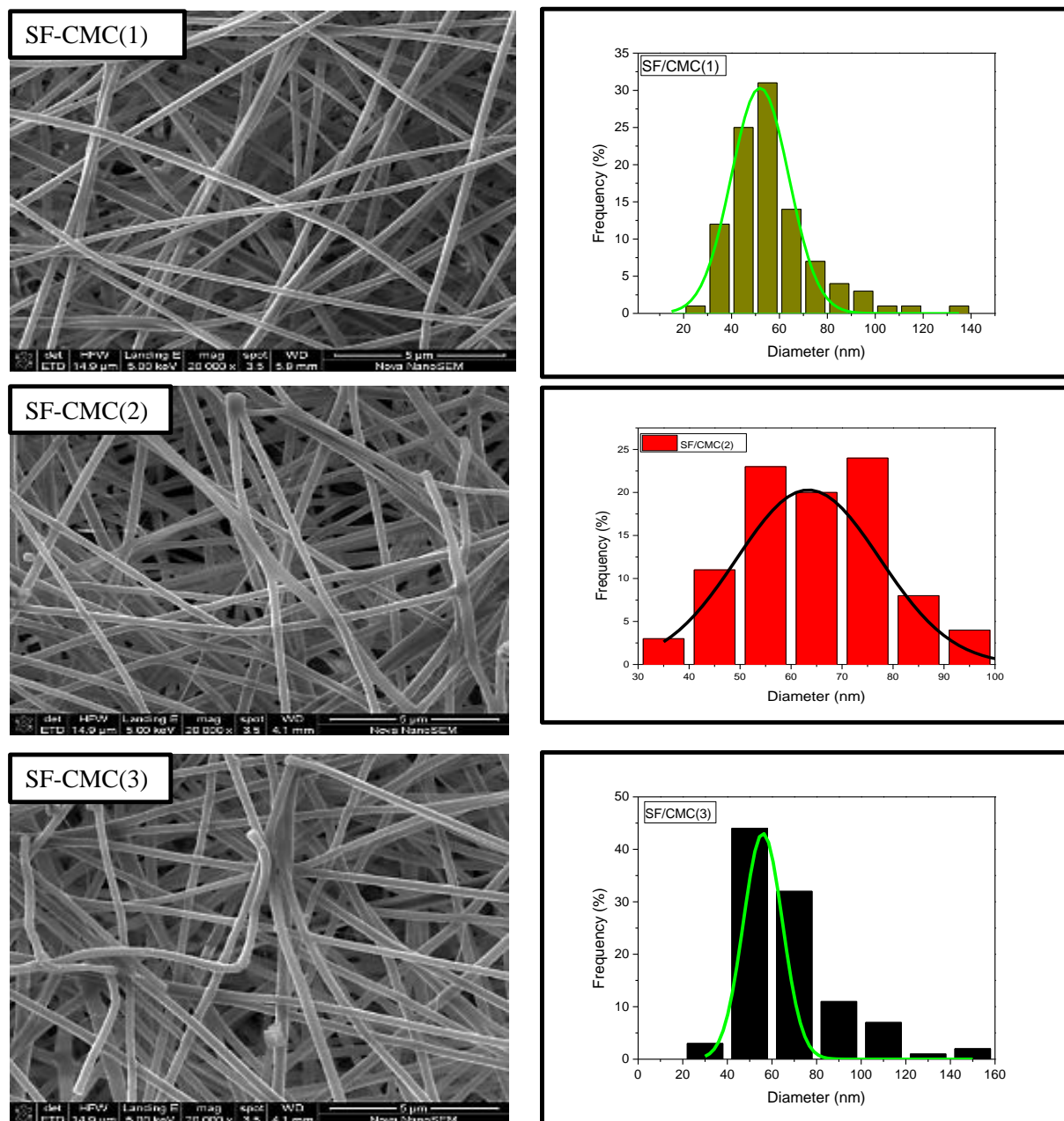


Figure 3.6: FE-SEM images of electrospun nanofibers: SF/CMC(1), SF/CMC(2) and SF/CMC(3)

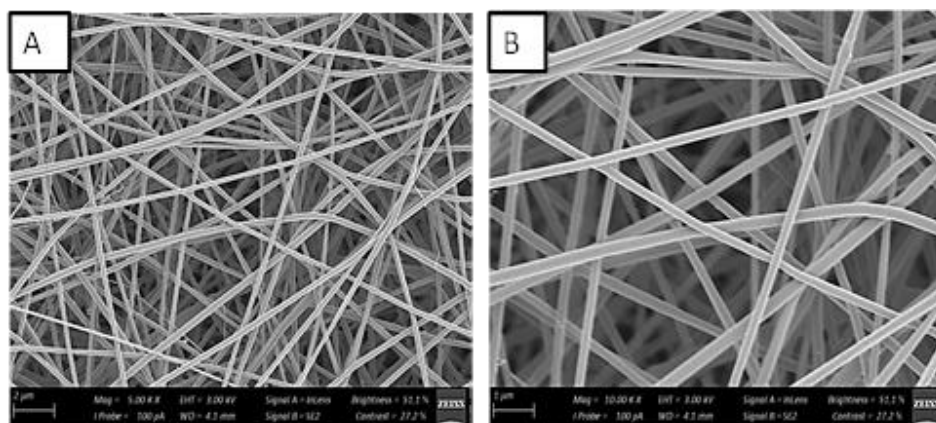


Figure 3.7: FE-SEM images of SF/CMC/SS electrospun nanofibers

3.5.4.2. Transmission electron microscopy (TEM)

The morphology of the SF/CMC blends was also studied via TEM analysis. Since most polymers are immiscible and form multiphase systems, it is important to be able to study their morphology.²⁰ The size domain, the shape of the polymer domains and the phase flow might differ by changing the process factors, and the resulting changes in the morphology can be studied using TEM.²¹ In this study, TEM was used to study the distribution of phases and morphology of each polymer in the various blends.

From the TEM images of the SF/CMC (1) blend nanofibers, in Figure 3.8, multiple necking formation and fragmentation at high rate of stretching of the nanofibers is observed. These results also indicate that the nanofibers have a compact shell such morphology might show because of a rapidly solvent evaporation during ES.

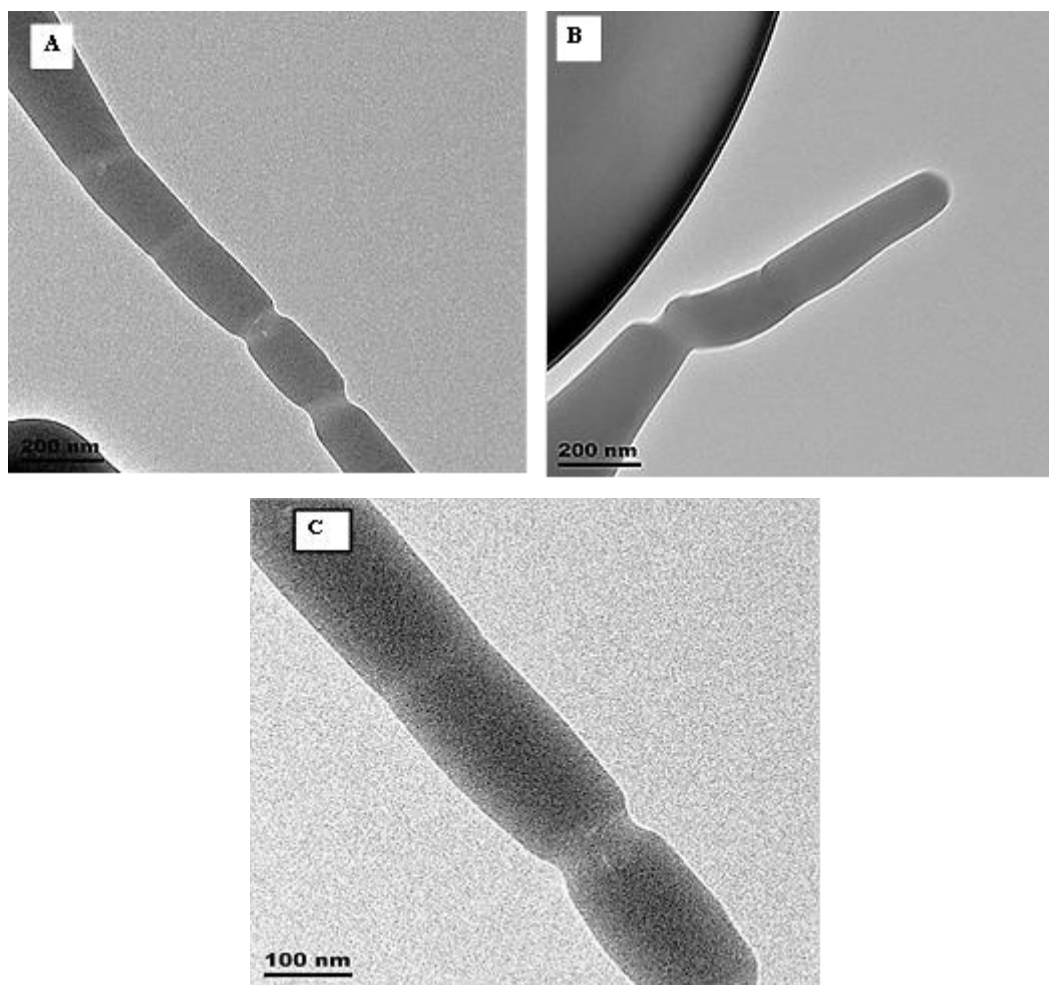


Figure 3.8: TEM images of electrospun SF/CMC (1) blend nanofibers.

3.5.5.1. FTIR

Macroscopic mechanical properties are normally associated with the microscopic structure.¹⁵ Thus, IR and SolSt-¹³C NMR analyses were both operated to study the conformational changes in the SF/CMC electrospun nanofibers, compared to the pure regenerated SF and CMC. Characteristic peaks of the amide I, amide II, and amide III of SF, observed at 1627 cm^{-1} , 1519 cm^{-1} and 1236 cm^{-1} respectively (Figure 3.9). These peaks in SF/CMC(2) became stronger, indicating the ability of CMC to facilitate conformational transition from random coils to β -sheets by developing extra intermolecular hydrogen bonds between the carboxyl groups of CMC and the amide groups of SF. The band at 1060 cm^{-1} is due to the $>\text{CH}-\text{O}-\text{CH}_2$ stretching of the CMC. This peak is visible on the spectra of CMC and SF/CMC blends, but not in the spectrum of SF. It is the only band peak that was observed on the SF/CMC blend that corresponds to the band peaks of CMC; the presence of this band is also reported in literature.^{4,5}

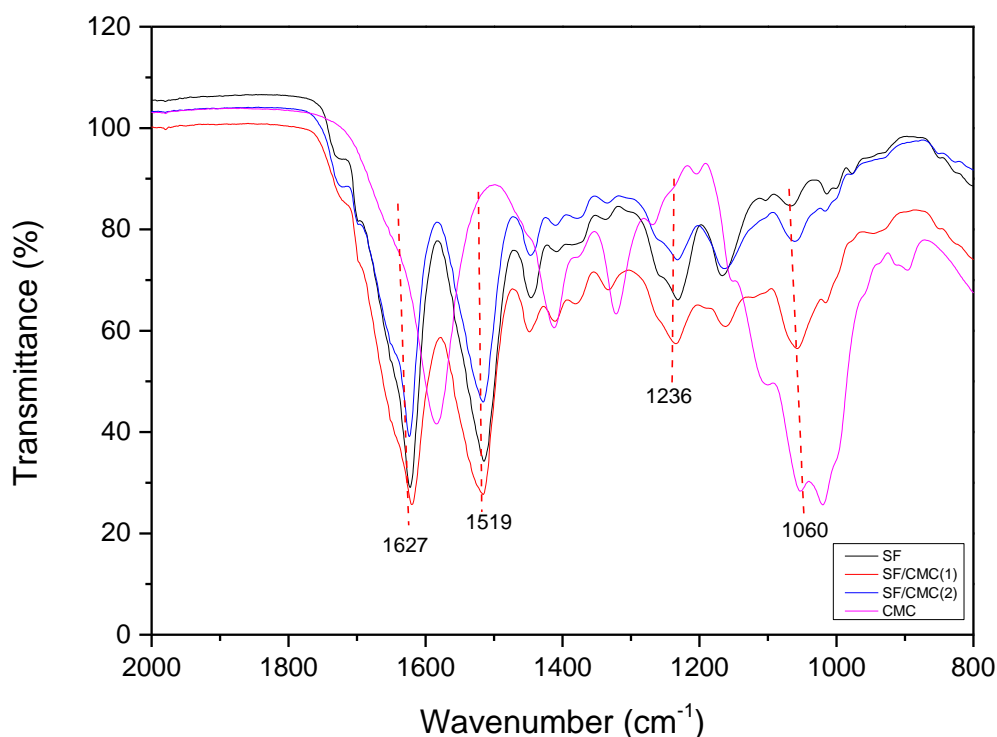


Figure 3.9: FTIR spectrum of the electrospun SF and SF/CMC blends.

3.5.5.2. SolSt-¹³C NMR

Going on with examining the SF/CMC blend nanofibers structure, the ¹³C NMR spectra of pure SF, CMC, and SF/CMC nanofibers were recorded, see Figure 3.10. Sung *et al.*²⁷ studied the conformation dependent ¹³C NMR chemical shift of SF in the SolSt. They reported that the carbonyl shifts of Ala C_α and C_β in the β-sheet structure were 48.2 and 19.9 ppm, respectively, and in the random structure they were 49.8 and 16.7 ppm, respectively. In this study, the peaks at 180 ppm represented by letter (b), 60.6 ppm presented by (d), 50.9 ppm which is indicated by letter (c), and 43.3 ppm represented by letter (a) in the ¹³C NMR spectra of pure SF nanofibers were assigned to the carbonyl carbons of SF.²⁸ The ¹³C NMR spectra of SF/CMC blend nanofibers showed characteristic chemical shifts of both SF and CMC. The absence of a characteristic peak at ~75 ppm (for carbon C₃) and at ~115 ppm (for carbon C₄), which corresponds to the crystalline structure of CMC, indicated an amorphous CMC structure in the SF/CMC blends.

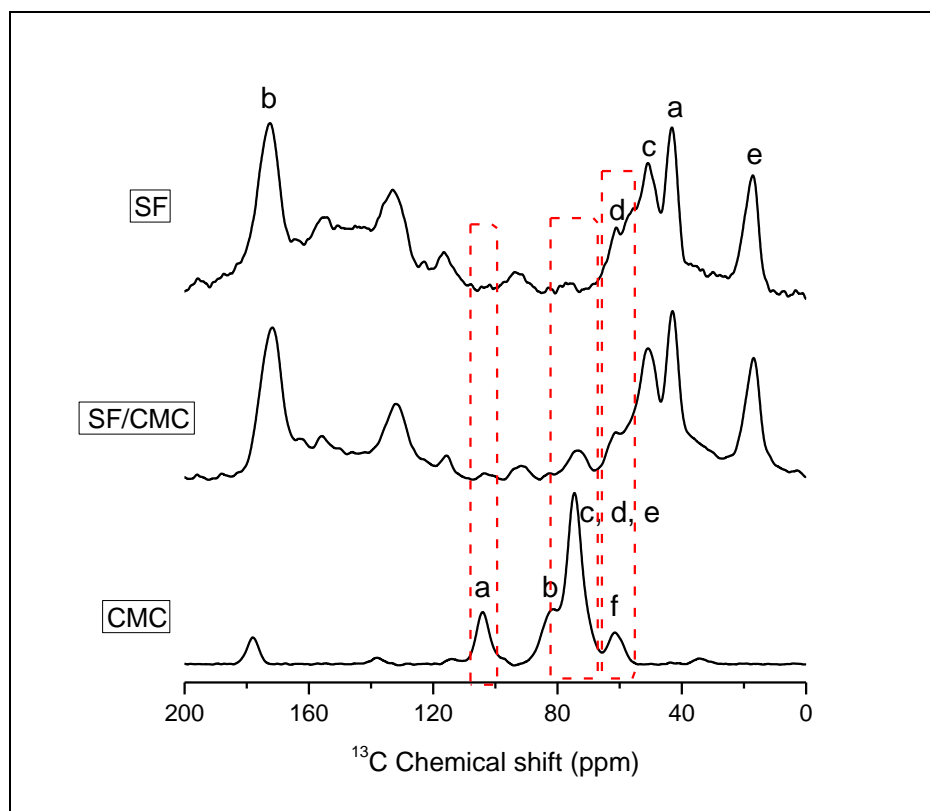


Figure 3. 10: SolSt- ^{13}C NMR of SF and CMC, and SF/CMC (1) nanofibers.

3.5.5.3. XRD

XRD is a useful analytical tool to examine the structure of semicrystalline polymers. XRD was used to study the SF/CMC blend nanofibers. Generally, silk fibers are composed of at least three types of conformation: a β -sheet, random coil, and helical structure; these conformations are indicated as silk I, silk II and silk III, respectively.⁴ The molecular interconnection between SF and CMC could be due to hydrogen bond development. The OH groups, C=O groups, and NH_2 groups of SF have ability of developing hydrogen bonds with the OH and C=O groups in CMC. The XRD diffractogram in Figure 3.11 shows XRD spectra of the electrospun SF and SF/CMC blends nanofibers. The SF/CMC fibers were essentially amorphous and there was a homogeneous dispersion of SF domains into a CMC matrix. The main diffraction peak in all samples appeared at $2\theta = 20.9^\circ$, which denotes the silk II structure. There were no peaks denoting silk I or silk III. Interaction between the amide groups of SF and the hydroxyl groups of the CMC molecules plays a vital part in the development of the β -sheet conformation and promotion of crystallization of the nanofibers. XRD patterns of the blended fibers revealed small different to those of pure SF fibers.¹⁸

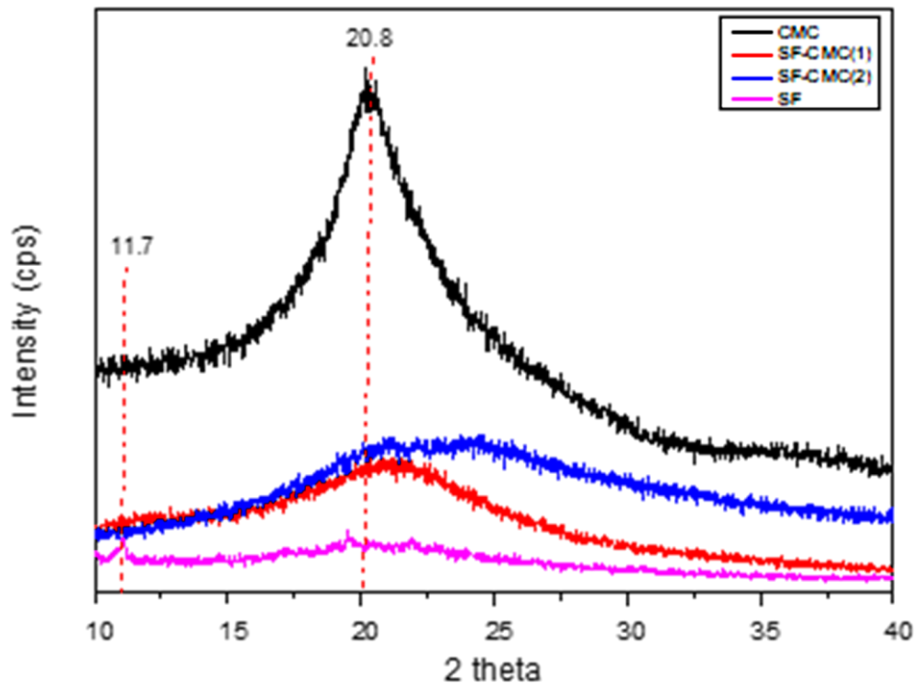


Figure 3.11: XRD spectrum of the electrospun SF and SF/CMC blend nanofibers.

3.5.5.4. Raman spectroscopy

Raman spectroscopy was operated as the secondary technique for examining the SF/CMC blends structure. See Figure 3.12. The Raman spectrum of CMC (Figure 3.12 A) shows a sharp peak at 2928.49 cm^{-1} because of the hydroxyl groups and a peak at 1451.63 cm^{-1} due to the carboxyl group. The SF spectra (Figure 3.12 B) shows strong peaks around $2950\text{--}2440\text{ cm}^{-1}$, due to the absorption of water. The bands at 1775 and 1467 cm^{-1} are evidence of the β -sheet crystallinity and the peak at 487.27 cm^{-1} is reported to be related with side chains of amino acids.⁶ The spectrum of the SF/CMC blends (Figure 3.12 C), slight shifts in all the peaks were observed, which indicate interactions between CMC and SF.

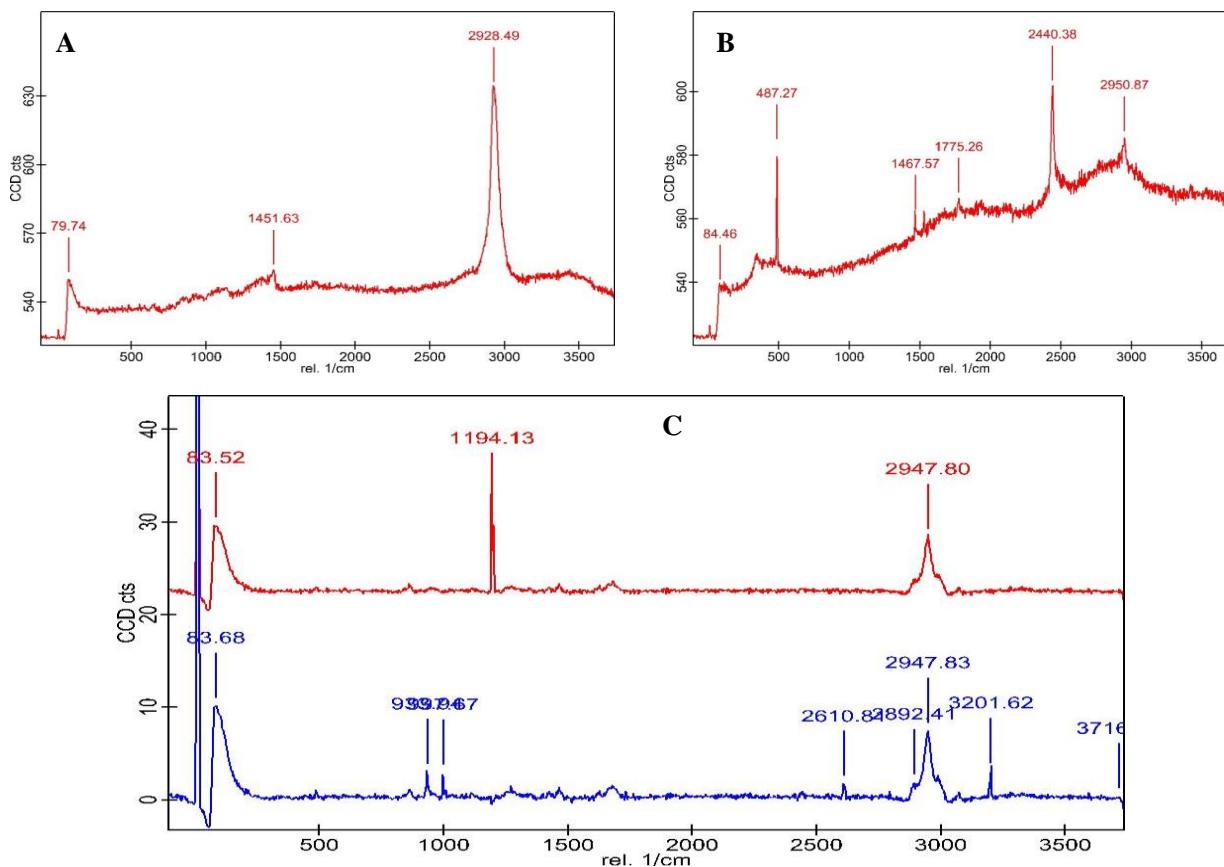


Figure 3.12: Raman spectrum of (A) CMC, (B) SF, and (C) SF/CMC(1) blend nanofibers.

3.5.7. Thermal characterization

3.5.7.1 TGA analysis

The thermal properties of SF, CMC, and SF/CMC blends nanofibers were studied using TGA. TGA curves are shown in Figure 3.13. A part of weight loss for temperature values up to 100 °C was observed from SF and SF/CMC samples, principally due to the loss of water (from environmental humidity). From 50 °C to 250 °C, the weight of CMC was almost unchanged. The primary thermal decomposition of CMC occurs between 250 and 400 °C. SF presented the highest water loss in comparison with CMC, indicating that SF has higher ability to absorb moisture from the ambient medium. Degradation of the blended nanofibers occurs in three steps: the initial mass loss is caused by the evaporation of water, the second weight loss is found in the temperature range of 250–350 °C, and the third weight loss is around 430 °C. During the first stage CMC seemed to be more stable so as the blends contains high ratio of CMC. SF nanofibers showed another part of weight loss between 270 and 380 °C with a peak at 274 °C that was related with the degradation of amino acid side groups and cleavage of peptide bonds.²⁹

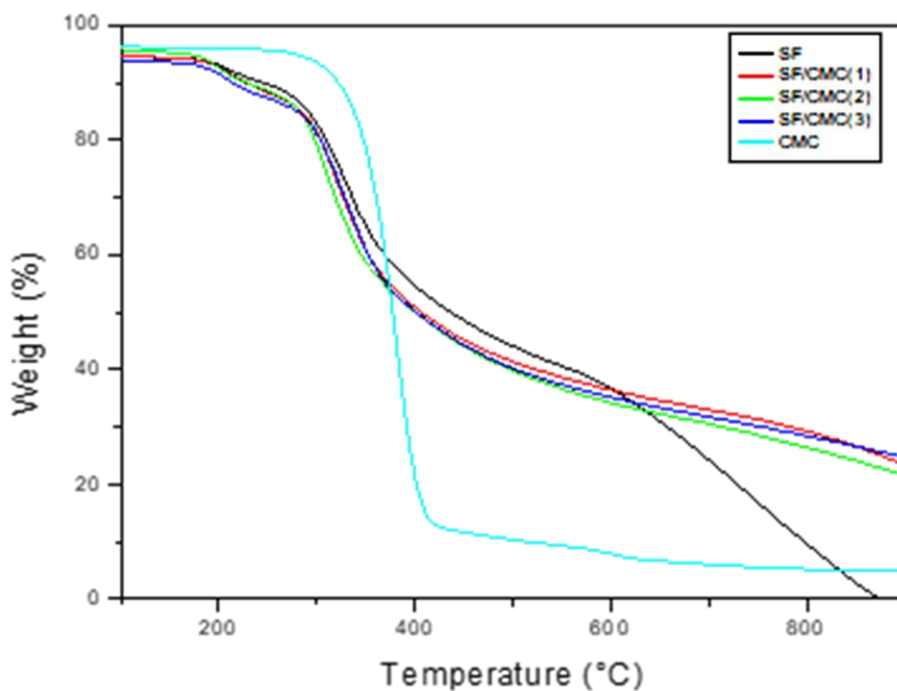


Figure 3. 13: TGA curves of the SF, CMC, and SF/CMC blends.

3.5.7.2. DSC analysis

The thermal behavior of the electrospun SF/CMC blends was further confirmed by DSC. Figure 3.14A shows the DSC results of pure CMC. The melting temperature was observed at 120 °C and cold crystallization peak was observed at 190 °C. The glass transition (T_g) peak was observed at 75 °C (as reported in literature). Moraes *et al.* studied the impact of various ratio of SF and chitosan on the thermal properties of SF/CS blends. They observed an exothermic peak below 150 °C for SF, which was assigned to crystallization during heating, from a silk I to a silk II structure.³⁰ Shen *et al.* reported an exothermic shift at about 220 °C and an endothermic peak at 278 °C for the SF, which was assigned to the heat induced β -sheet crystallization and the thermal decomposition of the SF, respectively.¹⁴ The SF (Figure 3.16B) shows two broad and large endothermic peaks which are around 75 °C, due to loss of moisture and about 275 °C, assigned to thermal degradation of the well oriented β -sheet crystalline conformation, which is consistent with the observation from TGA. The exothermic peak at 245 °C has been reported by Lau *et al.* as the crystallization during heating by forming the β -sheet structure from a random coil conformation.³¹ The T_g of SF is around 178 °C, which is close to the crystallization temperature of CMC, but is not observable in Figure 3.16B. There is no T_g of SF observed in the blends (Figure 3.16C). The reason could be that the T_g of SF is hidden within the crystallization peak of cellulose. Another reason could be that the blends are miscible and only a single T_g could be observed. The blends show the melting peak around 262 °C. Chen *et al.*

studied the thermal properties and phase transition in nylon-6 and SF blends, they concluded with the strong interaction between SF and nylon-6 prevents the SF from crystallizing.³²

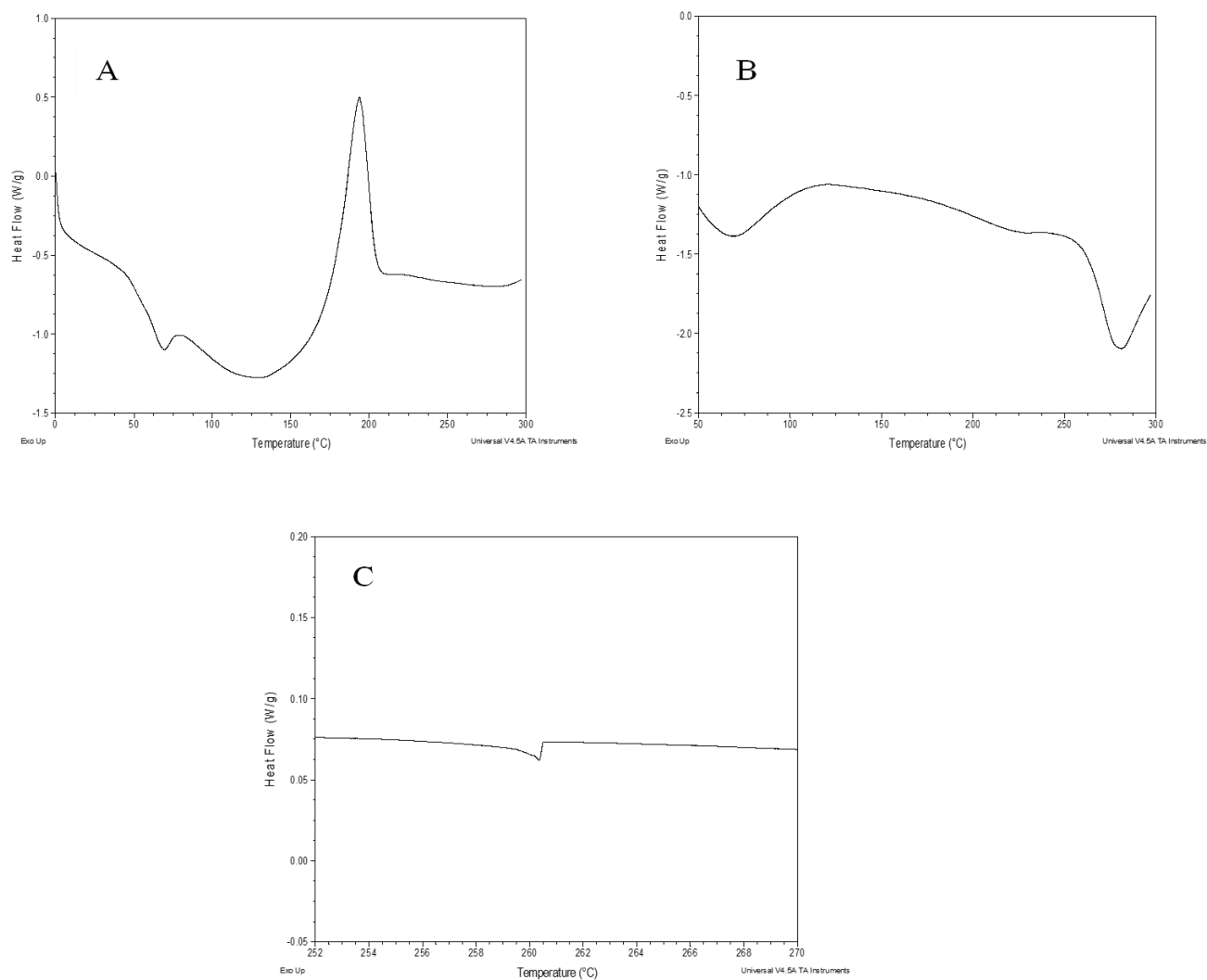


Figure 3. 14: DSC thermograms of the second heating runs of (A) CMC, (B) SF, and (C) SF/CMC (1) blend nanofibers.

3.6. Conclusion

Fabricating SF composites together with other polymers is the best way to alter properties of SF nanofibers. SF and CMC nanofiber composites (SF/CMC) were successfully prepared through the process of ES. The blended nanofibers resulted in uniform fibers, without the formation of beads, as confirmed by morphological analysis. The diameter of the electrospun mats increased gradually upon addition of CMC. Structural characterization using ATR-FTIR, XRD, Raman, and SolSt-¹³C NMR showed the transfiguration of silk fibroin from a random coil to a β -sheet in the electrospun blends with CMC. The carboxymethyl cellulose accounted for greater association of water molecules in the SF/CMC composites and upgraded their thermal conductivity during high temperatures. The TGA results of SF/CMC blended nanofibers showed thermal behavior almost similar or better than that of SF nanofibers.

3.7. References

1. Mai, Z. Membrane Processes for Water and Wastewater Treatment: Study and Modeling of Interactions Between Membrane and Matter. *English* **2014**, Ecole Cent.
2. Guzman-puyol, S. *et al.* Low-Cost and Effective Fabrication of Biocompatible Nanofibers from Silk and Cellulose-Rich Materials. *ACS Biomater. Sci. Eng* **2016**, *2*, 526–534.
3. Mondal, M., Trivedy, K. & Kumar, S. N. The silk proteins, Sericin and Fibroin in Silkworm, *Bombyx mori* Linn. A review. *Casp. J. Environ. Sci* **2007**, *5*, 63–76.
4. Kundu, J., Mohapatra, R. & Kundu, S. C. Silk Fibroin/Sodium Carboxymethylcellulose Blended Films for Biotechnological Applications. *J. Biomater. Sci. Polym. Ed* **2011**, *22*, 519–539.
5. Singh, B. N. Development of Novel Silk Fibroin / Carboxymethyl Cellulose Based Electrospun Nanofibrous Scaffolds for Bone Tissue Engineering Application. **2017**, National Institute of Technology Rourkela, PhD.
6. Mhuka, V. Characterization of Silk Protein from African Wild Silkworm Cocoons and Application of Fibroin Matrices as Biomaterials. **2014**, University of South Africa, PhD.
7. Casaburi, A., Montoya, Ú., Cerrutti, P., Analía, V. & Laura, M. Carboxymethyl Cellulose with Tailored Degree of Substitution Obtained from Cellulose. *Food Hydrocoll* **2018**, *75*, 147–156.
8. Mccool, J. Silk Fibroin-Based Scaffolds for Tissue Engineering Applications. **2011**, Virginia Commonwealth University, MSc.
9. Hu, X.; Liu, S.; Zhou, G.; Haung, Y. Electrospinning of Polymer Nanofibers for Delivery Application. *J. Control. Release* **2014**, *10*, 12-21.
10. Gule, N. P. Electrospun antimicrobial and antibiofouling nanofibres. **2011**, Stellenbosch University, PhD.
11. Rojas, J. & Azevedo, E. Functional and Crosslinking of Microcrystalline Cellulose in Aqueous Media: A Safe Economic Approach. *Int. J. Pharm. Sci. Rev. Res* **2011**, *8* (1).
12. Ostrowska, B., Jaroszewicz, J., Zaczynska, E. & Tomaszewski, W. Evaluation of 3D hybrid microfiber / nanofiber scaffolds for bone tissue engineering. *Science* **2014**, *62* (3), 551–556.

13. Maksimcuka, J. *et al.* X-ray Tomographic imaging of Tensile Deformation Modes of electrospun Biodegradable Polyester Fibers. *Front. Mater* **2017**, *4*, 1–11.
14. Shen, W., George, M., Mussone, P. & Montemagno, C. Physical Properties of Silk Fibroin and Cellulose Nanocrystals Blended Films: Thermal, Mechanical and Morphological Characterization. *IJRRAS* **2016**, *28*, 71–83.
15. Tian, D. *et al.* Conformations and Intermolecular Interactions in Cellulose/Silk Fibroin Blend Films: A Solid-State NMR Perspective. *J. Phys. Chem* **2017**, *121*, 6108–6116.
16. Kemp, R. Coaxial Electrospinning for the Reinforcement of Nanofibre Mats **2017**, Stellenbosch University, MSc.
17. Beachley, V. & Wen, X. Effect of Electrospinning Paramets on the Nanofiber Diameter and Length. *Mater. Sci. Eng. C Mater. Biol. Appl* **2009**, *29* (3), 663–668.
18. Liu, R., Zhang, F., Zuo, B. & Zhang, H. EDC-Crosslinked Electrospun Silk-Fibroin Fiber Mats. *Adv. Mater. Res* **2011**, *175–176*, 170–175.
19. Kweon, H. Y., Um, I. C. & Park, Y. H. Thermal behavior of Regenerated Antheraea pernyi Silk Fibroin Film Treated with Aqueous Methanol. *Polymer (Guildf)* **2000**, *41* (20), 7361–7367.
20. Hassander, H. Electron Microscopy Methods for Studying Polymer Blends Comparison of Scanning Electron Microscopy and Transmission Electron Microscopy. *Polym. Test* **1985**, *5*, 27-36.
21. Jinnai, H., Spontak, R. J. & Nishi, T. Transmission Electron Microtomography and Polymer Nanostructures. *Macromolecules* **2010**, *43* (4), 1675–1688.
22. Wang, C. T., Kuo, C. C., Chen, H. C. & Chen, W. C. Non-Woven and Aligned Electrospun Multicomponent Luminescent Polymer Nanofibers: Effects of Aggregated Morphology on the Photophysical Properties. *Nanotechnology* **2009**, *20* (37).
23. Shenoy, S. L., Bates, W. D., Frisch, H. L. & Wnek, G. E. Role of Chain Entanglements on Fiber Formation during Electrospinning of Polymer Solutions: Good Solvent, Non-Specific Polymer-Polymer Interaction Limit. *Polymer (Guildf)* **2005**, *46* (10), 3372–3384.
24. Luzio, A., Canesi, E. V., Bertarelli, C. & Caironi, M. Electrospun Polymer Fibers for Electronic Applications. *Materials (Basel)* **2014**, *7* (2), 906–947.

25. Nishikawa, Y., Baba, S. & Takahashi, M. Optimization of X-Ray Computerized Tomography for Polymer Materials. *Int. J. Polym. Mater* **2013**, 62 (5), 295–300.
26. Lai, G. & Chen, J. Response of Human Mesenchymal Stem Cells to Intrafibrillar Nanohydroxyapatite Content and Extrafibrillar Nanohydroxyapatite in biomimetic Chitosan/Silk/Nanohydroxyapatite Nanofibrous Membrane Scaffolds. *Int. J. Nanomed* **2015**, 10, 567–584.
27. Sung-Won, H., Alan, T. & Hudson, S. Structural studies of Bombyx mori Silk Fibroin During Regeneration from Solutions and Wet Fiber Spinning. *Biomacromolecules* **2005**, 6 (3), 1722–1731.
28. Zhang, K., Yu, Q. & Mo, X. Fabrication and Intermolecular Interactions of Silk Fibroin / Hydroxybutyl Chitosan Blended Nanofibers. *Int. J. Mol. Sci* **2011**, 12 (4), 2187–2199.
29. Motta, A., Fambri, L. & Migliaresi, C. Regenerated Silk Fibroin Films: Thermal and Dynamic Mechanical Analysis. *Macromol. Chem. Phys* **2002**, 203, 1658–1665.
30. Moraes, M. A. De, Nogueira, G. M., Weska, R. F. & Beppu, M. M. Preparation and Characterization of Insoluble Silk Fibroin/Chitosan Blend Films. *Polymer (Guildf)* **2010**, 2 (4), 719–727.
31. Jaramillo-quiceno, N., Álvarez-lópez, C. & Restrepo-osorio, A. Structural and Thermal Properties of Silk Fibroin Films Obtained From Cocoon and Waste Silk Fibers as Raw Materials. *Procedia Eng* **2017**, 200, 384–388.
32. Chen, H., Hu, X. & Cebe, P. Thermal Properties and Phase Transitions in Nylon-6 and Silk Fibroin Blends. *J. Therm. Anal. Calorim* **2008**, 93, 201–206.

Chapter 4: Biodegradation and antimicrobial evaluation of the electrospun mats

4.0. Summary

In this chapter the antimicrobial and biodegradability evaluation of the fabricated nanofiber membranes are reported. It includes a brief discussion on the crosslinking and antimicrobial assay of these nanofiber mats. The electrospun fibers were crosslinked with *N*-(3-dimethylaminopropyl)-*N'*-ethylcarbodiimide hydrochloride, a nontoxic crosslinking agent, and *N*-hydroxysuccinimide, that is able to speed up the reaction. The antimicrobial action for ES fibers was investigated towards various organisms involving *Staphylococcus aureus* (Gram-positive) and *Escherichia coli* (Gram-negative). Several techniques were applied for the evaluation of antimicrobial action including zone inhibition and fluorescence imaging. The enzymatic biodegradation evaluation of the materials was studied using cellulase extracted on *Aspergillus niger* and protease XIV (*Streptomyces griseus*). Different tools such as SEM and FTIR were used to evaluate degradation of the electrospun mats.

4.1. Introduction

Polymers that can decompose naturally derived from renewable resources has gained great awareness in past decades.¹ The biodegradability of natural polymers in the natural setting is one of the most interesting properties of this class of polymers.² Polymer degradation can be defined as the change in the properties (tensile strength, color, shape, etc.) of a polymer or polymer-based product under the influence of one or more environmental parameters such as chemicals, moisture, heat, light, etc.³ These changes in properties are often called 'ageing'. Biodegradation occurs via an activity mode of enzymes or through chemical stagnation related with living organisms. Biodegradability does not only rely on the source of the polymer but also on its chemical structure and degrading environmental constrain.^{1,4} The mechanical behavior of the biodegradable materials depends on their chemical composition and the application conditions. Degradation can be helpful for recycling or reusing polymer waste, to prevent or reduce environmental pollution. It can also be made purposely to help structure determination.^{5,6}

4.1.1. The biodegradation behavior of SF and CMC nanofiber membranes

Biological degradation by proteolytic enzymes can be harmful to silk fibroin due to its protein nature.⁷ The features of breaking down silk behavior differs based on the enzyme used. Previous

reports has reported the degradation behavior of SF exposed to different proteolytic enzymes for various periods of time. Chymotrypsin has been used to degrade the amorphous region of fibroin to obtain highly crystallizable fibroin protein. When protease (protease XIV) was compared with α -chymotrypsin, it was observed that when SF is incubated in the protease XIV enzyme, there was a significant decrease in mass and ultimate tensile strength (UTS) within a week.^{8,9} Whereas, in α -chymotrypsin, the UTS and mass of the SF remained unchanged. The α -chymotrypsin can degrade the dissolved fibroin proteins but not the fibroin sheets. In contrast, other enzymes (particularly protease XIV) extensively degraded fibroin sheets, demonstrating the potential of protease degradation of SF. Biodegradation of CE proceeds by enzymatic oxidation with peroxidase secreted by fungi. CE can also be degraded by bacteria.⁹ For ease of application in many advanced fields, cellulose (which is insoluble in many solvents) is usually modified via a reaction on one or more of the hydroxyl groups present in its repeating unit. Biodegradation of cellulose derivatives depends on the degree of substitution/modification. The biodegradation decreases as the DS increases.¹⁰

4.2. Crosslinking of silk and cellulose nanofibers

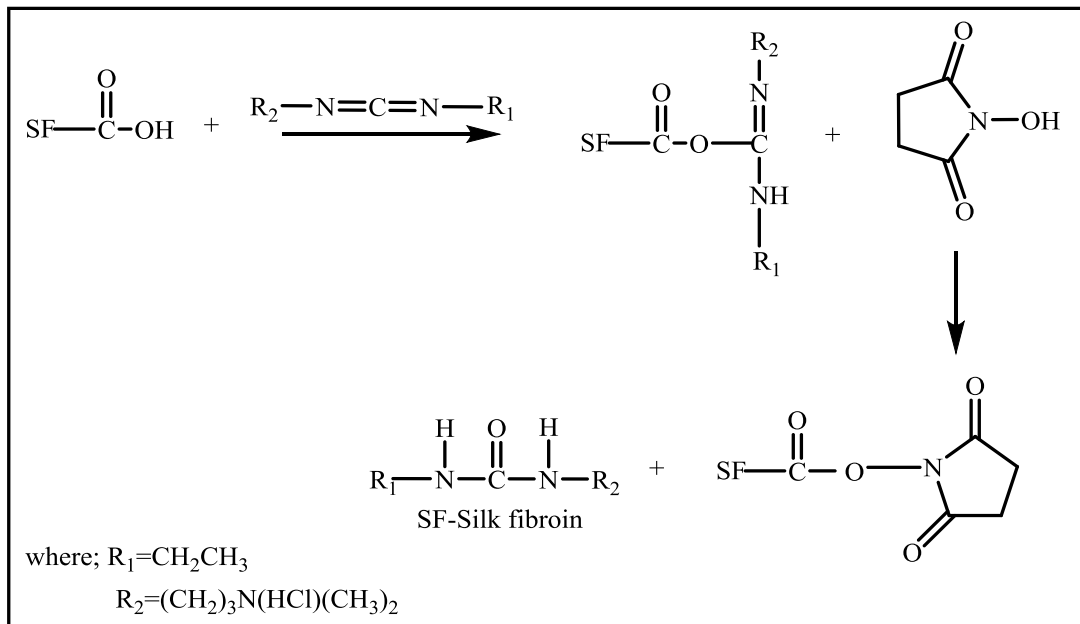
CE, the greatest polymer in the universe that construct greatest amount of a plant's cell wall. Even though CE cannot dissolve in water and in most organic solvents.¹¹ Like, CA can dissolve in acetone, tetrahydrofuran, and other organic solvents while ethyl cellulose, methylcellulose and carboxymethyl cellulose are soluble in water. CE derivatives can be dissolved either at a molecular level or dispersed on a colloidal level.¹²

CMC, which is the CE derivative used in this study, is water soluble carboxymethyl ether of cellulose, the ubiquitous polysaccharide composed of the fibrous tissue of plants. It has many used in food, pharmaceutical, personal care/cosmetic, paper and other industries.¹³ On the other hand, a RSF structure is mainly composed of α -helix and random coil conformations resulting in poor mechanical properties and water resistance. Mechanical integrity is important in most uses, such as water filtration. The blend of CMC and SF as reported in this study will be soluble in water, which would make it unsuitable for water filtration. Hence, post-treatment crosslinking of these biopolymers was a prerequisite.

N-(3-dimethylaminopropyl)-*N*'-ethylcarbodiimidehydrochloride(EDC)/*N*-

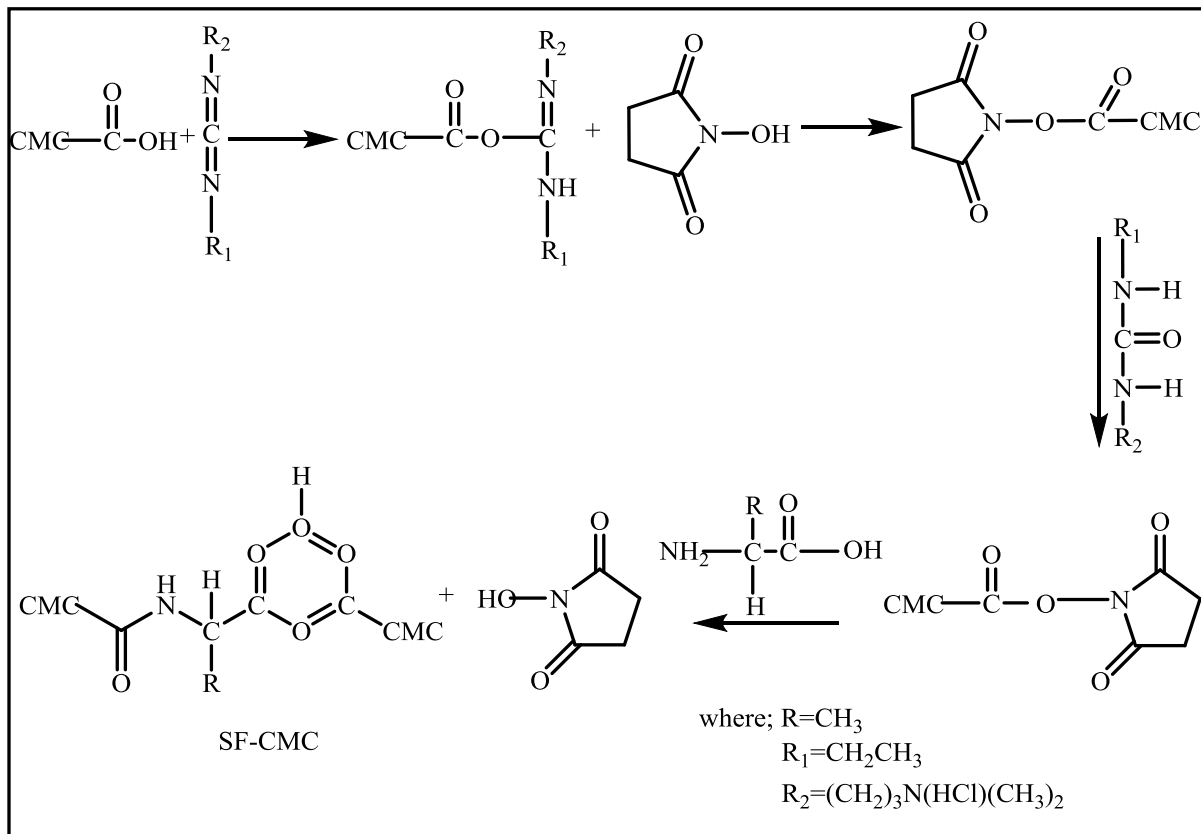
hydroxysuccinimide (NHS) is a nontoxic cross-linking agent that has been enormously investigated and announced to upgrade the mechanical properties of silk and cellulose electrospun nanofibers.¹⁴ EDC is defined as the well-known carbodiimide applied in

conjugating biological material having carboxylates and amines. It is well known by its role on particle and surface conjugating methods, together with NHS.¹⁵



Scheme 4. 1: Reaction mechanism of EDC with carboxyl and amino group in the SF.¹⁶

SF protein contains carboxyl group and amino groups, while CMC obtained the carboxyl groups and hydroxyl groups. During exposure of the ES fibers to the crosslinking mixture chemical process occurs that provide enough gap for the movement of molecular chains. The carboxylic acid remains of CMC are initiated with EDC, and the formation of the amide bond by nucleophilic attack of available amine group from silk fibroin on the initiated carboxylic groups. Meanwhile NHS is applied together with EDC for restraining fast hydrolysis of *O*-acylisourea intermediate group, in the development of strong NHS-ester intermediate. Hence, EDC/NHS mixture promotes crosslinking of SF/CMC fibers via covalent bonding.^{15,16} see Scheme 4.2.



Scheme 4. 2: Crosslinking reaction process of SF/CMC nanofiber membranes.¹⁵

4.3. Materials and techniques

All the reagent that were used for crosslinking experiment were used without any further purification unless stated otherwise. Ethylcarbodiimide hydrochloride (molecular weight ~ 191.7), was obtained from Sigma-Aldrich, South Africa. N-hydroxysuccinimide (molecular weight ~ 115.7) was also obtained from Sigma-Aldrich. Ethanol purchased from Merck and DI water were used as solvents.

4.3.1. Crosslinking of the electrospun nanofibers

Electrospun mats (prepared as described in Section 3.3.3) were exposed to EDC and NHS. An ethanol solution of EDC/NHS was prepared as the crosslinking solution. EDC (10.0g, 0.0125 mol) and 5.0g NHS (0.0125 mol) were dissolved into ethanol ($V_{\text{Ethanol}}/V_{\text{H}_2\text{O}} = 95/5$) at RT to give solutions of three different concentrations (3 wt%, 5 wt %, and 7.5 wt %). The respective solutions were stirred for 10 min to afford homogeneous solutions. Electrospun mats were cut into 50 mm × 50 mm rectangles, and then placed into the crosslinking solution (10 mL) for 24 h and 48 h. Then the mats were rinsed in DI water to remove the residual crosslinking agent and dried in the vacuum oven at 40 °C for 24 h. The mass loss, morphology, structural and

thermal changes were studied. The experiments were performed at RT. The average mass loss was described by weighing each sample prior and after crosslinking.

$$\text{Mass loss (\%)} = \frac{M_1 - M_2}{M_1} \dots\dots\dots (1)$$

4.3.2. Antimicrobial characterization

The antimicrobial behaviour of the crosslinked nanofibers was measured by making use zone inhibition test technique and fluorescence microscopy. Organisms that were applied for the tests were both Gram-negative *Escherichia coli* (*E. coli*) and gram-positive *Staphylococcus aureus* (*S. aureus*). The efficacy of the sample towards investigated organisms was evaluated through the growth inhibition zones. The area of inhibition is observed as clear regions all over the disc because of the spreading of the antimicrobials into the agar plate.

4.3.2.1. Evaluation by zone inhibition test

Preparation of agar plates

The agar plates were produced with a growth medium, Mueller-Hinton agar (composition in Gram/Litre; meat infusion 2.0g, casein hydrolysate 17.5g, soluble starch, agar 1.5g dissolved in 1L of DI). The agar was prepared as per the packaging instructions and then autoclaved. The autoclaved solution was cooled to the point at which the container could be comfortably handled and then subsequently poured into the plates and left to solidify overnight.

The bacteria were inoculated in nutrient broth (Biolab Diagnostics) and prepared according to the instructions on the container (composition in g/L: meat extract, yeast extract, peptone). The mixture of the broth was added to test tubes, in duplicate, and autoclaved. The bacteria were deposited to respective test tubes by collecting a bacteria colony in a plastic syringe tip and placing it in the broth. The test tubes containing the bacteria were then placed on a rotating incubator at 37 °C for 24 h. Hereafter, the bacteria were transferred to the plates and spread to form a lawn.

Agar disk diffusion method

Agar plates were inoculated with a standardized inoculum of the tested microorganisms (*S. aureus* and *E. coli*). Filter paper discs (about 6 mm in diameter), containing the antimicrobial agent of the concentration of choice, were placed on the agar surface, then the petri dishes were incubated at 37 °C for 24 h. Normally, the antimicrobial agent spreads into the agar and

terminate germination and growth of the test microorganisms. The diameters of the inhibition growth zones are then calculated.

4.3.2.2. Evaluation using fluorescent microscopy

The bacteria (*S. aureus* and *E. coli*) were streaked out into Luria Bertani broth (LB) agar plates (1.5% agar) and incubated overnight at 37 °C. This was followed by the inoculation of 4–5 colonies into 20 mL of clean LB medium (1% tryptone, 1% NaCl, 0.5% yeast extract) and overnight incubation, with angle rotation at 120 rpm at 37 °C. The culture was diluted to an optical density of 0.0025 (OD600 nm) in LB broth. The cell suspension (500 µL) was dispensed into sterile Eppendorf tubes. Electrospun nanofiber mat was inserted into each tube containing cell suspension. All tubes were placed on an orbital shaker (120 rpm) at 37 °C for 24 h.

Fluorescent staining

Fibers were withdrawn from the cell suspension and stained with PI and SYTO 9 known commercially as “LIVE/DEAD” BacLight bacteria viability kits. These dyes are used to monitor the viability of the bacteria as a function of the cell membrane integrity. The cells were then envisaged by a Carl Zeiss LSM780 laser scanning microscope (Carl Zeiss, Germany) and data refined with the ZEN 2011 imaging software (Carl Zeiss). PI fluoresces red around 561 nm / SYTO 9 fluoresces green around 488 nm. Metabolically viable/alive bacteria produce green fluorescence while dead bacteria produce red fluorescence.

4.3.3. Biodegradation evaluation

The degradation of the electrospun mats was studied using the enzymes cellulase extracted on *Aspergillus niger* and protease XIV from *Streptomyces griseus*. The initial weight of dry electrospun nanofiber mats was weighed and recorded (W_o). The nanofiber mats were incubated at 37°C, silk nanofibers were soaked in protease XIV solution (0.1 mg/ml) developed in PBS mixture and soaked in the PBS without the enzyme (control). Then SF/CMC nanofiber membranes were also soaked in cellulase and the mixture of protease and cellulase (1:1 w/w), which were also prepared in the PBS solution and soaked in PBS without the enzyme. After incubation for about 3–14 days, nanofiber mats were removed, washed with DI water and lyophilized, then weighed again; that weight was noted as the final weight (W_F). Finally, degradation percent was calculated using the initial weight (W_o) and the final weight (W_F) of the nanofiber mats, by applying Equation 2. The degradation of electrospun mats was also examined structurally with ATR-FTIR and morphological changes were examined by SEM.

$$\text{Percentage degradation} = \frac{W_o - W_F}{W_o} \times 100 \dots\dots\dots (2)$$

4.4. Results and discussion

4.4.1. Effect of the crosslinking agent on the crosslinked nanofibers

4.4.1.1. Effect of concentration of crosslinking agent

An intensity in the crosslinking agent available on the polymer is the valuable factor for the degree of crosslinking in the resultant polymer matrix .¹⁸ Intensity effect of crosslinking agent (EDC/NHS) on mass loss, morphology even on fiber diameter were investigated. An average mass loss of SF and SF/CMC nanofibers mats during the crosslinking reaction is shown in Figure 4.1. Results indicate that, at low concentration of EDC/NHS, crosslinked nanofibers led to 8-10% mass loss. The final mass loss decreased with rise in crosslinking agent intensity.

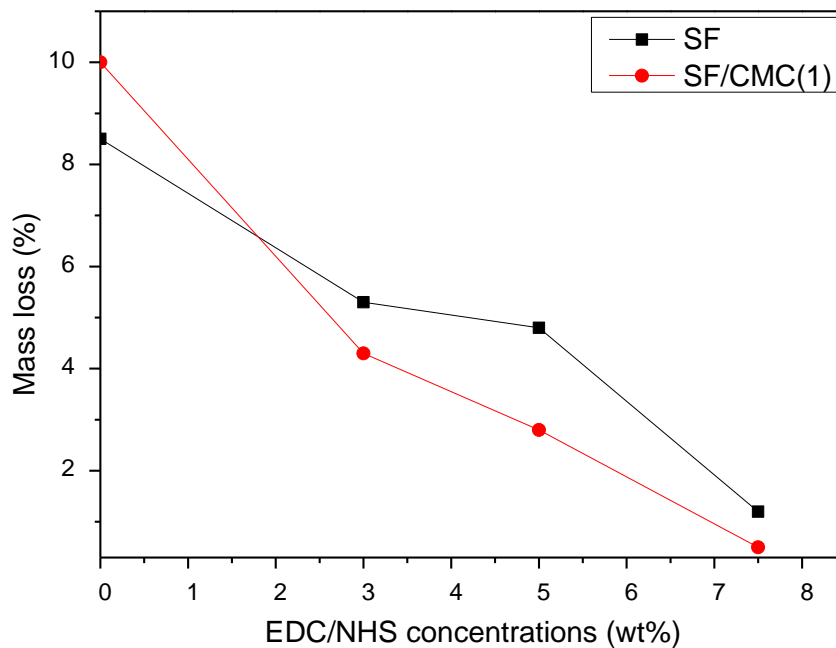


Figure 4.1: Final Mass loss of SF and SF/CMC(1) nanofiber mats as the EDC/NHS concentration increases.

The uncrosslinked SF fiber looked soft and wide gap in between the nanofibers was observed due to the presence of electrostatic between nanofibers as demonstrated in Figure 4.2 A. At low concentrations from 3wt% to 5wt%, the morphology of the crosslinked nanofiber mats was closely packed, and the nanofibers were intertwined. As the concentration of the crosslinking

agent increased, to 7.5 wt%, the morphology of the crosslinked nanofiber mats showed less swelling, see Figure 4.2B, C, and D. The diameter of fibers calculated by make use of Axiovision software. The average diameter appeared to decrease as the intensity of the crosslinking agent increased.

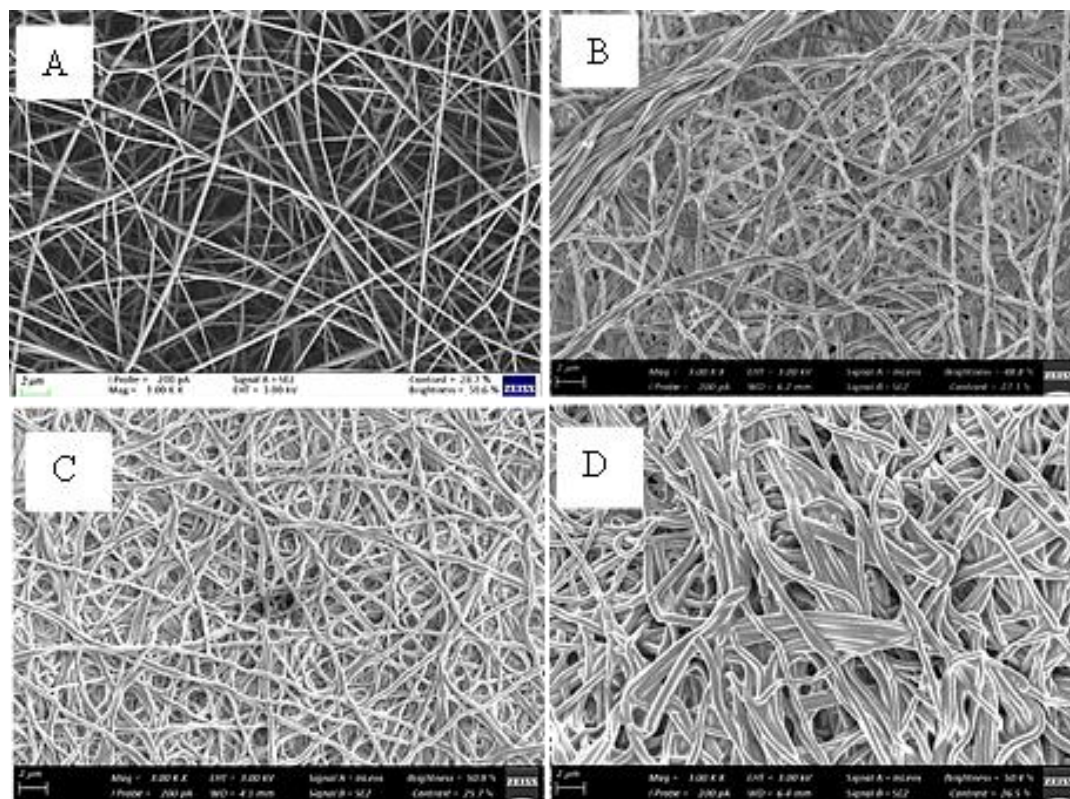


Figure 4.2: FESEM images of SF crosslinked nanofibers (A) uncrosslinked nanofiber mats, (B) 3 wt% EDC/NHS, (C) 5 wt% EDC/NHS, and (D) 7.5 wt% EDC/NHS.

The uncrosslinked SF/CMC nanofibers looked soft and wide gap in between the nanofibers was observed, see Figure 4.3A. The morphology of the crosslinked nanofiber mats became intertwined at low concentration of the crosslinking agent increase and the diameter of the crosslinked nanofiber mats was decreasing compared to the diameter of uncrosslinked fibers.

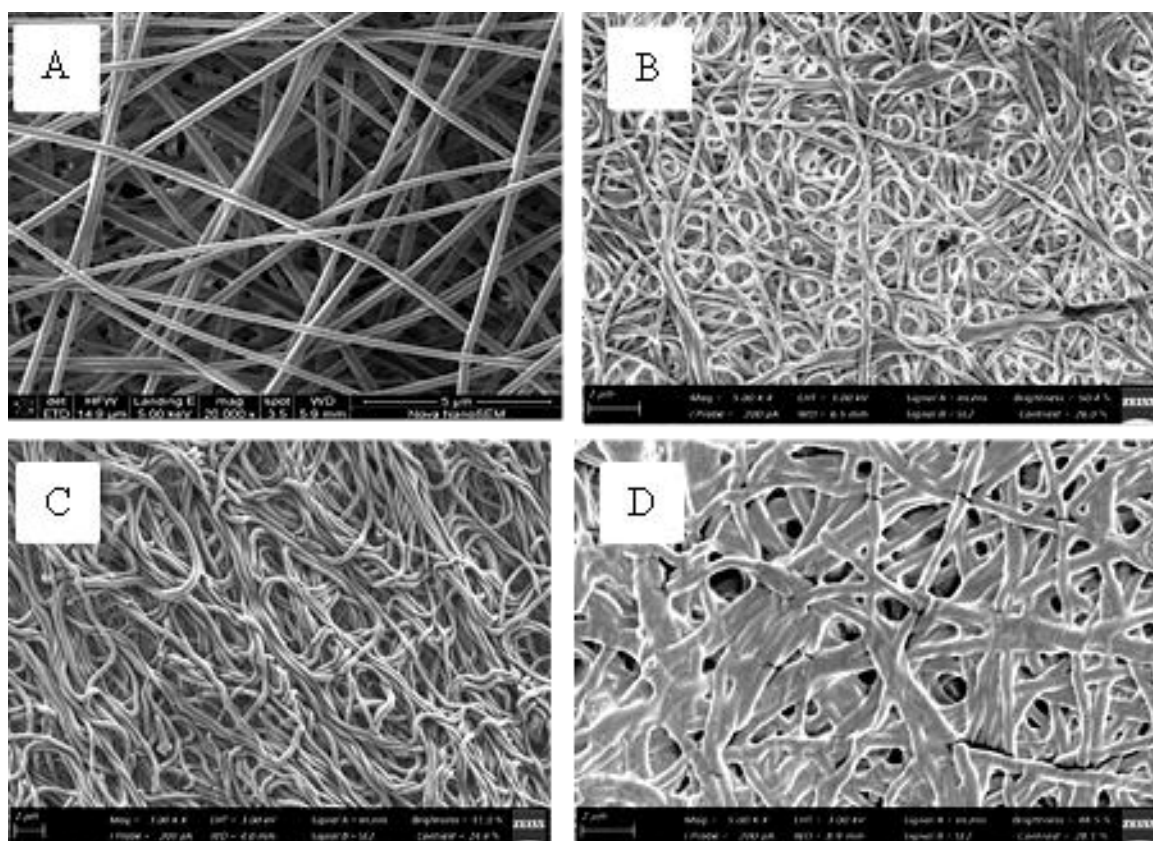


Figure 4.3: FESEM images of SF/CMC(1) crosslinked nanofibers (A) uncrosslinked nanofiber mats, (B) 3 wt% EDC/NHS, (C) 5 wt% EDC/NHS, and (D) 7.5wt% EDC/NHS.

4.4.1.2. Effect of crosslinking agent exposure time on nanofiber stability

In applications where high surface region-to-mass ratio are favoured keeping the morphology of fiber is significant. Thus, in this portion an impact of the exposure period in the crosslinking agent and stability of the crosslinked fibers was investigated. The stability of the crosslinked fibers were tested by immersing crosslinked nanofibers and uncrosslinked nanofibers in water at RT for 24 h as demonstrated by Figures 4.4 and 4.5, showing the difference in morphology on the fibers prior and after crosslinking. Uncrosslinked nanofibers showed well separated morphology before soaked in water as shown in Figure 4.4 and 4.5A, after these nanofibers (uncrosslinked) where soaked in water, they rapidly fused in water and form an unstable morphology in that they partially dissolved and form a film, as is evident in both Figures 4.4B and 4.5B. The crosslinked nanofibers that were exposed to the 7.5wt% crosslinked agent for 24h after immersion in water showed did not maintain the nanofiber morphology shown in Figure 4.4D and 4.5D. Increasing the exposure time into the 7.5wt% crosslinking agent to 48h created adjoining nanofiber components to swell among themselves (see Figure 4.4E and 4.5E),

but the nanofibers exhibited higher stability to water as the fibers did not lose their intact morphology that left behind the nanofiber properly separated or not intertwined, as is evident in Figures 4.4F and 4.5F. The exposure time in the crosslinking agent was observed to influence morphology of the crosslinked nanofibers prior and after soaking in water. As the exposure time was increased, the crosslinked nanofibers obtained more stability in water and the morphology was maintained.

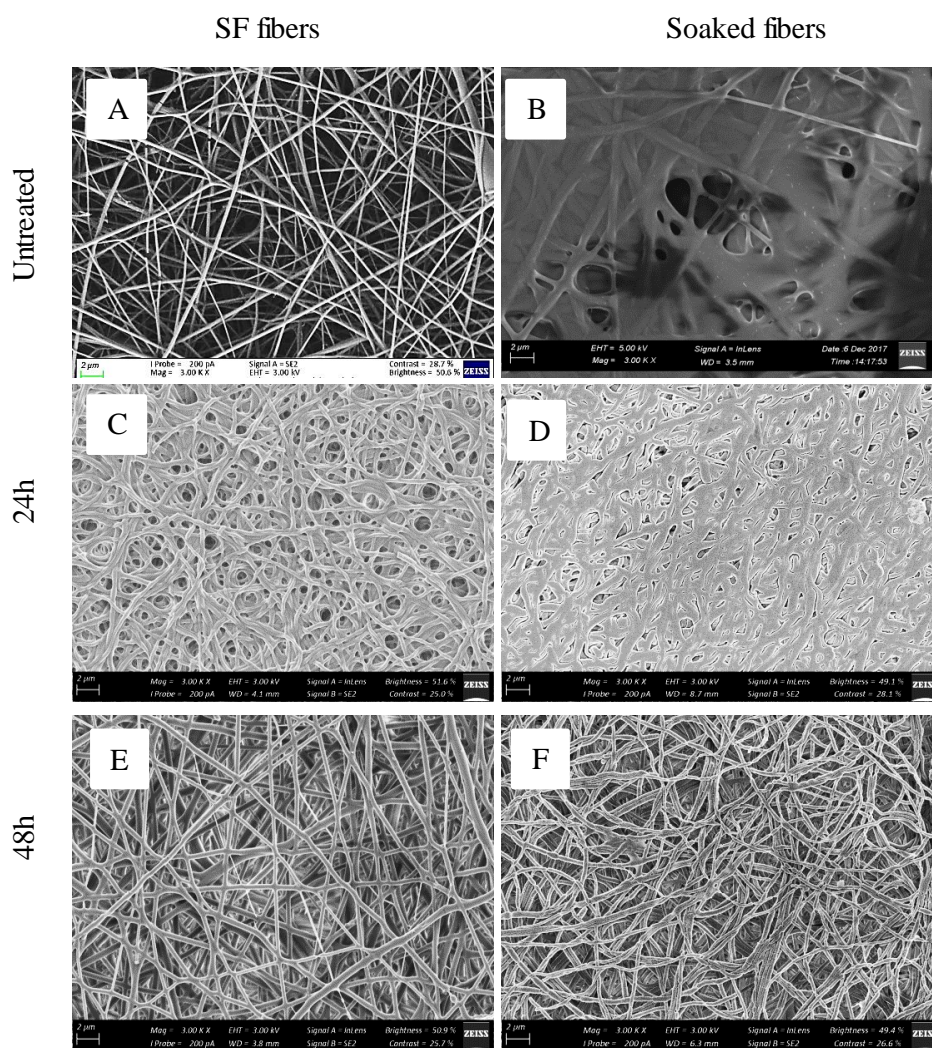


Figure 4.4: FE-SEM images of SF, (A) untreated SF nanofiber mats, (B) untreated SF fiber mats after soaking in water, (C) SF fibers exposed for 24 h to the 7.5wt% EDC/NHS, (D) after soaking in water, (E) SF nanofibers mats exposed for 48 h to the 7.5wt% EDC/NHS and (F) after soaking in water.

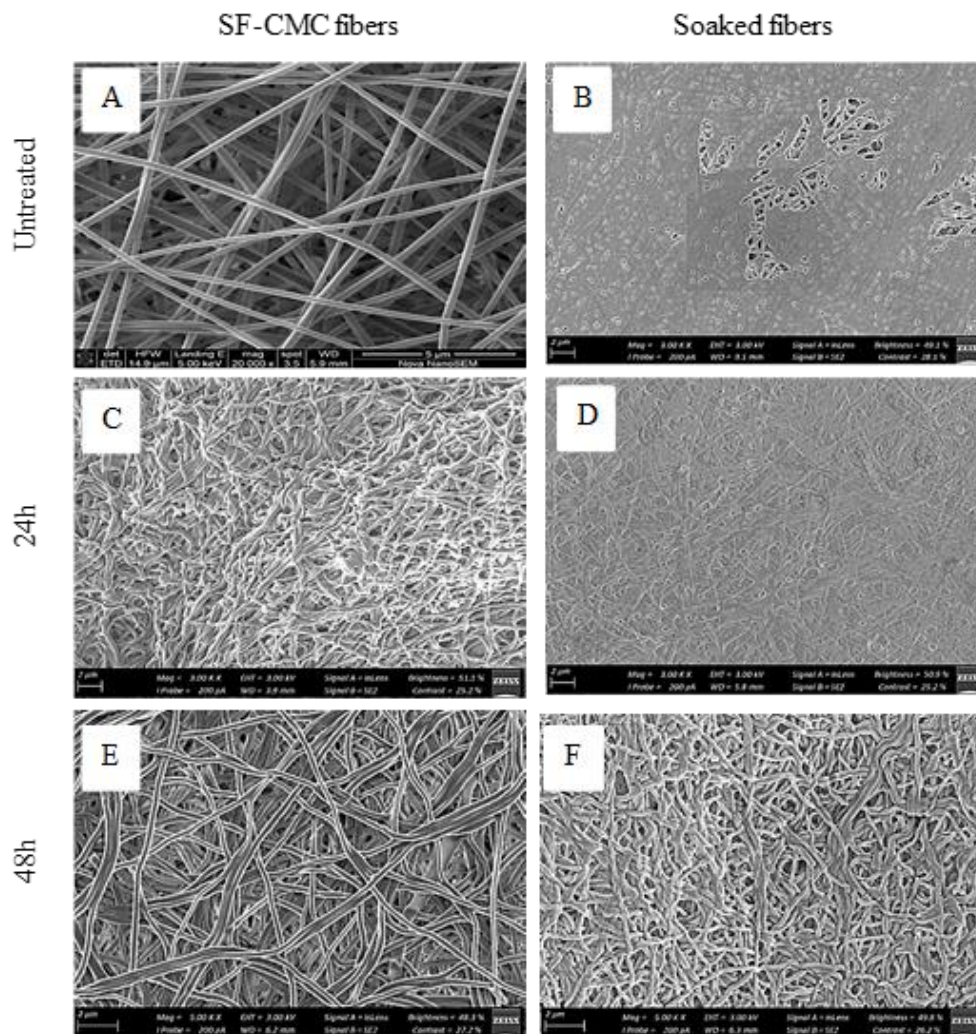


Figure 4.5: FE-SEM images of SF/CMC (1) fibers, (A) untreated fibers, (B) untreated fiber mats after soaking in water, (C) nanofiber mats exposed for 24 h to the 7.5wt% EDC/NHS, (D) after soaking in water, (E) nanofiber mats exposed for 48 h to the 7.5wt% EDC/NHS and (F) after soaking in water.

4.4.2. Characterization of crosslinked nanofiber membranes

4.4.2.1. Attenuated total reflectance infrared spectroscopy (ATR-IR)

Structural changes that took place in crosslinked nanofiber mats were confirmed by FTIR. The results shown in the figures that follow demonstrate the effect of crosslinking in the spectra of crosslinking nanofibers. Figure 4.6 indicates while the concentration of the crosslinking agent increased so too did the intensity of the absorption peaks, compared to the uncrosslinked silk fibroin peaks. The intermolecular and intramolecular hydrogen bonds were observed by a broad peak around 3500 to 3300 cm^{-1} . These signals overlapped with the absorbance of water. An infrared spectra region around 1700 to 1600 cm^{-1} was allocated with the peptide backbone of

amide I that has been reported to determine the crystallinity of SF nanofibers. The peaks at 1530 cm^{-1} and 1235 cm^{-1} were assigned as amide II and amide III, individually. A band at 965 cm^{-1} was assigned as amide IV.

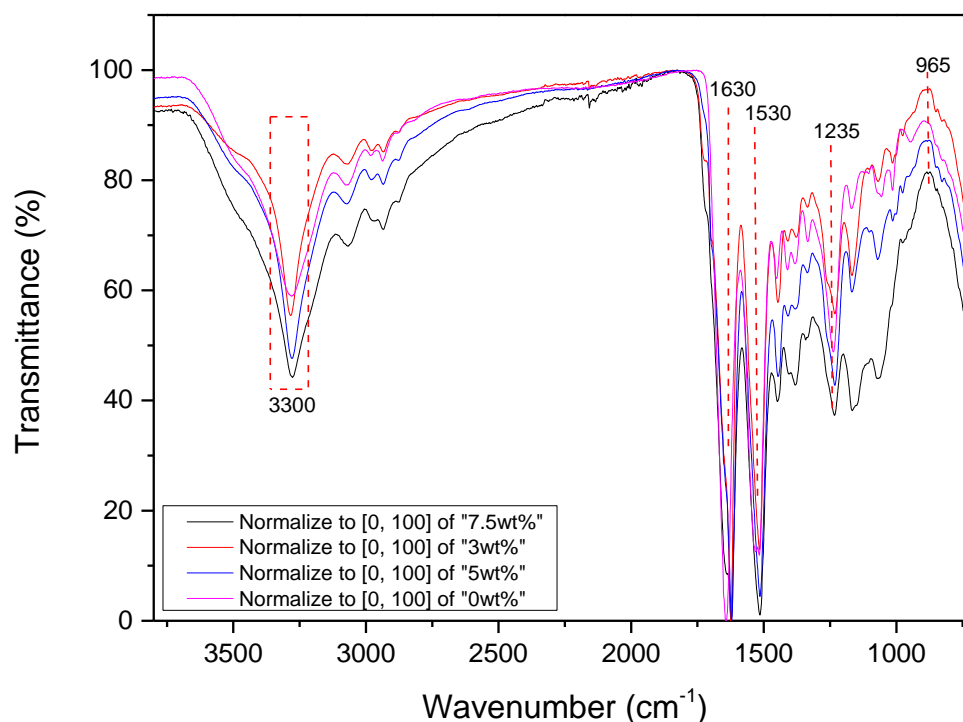


Figure 4.6: FTIR spectrum of SF crosslinked nanofibers with different concentrations of the crosslinking agent: 0%, 3 wt%, 5 wt%, 7.5 wt% EDC/NHS.

Figure 4.7 shows the spectrum of the crosslinked SF/CMC blended nanofiber membranes. The crosslinked blends show band around 1630 cm^{-1} (amide I), 1560 cm^{-1} (amide II), and 1230 cm^{-1} (amide III); these peaks represent the transformation of random coil conformation to β -sheet conformation and the intensity of these peaks was seen to increase with increase in concentration of the crosslinking agent. A band around 1060 cm^{-1} representing $>\text{CH}-\text{O}-\text{CH}_2$ stretching of the CMC.

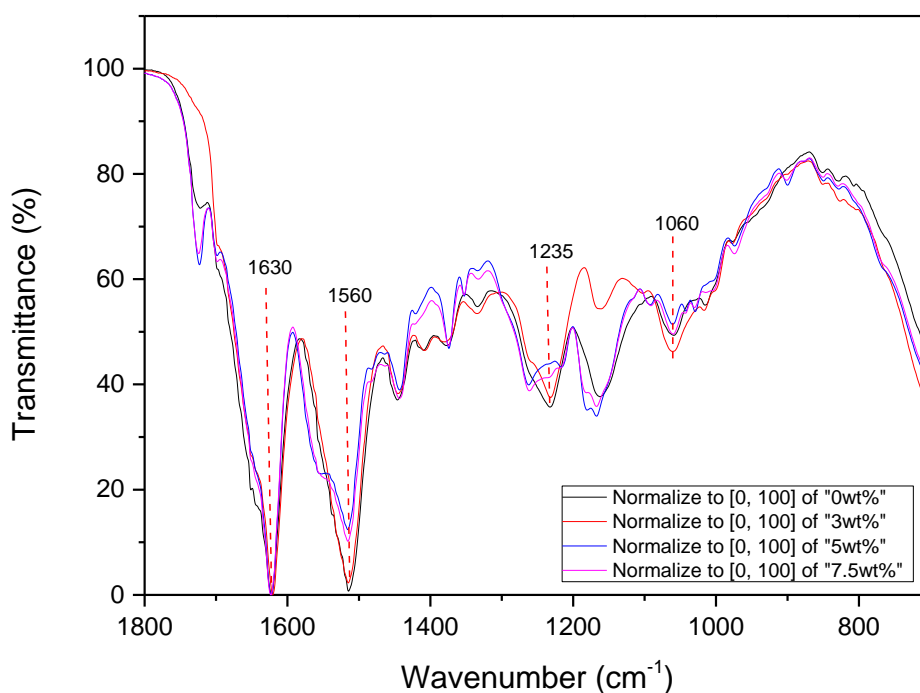


Figure 4.7: FTIR spectrum of SF/CMC(1) crosslinked nanofibers with different concentrations of the crosslinking agent: 0%, 3 wt%, 5 wt%, 7.5 wt% EDC/NHS.

4.4.2.2. Thermal gravimetric analysis (TGA)

Decomposition and conductivity of heat on crosslinked SF nanofibers and SF/CMC blended nanofibers mats was performed by TGA. The TGA tool describes the relationship in temperature and the weight of the material, which then interpret the capacity of a substance to resist elevated temperature. The percentage mass loss was observed by increasing the temperature varying between 0–900°C. The first mass loss from all samples, because of moisture loss, was observed at around 100 °C. Figure 4.8 shows the thermograms of crosslinked SF nanofibers with various concentrations of the crosslinking agent. A huge mass loss around 200–400 °C was noticed and was related to the decomposition of the amino acids also the fractionation of the peptide's bonds. A decrease in the weight loss with increase in temperature was observed as the concentration of crosslinking agent was increasing. As the temperature was rising to 900 °C, about 80% of the weight decomposed for the uncrosslinked nanofiber mats, whereas for the crosslinked nanofiber mats were still thermal stable.

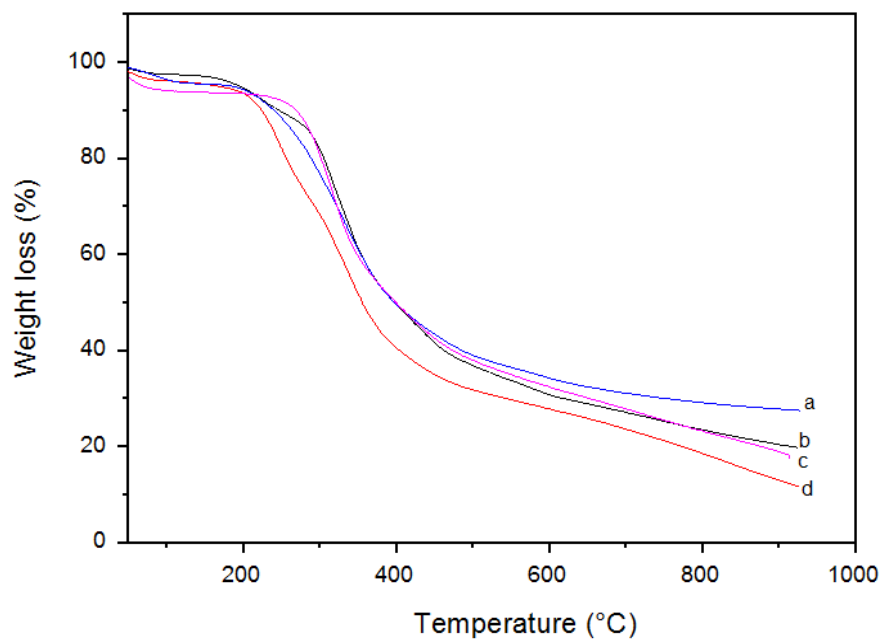


Figure 4.8: TGA spectra of SF crosslinked nanofibers with different concentrations of the crosslinking agent: (a) 7.5 wt% EDC/NHS, (b) 5 wt% EDC/NHS, (c) 3 wt% EDC/NHS; and (d) uncrosslinked SF nanofibers.

The thermograms of crosslinked SF/CMC(1) blended nanofiber mats are shown in Figure 4.9 and indicate two phases of weight loss. The initial weight loss occurred due to the moisture content. The remaining weight at 900 °C of blended nanofibers was like the crosslinked SF nanofibers. As the concentration of the crosslinking agent increased, the crosslinked samples were all pretty much the same, only the uncrosslinked sample showed less thermal stability.

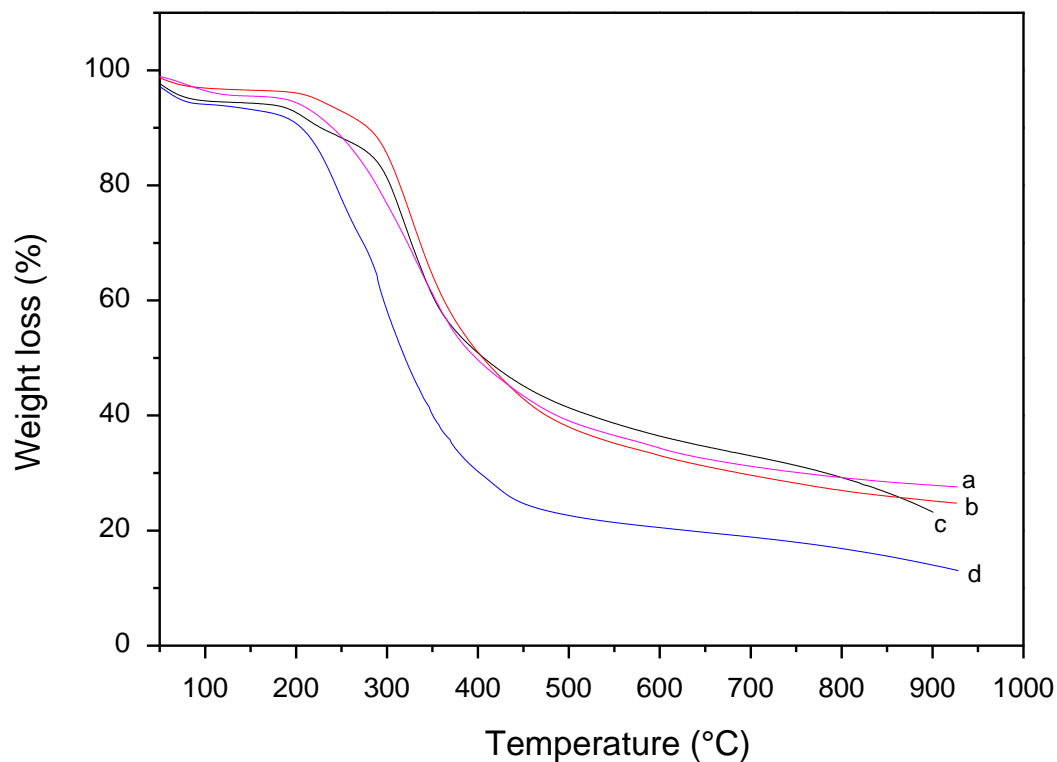


Figure 4.9: TGA thermograms for SF/CMC(1) crosslinked nanofibers with different concentration of the crosslinking agent: (a) 7.5 wt% EDC/NHS, (b) 5 wt% EDC/NHS, and (c) 3 wt% EDC/NHS; and (d) uncrosslinked SF/CMC(1) nanofibers.

4.4.3. Antimicrobial evaluation of the crosslinked nanofibers

To study antimicrobial properties towards the fabricated nanofiber mats was also some of the objectives of this work. The antimicrobial activity of the produced nanofibers was evaluated using two methods: zone inhibition (Section 4.4.3.1) and fluorescence microscopy (Section 4.4.3.2).

4.4.3.1. Zone inhibition test

Some silk fibers have been reported to be antimicrobial. Khalid *et al.*¹⁹ investigated an effect of antibacterial action of SS extracted on *Bombyx mori*. They discovered that the innate SS (which is defined as the glue-like material that keeps the strand of the fibroin together within the silk threads) has good antimicrobial activity against *Micrococcus leutus*, *Pseudomonas aeruginosa*, *Staphylococcus aureus*, and *Escherichia coli*. Previous work by Waraluk *et al.*²⁰ described antimicrobial properties of the sericin extracted from Eri (which is a wild species of the non-mulberry silk moth). The potency of Eri sericin as an antibacterial agent was

demonstrated by putting a disc on top of the culture and reducing concentration micromethod, as well as by evaluating the effect of Eri sericin on bacterial growth. Eri sericin was found to be bactericidal.

In this study CMC, SS and SF were investigated for the mode of activity in opposition to *Staphylococcus aureus* and *Escherichia coli*. their blends were also evaluated. The technique of the disc diffusion was applied to describe a sensitivity of both (*S. aureus* and *E. coli*) towards nanofiber samples. An action of antibacterial material can be explained by noticing a region of inhibition all over the sample.

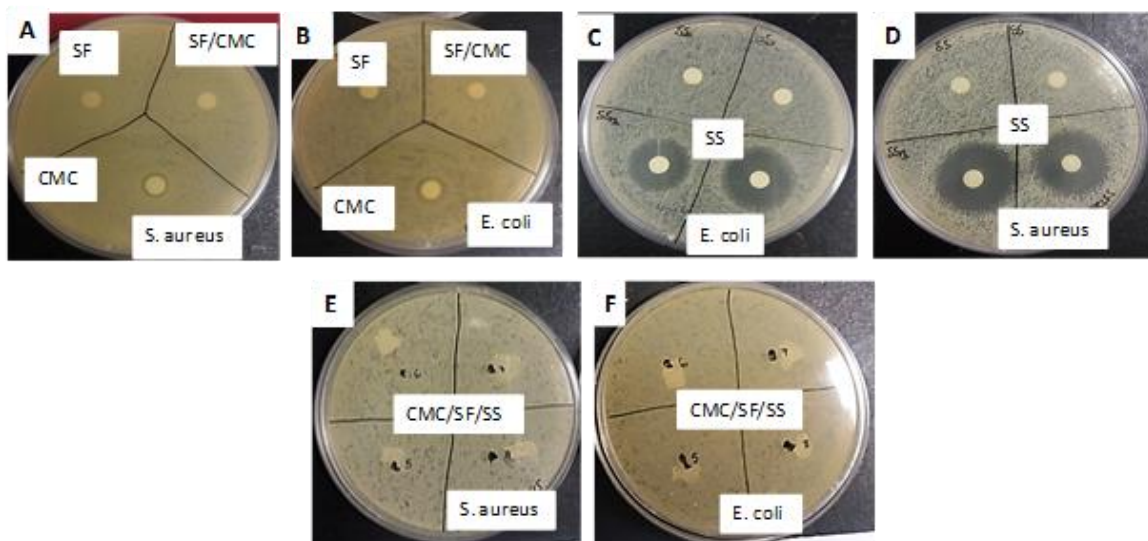


Figure 4.10: Results of the zone-inhibition method used to determine the susceptibility of *E. coli* (Gram-negative) and *S. aureus* (Gram-positive) to (A) SF, CMC, SF/CMC, (C) SS and (E) SF/CMC/SS blend nanofiber membranes.

The results of the zone inhibition test against *S. aureus* and *E. coli* did not show any susceptibility around SF and SF/CMC nanofiber as demonstrated in Figure 4.10A and B, only CMC showed a slight activity on both bacteria (*S. aureus* and *E. coli*). According to the literature,²⁰ SS is antimicrobial. The activity of the antibacterial was examined on the SS against *S. aureus*. Outcomes of the test are indicated in Figure 4.10A. Zone of inhibition was noticed as the clearing around the samples, which proved that SS possess antimicrobial activity. The zone of the inhibition was also observed when SS was tested against *E. coli*, as demonstrated in Figure 4.10D. The experiment indicates that the SS had antimicrobial activity against both bacteria tested, but the amount of the activity fluctuated, depending on the bacteria used. These results were found to be consistent with what is reported on the literature. The blend

of SF/CMC/SS nanofibers did not show any activity against all the organisms that were used, and this was thought to be due to the low ratio of sericin in the SF/CMC/SS blends nanofibers. Table 4.1 summarizes the results of the zone inhibition test done on all the electrospun nanofibers, results shows that the antibacterial effect of the samples fluctuated, due to which type of bacteria was used. Inconsistence of inhibition area around the sample was not studied but the experimental test were described as positive or negative based on antibacterial action.

Table 4. 1: Summary of antimicrobial activity of the electrospun nanofiber membranes

Sample	<i>S. aureus</i>	<i>E. coli</i>
SF (degummed silk)	No activity	No activity
SS (Silk sericin)	Very active	Very active
CMC(Carboxymethyl Cellulose)	Slightly active	Slightly active
SF/CMC	No significant activity	No significant activity
SF/CMC/SS	No activity	No activity

4.4.3.2. Fluorescence microscopy

Fluorescence microscopy was used in efforts to examine the mechanism of action of fibers against bacteria cells. The experimental outcomes for the live/dead bacteria with *S. aureus* and *E. coli* are shown in Figure 4.11. The test was done by exposing the bacteria to the samples for 15 min before imaging. The colonies are the brightly colored dots that are visible on top of the fiber surfaces, due to some dye being absorbed. The controls show great number of connected colonies, that were not immersed in PI, showing that they were living. When small pieces of SF fibers were placed in the bacterial solution, the appearance of red fluorescent cells was observed, that shows the cells are not alive. The death of the bacterial cells is most likely a result of disruptive interaction on the cell wall at the lipid interface, damaging the membrane, then followed by cell lysis. The mode of the cell death depended on the type of bacteria used. In the case of SF fibers, more cell death was observed investigating the matter of the *S. aureus* (gram-positive) than *E. coli* (Gram-negative). For SF/CMC blends nanofibers, very few cell deaths were observed; most bacteria were alive. These results could be due to the insufficient sericin in the SF of our mix. The literature reports¹⁹ the antimicrobial properties of sericin rather than the SF. Of importance to note here, from the point of view of novelty, there is no literature (openly available) describing the antimicrobial properties of SF/CMC blends.

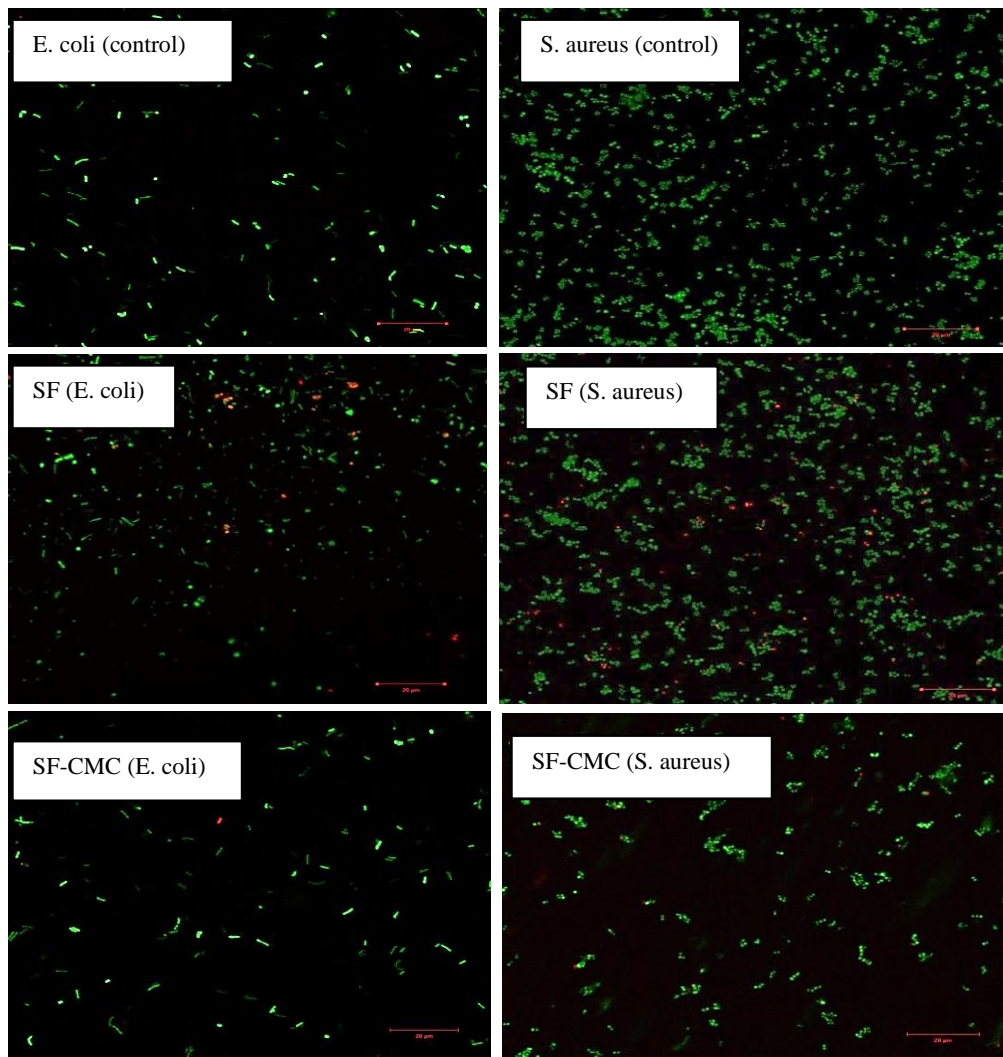


Figure 4.11: Fluorescent microscope images of incubated fibers, SF, and SF/CMC blend *with S. aureus* and *E. coli* in saline solution.

4.4.4. Biodegradation evaluation

4.4.4.1. Weight loss in the degradation process

Certain enzymes such as protease XIV, cellulase enzymatic solutions and PBS solution were used to study a degradation behavior of the fabricated SF and SF/CMC nanofiber membranes. Figure 4.12 indicates a degradation rate with reference to the weight loss of the nanofiber mats. Figure 4.12(A) 14 days later in the phosphate buffer solution results indicate that there was not much change in the weight loss of the nanofiber mats, act as controls. Only about 10–35% of the weight was lost in all samples. Following the incubation in the Protease XIV solution at 37 °C for 3–7 days (Figure 4.12(B), the weight loss of silk fibroin fibers was ~40–88% and the SF/CMC blends nanofibers shows slightly slower degradation compared to silk fibroin fibers,

the weight loss of the SF/CMC blend nanofibers was ~20–70%. SF/CMC blend nanofiber mats were also incubated in the cellulase solution at 37°C for 3–7 days indicated with Figure 4.12(C), a decrease in the mass was observed to ~35–45%, which was much lower than when they were incubated in protease XIV but higher when compared with the controls. Figure 4.12(D) shows the weight loss of the SF/CMC blend nanofibers when the solutions of these two enzymes were combined, the weight loss of SF/CMC blends after two weeks was observed to be ~40–65%.

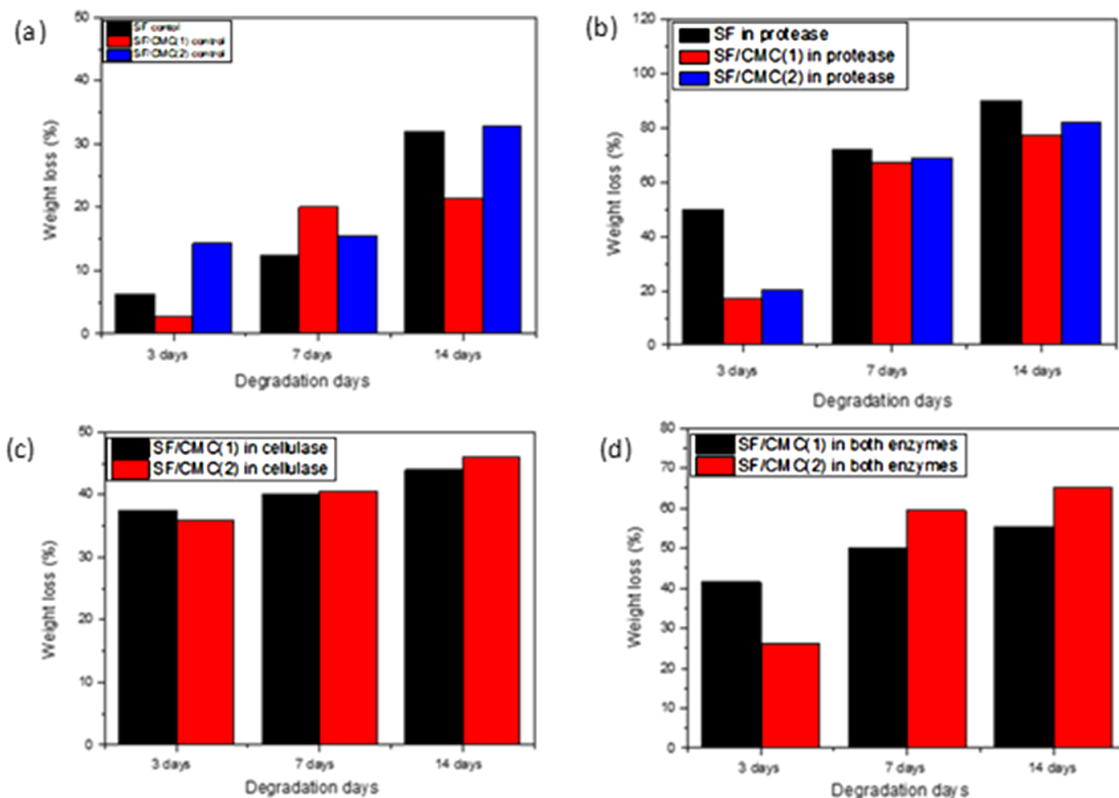


Figure 4.12: Degradation behavior of SF, SF/CMC(1), and SF/CMC(2) after incubation in the following solutions: (A) PBS solution (controls), (B) protease XIV solution, (C) cellulase solution, and (D) a solution of both enzymes.

4.4.4.2. The changes in the morphology of nanofiber membranes

The difference in the morphology of the crosslinked nanofibers during degradation was examined by scanning electron microscopy imaging. Figure 4.13 shows the morphological changes of SF nanofibers after incubation into phosphate buffer solution and protease XIV solution for 3–7 days. After two weeks in PBS solution (pH 7.4) at 37 °C, irrelevant morphological changes in the SF fibers was observed during the degradation. But after 3 days in protease XIV solution, surface defects (microcracks) were observed on SF nanofibers. This

led to fiber rupture after 7 days of degradation; no silk fibroin fibers were observed after 14 days. The difference in the degradation rates of nanofibers was thought to be due to the fiber diameters (external region).

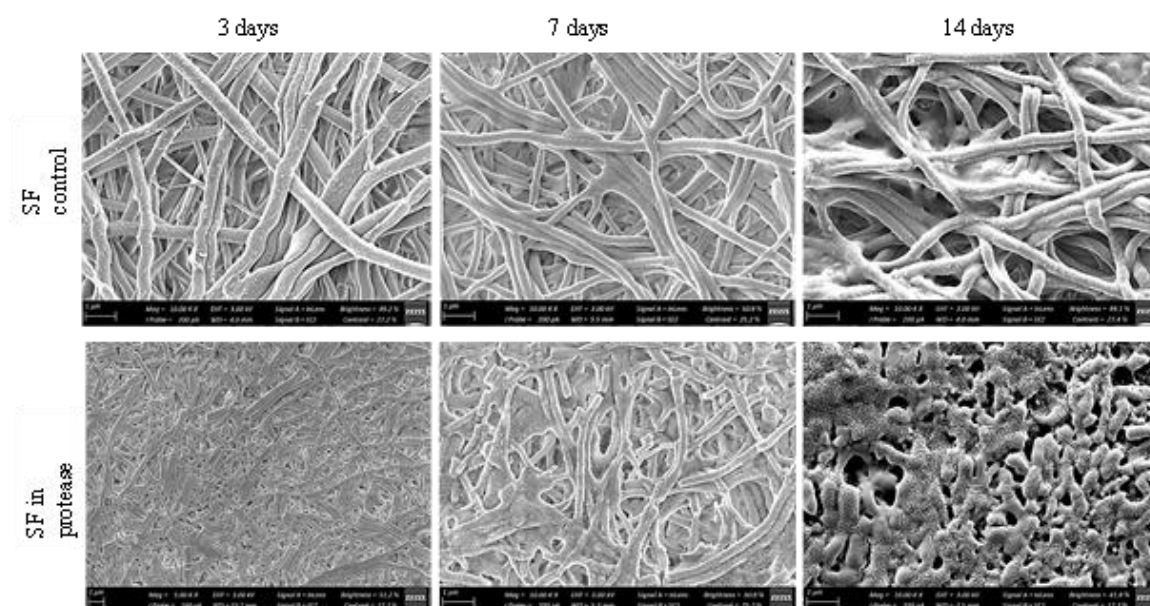


Figure 4.13: SEM images of the SF nanofibers after incubation in PBS (controls) and protease XIV solution at 37 °C for 3, 7, and 14 days.

Degradation of the developed electrospun SF/CMC blend nanofibers was investigated by exposing the blend nanofibers to protease XIV, cellulase, and a mixture of the two enzymes at 37°C for periods of 3, 7, and 14 days. The reasoning behind selecting these conditions was the following: protease XIV degrades the silk and cellulase degrades cellulose. Then, by selecting a combination of the two enzymes, the main objective was to check whether the enzyme will be selective in a mixed matrix environment.

The morphology of the degraded SF/CMC blend nanofibers in PBS solution as control, and in protease XIV, cellulase, and a mixture of two enzymes is shown in Figure 4.14. After 2 weeks of degradation in PBS, the surface of the SF/CMC blend nanofibers were homogeneously smooth in appearance. After 3 days of degradation in the enzymatic solution, some of the SF/CMC nanofibers has degraded. A considerable number of fibers had degraded after 7 days. Then after 2 weeks of degradation, the nanofibers matrix of the SF/CMC blends changed into ‘chunks’, consisting of the short fiber fragments.

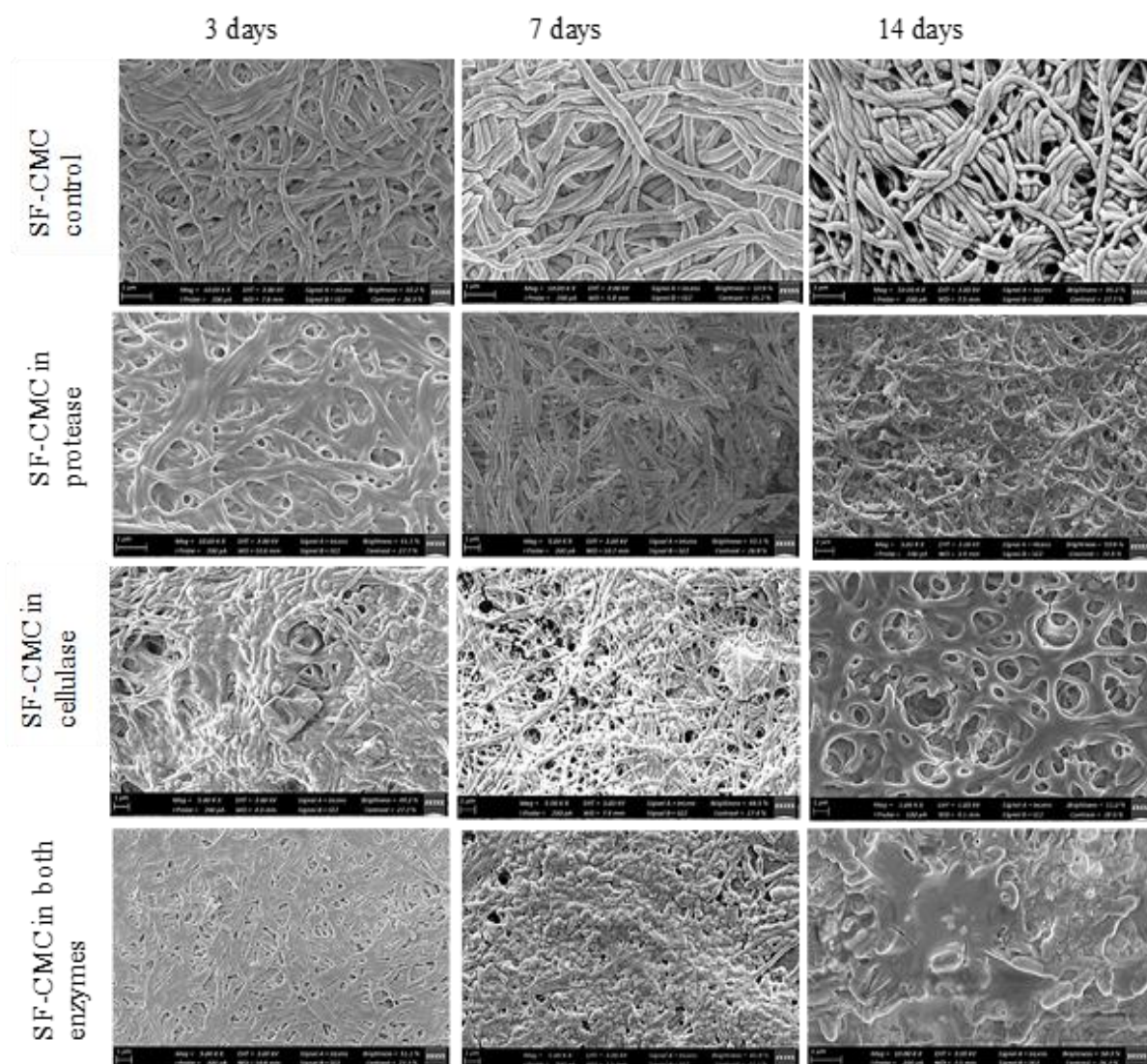


Figure 4.14: SEM images of the SF/CMC blends nanofibers after incubation in PBS and enzymatic solution at 37°C for 3–14 days.

4.4.4.3. Structural changes during the degradation process

Structural changes in the degradation process were unveiled by using ATR-FTIR instrument. Prior to degradation, the nanofiber mats showed large bends around 1660 cm^{-1} (random coil, amide I) and at 1530 cm^{-1} (α -helix, amide II), as demonstrated in Figure 4.15(A). The structural changes in the degraded nanofibers after 3 days are demonstrated in Figure 4.15(B); weak peaks were observed around 1521 cm^{-1} (β -sheet, amide II). Additionally, SF/CMC blend nanofibers showed a large band at 1060 cm^{-1} (carboxymethyl group). After 14 days of degradation, a weak peak at 1660 cm^{-1} was observed, but the amide II and amide III had disappeared. The outcomes reveal that, before degradation, the secondary structure of the RSF and SF/CMC blend nanofiber existed mostly in random coil and α -helix. The β -sheet structure at the remains of SF

nanofibers after degradation showed some broad bands, although the bend (amide III region) is proportional to the random coil and α -helix conformations structure became fragile/had disappeared. The remaining SF/CMC blend nanofibers showed tough bands around 1660 cm^{-1} (β -sheet, amide I) and at 1060 cm^{-1} (carboxymethyl group). These results demonstrated that the secondary structures of the residual SF and SF/CMC blend nanofibers were mainly β -sheet structures after degradation.

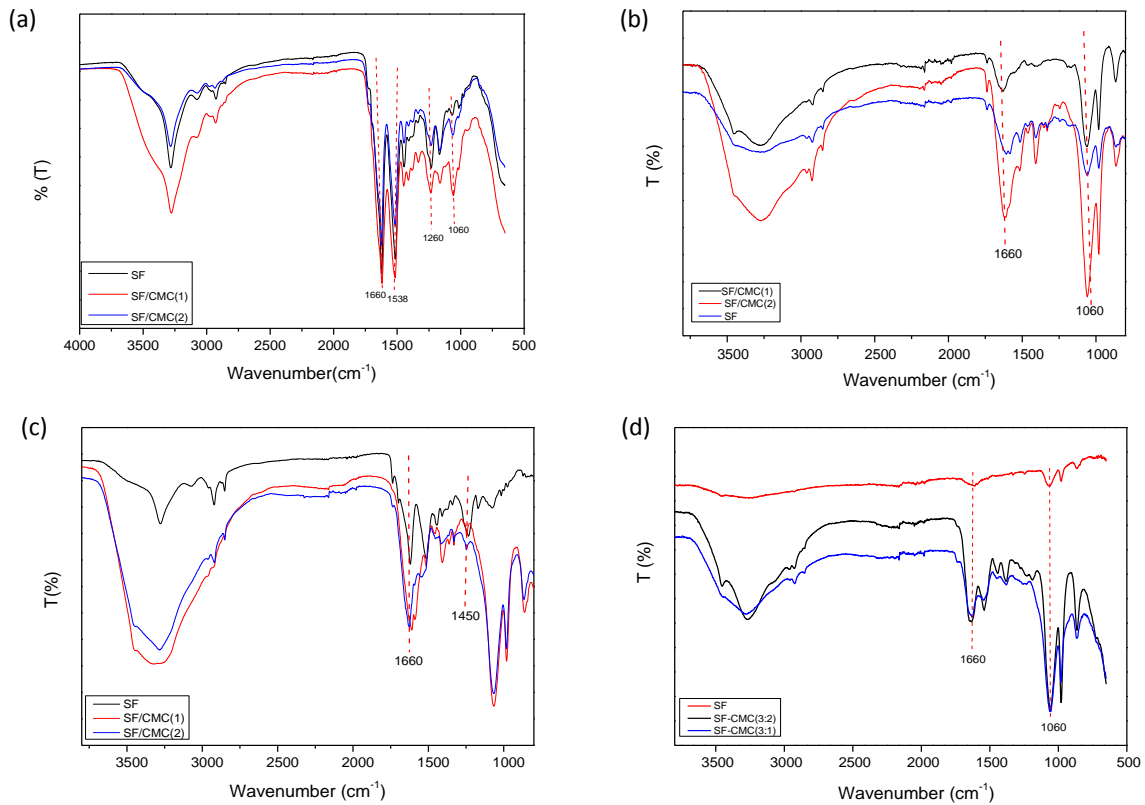


Figure 4.15: FTIR spectrum for CMC, SF, and SF/CMC blend nanofibers: (A) before degradation, (B) 3 days later of degradation, (C) 7 days later of degradation, and (D) 14 days later of degradation.

4.5. Conclusion

In this chapter, the crosslinking of the nanofiber mats prior to being assessed on the envisaged application as well as the antimicrobial and biodegradation evaluation of all electrospun nanofibers is reported. The SF and SF/CMC blends nanofibers were all successfully crosslinked by different concentration of EDC/NHS crosslinking agent (3wt%, 5wt% and 7.5wt %). The crosslinked nanofiber composites were studied, morphology using SEM, microstructure using ATR-FTIR and thermal behavior using TGA. After crosslinking, it was observed that the nanofiber mats became more pliable and their average diameter increased compared to the non-

crosslinked nanofiber mats. The stability in water was achieved due to the highly concentrated EDC/NHS agent. This water-stability property of the crosslinked nanofiber mats would be good candidates in the uses of water purification.

Antibacterial experiments on the composites that were conducted in opposition to a Gram-positive bacteria strain (*S. aureus*) together with the Gram-negative bacteria strain (*E.coli*) proved that SF shows moderate activity and inconsiderable results were obtained in all SF/CMC nanofiber membranes

Biodegradable materials are preferred candidates to respond to an increased awareness of the need to protect the environment. The degradation of all electrospun nanofibers was investigated through an action of enzymes. The results show that SF and CMC can be classified as enzymatically degradable polymers. The changes in morphology and in microstructure during the degradation process were observed by using SEM and ATR-FTIR. An increase in weight loss as the degradation period increased was observed, and this was confirmed by the microstructure of the degraded nanofibers because some of the SF and SF/CMC bonds were broken.

4.6. References

- (1) Kumar, A. A.; Karthick, K.; Arumugam, K. P. Applications of Biodegradable Materials. **2011**, *1* (3), 1–4.
- (2) Vroman, I.; Tighzert, L. Biodegradable Polymers. *Materials* **2009**, *2* (2), 307–344.
- (3) Kaushik, K.; Sharma, R. B.; Agarwal, S. Natural Polymers and Their Applications. *Int. J. Pharm. Sci. Rev. Res.* **2016**, *37* (2), 30–36.
- (4) Morris, G.; Harding, S. Polysaccharides, Microbial. *Appl. Microbiol.* **2009**, 482–494.
- (5) Olatunji, O.; Richards, O. Processing and Characterization of Natural Polymers. *Natural Polymers*. Springer International, **2017**.
- (6) Paull, R. E.; Chen, N. J. Postharvest Variation in Cell Wall-Degrading Enzymes of Papaya during Fruit Ripening. *Plant Physiol.* **1983**, No. 2699, 382–385.
- (7) Lu, Q.; Zhang, B.; Li, M.; Zuo, B.; Kaplan, D. L.; Huang, Y.; Zhu, H. Degradation Mechanism and Control of Silk Fibroin. *Biomacromolecules* **2011**, *12* (4), 1080–1086.
- (8) Gross, R. A. Biodegradable Polymers for the Environment. *Science* (80). **2002**, *297* (5582), 803–807.
- (9) Xu, Y.; Wang, Y.; Jiao, Y.; Zhang, C.; Li, M. Enzymatic Degradation Properties of Silk Fibroin Film. *J. Fiber Bioeng. Informatics* **2011**, *4* (1), 35–41.
- (10) Juturu, V.; Wu, J. C. Microbial Cellulases: Engineering, Production and Applications. *Renew. Sustain. Energy Rev.* **2014**, *33*, 188–203.
- (11) Song, D. W.; Kim, S. H.; Kim, H. H.; Lee, K. H.; Ki, C. S.; Park, Y. H. Multi-Biofunction of Antimicrobial Peptide-Immobilized Silk Fibroin Nanofiber Membrane: Implications for Wound Healing. *Acta Biomater.* **2016**, *39*, 146–155.
- (12) Jamshaid, A.; Hamid, A.; Muhammad, N.; Naseer, A.; Ghauri, M.; Iqbal, J.; Rafiq, S.; Shah, N. S. Cellulose-Based Materials for the Removal of Heavy Metals from Wastewater - An Overview. *ChemBioEng Rev.* **2017**, *4* (4), 240–256.
- (13) Lopez, C. G.; Rogers, S. E.; Colby, R. H.; Graham, P.; Cabral, J. T. Structure of Sodium Carboxymethyl Cellulose Aqueous Solutions. *J. Polym. Sci. Part B Polym. Phys.* **2015**, *53* (7), 492–501.
- (14) Vashist, S. K. Comparison of 1-Ethyl-3-(3-Dimethylaminopropyl) Carbodiimide Based Strategies to Crosslink Antibodies on Amine-Functionalized Platforms for Immunodiagnostic Applications. *Diagnostics* **2012**, *2* (4), 23–33.
- (15) Singh, B. N. Development of Novel Silk Fibroin / Carboxymethyl Cellulose Based Electrospun Nanofibrous Scaffolds for Bone Tissue Engineering Application. National Institute of Technology Rourkela **2017**, PhD.

- (16) Liu, R.; Zhang, F.; Zuo, B. Q.; Zhang, H. X. EDC-Crosslinked Electrospun Silk-Fibroin Fiber Mats. *Fibers Polym.* **2012**, *13* (5), 613–617.
- (17) Balouiri, M.; Sadiki, M.; Ibnsouda, S. K. Methods for in Vitro Evaluating Antimicrobial Activity: A Review. *J. Pharm. Anal.* **2016**, *6* (2), 71–79.
- (18) Gule, N. P. Electrospun Antimicrobial and Antibiofouling Nanofibres. Stellenbosch University. **2011**, PhD .
- (19) Khalid, N. J.; Omar, J. A. Study of the Antimicrobial Activity of Silk Sericin from Silkworm Bombyx Mori. *J. Comm. Med* **2010**, *23* (April), 130–133.
- (20) Waruluk, S.; Suporn, N.; Sivilai, S.; Thanaset, S.; Privina, K. Antibacterial Action of Eri (Samia Ricini) Sericin against Escherichia Coli and Staphylococcus Aureus. *Asian J. Food Agro-Ind.* **2009**, *2*, 222-228.

Chapter 5: Conclusions and recommendations for future research

5.0. Summary

This section summarizes the overall conclusions from the study based on the original objectives that's are described in Chapter 1. Additionally, suggestions for future work are given.

5.1. Conclusions

The research in this thesis focused on the preparation of SF/CMC based electrospun nanofiber mats for water treatment applications. Nanofibers of SF/CMC blends were successfully prepared via the ES process, using various compositions of SF/CMC blend solutions: 3:2, 3:1, and 2:1 (w/w) SF/CMC. The electrospun nanofibers were crosslinked with different concentrations of the crosslinking agent EDC/NHS (3 wt%, 5 wt%, and 7.5 wt%). Major development in different chemical and thermal properties of nanofiber obtained by the blending of SF and CMC (better properties were achieved than with pure SF nanofibers). During different blends considered, SF/CMC with blend ratio of 3:2 w/w (SF/CMC(1)) was found to have suitable; it had superior nanofiber properties than pure SF nanofibers.

The fabricated nanofibers were characterized for their morphology using SEM, and TEM. They were characterized structurally using FTIR, XRD, SolSt-¹³C NMR, and Raman spectroscopy and thermally using TGA and DSC. The average diameter of the nanofiber blends increased after CMC was added; the diameters of pure SF nanofibers were 100 ± 20 nm while that of SF/CMC(1) was measured to be 153 ± 28 nm. Nanofibers of the electrospun blends showed better chemical properties and thermal conductivity, in contrast with pure *Bombyx mori* SF.

The antimicrobial properties of silk sericin which is the gummy substance usually removed for processability of silk fibers are well reported in literature. In this study, pure sericin was evaluated for antimicrobial activity as well as pure silk fibroin and a cellulose derivative (CMC). Silk sericin showed great potency against both *E. coli* and *S. aureus* while pure cellulose indicated slight activity which has been reported in literature and as expected, silk fibroin did not have any activity. The blends of SF/CMC and SF/CMC/SS were also tested for their antimicrobial activity. The activity towards the Gram-positive bacteria (*S. aureus*) and Gram-negative (*E. coli*) bacteria was very poor. This could be attributed to the blending

technique observed in this study, immobilization of the sericin as a shell around the nanofiber membranes could improve the activity.

The biodegradation of the fabricated nanofiber membranes by an action of enzymes was done to determine the time it took for the nanofibers to degrade under certain conditions. Silk is a protein-based polymer; therefore, it is susceptible to biological degradation by proteolytic enzymes. The results revealed biodegradation after 2 weeks of incubation in a protease XIV solution at 37°C. The mass of the biodegraded nanofibers increased with an increase in exposure time. Pure SF nanofibers had obvious signs of degradation compared to those in the control experiment (SF nanofibers incubated in buffered solution without the enzyme). It was also observed that SF nanofibers degraded faster than the SF/CMC nanofibers. Hence, the nanofiber blends were further exposed to cellulase solution and to a mixture of the two enzymes. Decrease in the mass, change of the morphology, and distorted structure were observed by SEM and ATR-FTIR.

The work presented in this thesis contributes to a more detailed understanding of the structure of silk and carboxymethyl cellulose (SF/CMC) blend nanofibers, as candidates for water treatment. To our knowledge, this was the first study for SF to be used in water treatment and hence lays a foundation for many applications of natural fibers.

5.2. Recommendations

Recommendations for further studies include:

- i. Use of co-axial electrospinning as the fabrication technique for these two biopolymers
- ii. The development of the sponges as the potential candidates for filtration